Walter A. Rosenblith New Investigator Award

RESEARCH REPORT

HEALTH EFFECTS INSTITUTE

Number 209
February 2022

Associations of Air Pollution on the Brain in Children: A Brain Imaging Study

Mònica Guxens, Małgorzata J. Lubczyńska, Laura Pérez-Crespo, Ryan L. Muetzel, Hanan El Marroun, Xavier Basagaña, Gerard Hoek, Henning Tiemeier

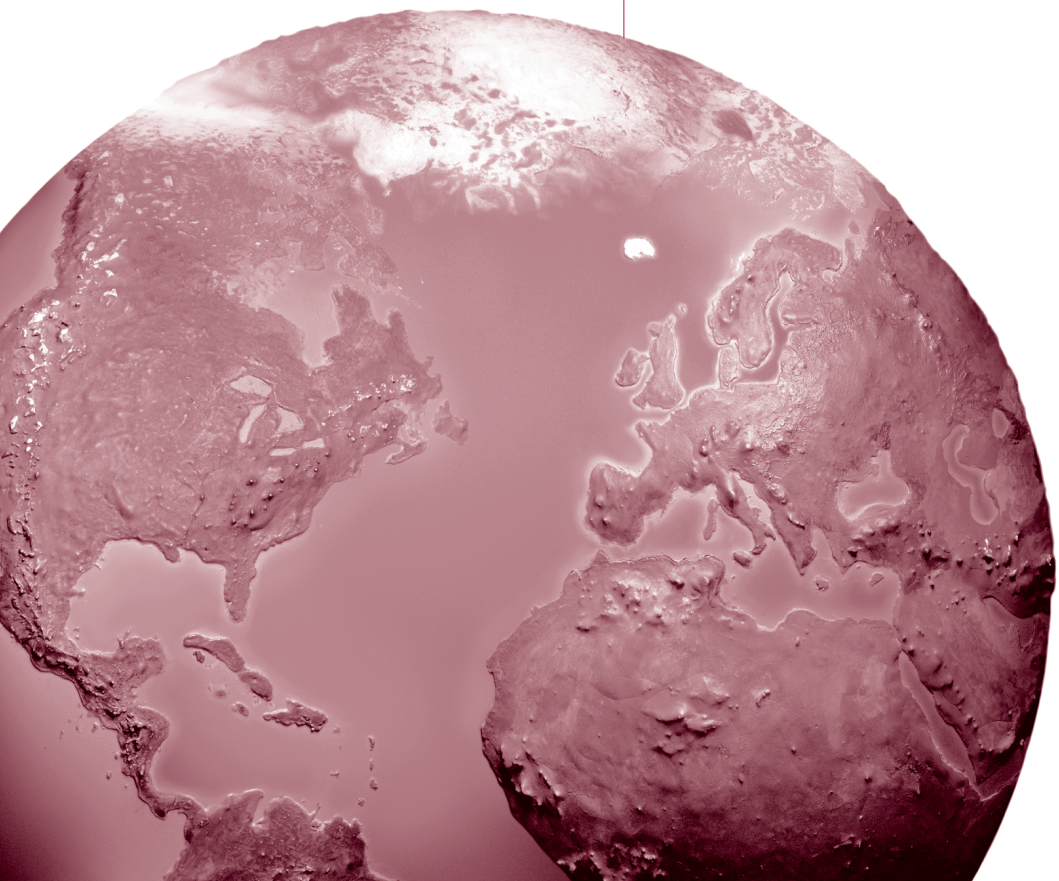

ISSN 1041-5505 (print)
ISSN 2688-6855 (online)

Associations of Air Pollution on the Brain in Children: A Brain Imaging Study

Mònica Guxens, Małgorzata J. Lubczyńska, Laura Pérez-Crespo, Ryan L. Muetzel, Hanan El Marroun, Xavier Basagaña, Gerard Hoek, Henning Tiemeier

---

with a Critique by the HEI Review Committee

Research Report 209

Health Effects Institute

Boston, Massachusetts

Trusted Science · Cleaner Air · Better Health

Publishing history: This document was posted at *www.healtheffects.org* in February 2022.

Citation for document:

Guxens M, Lubczyńska MJ, Pérez-Crespo L, Muetzel RL, El Marroun H, Basagaña X, et al. 2022. Associations of Air Pollution on the Brain in Children: A Brain Imaging Study. Research Report 209. Boston, MA: Health Effects Institute.

© 2022 Health Effects Institute, Boston, Mass., U.S.A. David A. Wade, Virginia Beach, Va., Graphic Designer.
Library of Congress Catalog Number for the HEI Report Series: WA 754 R432.

CONTENTS

About HEI v
About This Report vii
Contributors ix

HEI STATEMENT 1

INVESTIGATORS' REPORT *by Guxens et al.* 3

ABSTRACT 3

INTRODUCTION 4

SPECIFIC AIMS 5

METHODS AND STUDY DESIGN 5

Human Study Approval 5
Study Design and Population 5
Air Pollution Assessment 6
Brain MRI 7
Brain Structural Morphology 8
Brain Structural Connectivity 9
Brain Functional Connectivity 9
Cognitive Function 9
Attention and Executive Functioning Domain 10
Memory and Learning Domain 10
Potential Confounding Variables 10

STATISTICAL METHODS AND DATA ANALYSIS 10

Missing Data 10
Nonresponse Analysis 11
Exposure–Outcome Associations 11
Air Pollution Exposure and Brain Structural Morphology 11
Air Pollution Exposure and Brain Structural Connectivity 12
Air Pollution Exposure and Brain Functional Connectivity 13
Statistical Packages 13

RESULTS 13

Descriptive Analysis 13
Air Pollution Exposure and Brain Structural Morphology 14
Exposure During Pregnancy and Childhood — Brain Volumes in School-Age Children and Pre-adolescents 14
Exposure During Pregnancy and Childhood — Cortical Thickness and Surface Area in School-Age Children and Pre-adolescents 21
Exposure During Pregnancy — Cortical Thickness and Cognitive Function in School-Age Children 22
Air Pollution Exposure and Brain Structural Connectivity 22

Exposure During Pregnancy and Childhood — Global FA 22
Exposure During Pregnancy and Childhood — Global MD 23
Exposure During Pregnancy and Childhood — Specific FA and MD Tracts 23
Quantification of the Measurement Error 24
Air Pollution Exposure and Brain Functional Connectivity 24
DISCUSSION 25
Main Findings 25
Air Pollution Exposure and Brain Structural Morphology 25
Air Pollution Exposure and Brain Structural Connectivity 31
Air Pollution Exposure and Brain Functional Connectivity 31
Air Pollutants Related to Impaired Brain Development 32
Limitations 33
Air Pollution Exposure Assessment 33
Single Time Point for Outcome Data 34
Confounding 34
Generalizability 35
CONCLUSIONS 35
IMPLICATIONS OF FINDINGS 35
ACKNOWLEDGEMENTS 36
REFERENCES 36
HEI QUALITY ASSURANCE STATEMENT 43
MATERIALS AVAILABLE ON THE HEI WEBSITE 44
ABOUT THE AUTHORS 44
OTHER PUBLICATIONS RESULTING FROM THIS RESEARCH 45
CRITIQUE *by the Review Committee* 47
INTRODUCTION 47
SCIENTIFIC BACKGROUND 48
Approach 48
Methods 48
Summary of Results 50
HEI REVIEW COMMITTEE'S EVALUATION 54
Substantial Temporal and Spatial Misalignment of the Exposure Data 54
Statistical Analyses 55
Multipollutant Modeling 55
Generalizability of the Findings 56
Summary and Conclusion 56
ACKNOWLEDGMENTS 57
REFERENCES 57
Related HEI Publications 59
Abbreviations and Other Terms 61
HEI Board, Committees, and Staff 63

ABOUT HEI

The Health Effects Institute is a nonprofit corporation chartered in 1980 as an independent research organization to provide high-quality, impartial, and relevant science on the effects of air pollution on health. To accomplish its mission, the Institute

- Identifies the highest-priority areas for health effects research;
- Competitively funds and oversees research projects;
- Provides intensive independent review of HEI-supported studies and related research;
- Integrates HEI's research results with those of other institutions into broader evaluations; and
- Communicates the results of HEI's research and analyses to public and private decision makers.

HEI typically receives balanced funding from the U.S. Environmental Protection Agency and the worldwide motor vehicle industry. Frequently, other public and private organizations in the United States and around the world also support major projects or research programs. HEI has funded more than 340 research projects in North America, Europe, Asia, and Latin America, the results of which have informed decisions regarding carbon monoxide, air toxics, nitrogen oxides, diesel exhaust, ozone, particulate matter, and other pollutants. These results have appeared in more than 260 comprehensive reports published by HEI, as well as in more than 2,500 articles in the peer-reviewed literature.

HEI's independent Board of Directors consists of leaders in science and policy who are committed to fostering the public–private partnership that is central to the organization. The Research Committee solicits input from HEI sponsors and other stakeholders and works with scientific staff to develop a Five-Year Strategic Plan, select research projects for funding, and oversee their conduct. The Review Committee, which has no role in selecting or overseeing studies, works with staff to evaluate and interpret the results of funded studies and related research.

All project results and accompanying comments by the Review Committee are widely disseminated through HEI's website (*www.healtheffects.org*), printed reports, newsletters and other publications, annual conferences, and presentations to legislative bodies and public agencies.

ABOUT THIS REPORT

Research Report 209, *Associations of Air Pollution on the Brain in Children: A Brain Imaging Study*, presents a research project funded by the Health Effects Institute and conducted by Dr. Mònica Guxens of Barcelona Institute for Global Health (ISGlobal), Barcelona, Spain, and her colleagues. This research was funded under HEI's Walter A. Rosenblith New Investigator Award Program, which provides support to promising scientists in the early stages of their careers. The report contains three main sections.

The HEI Statement, prepared by staff at HEI, is a brief, nontechnical summary of the study and its findings; it also briefly describes the Review Committee's comments on the study.

The Investigators' Report, prepared by Guxens and colleagues, describes the scientific background, aims, methods, results, and conclusions of the study.

The Critique, prepared by members of the Review Committee with the assistance of HEI staff, places the study in a broader scientific context, points out its strengths and limitations, and discusses remaining uncertainties and implications of the study's findings for public health and future research.

This report has gone through HEI's rigorous review process. When an HEI-funded study is completed, the investigators submit a draft final report presenting the background and results of the study. This draft report is first examined by outside technical reviewers and a biostatistician. The report and the reviewers' comments are then evaluated by members of the Review Committee, an independent panel of distinguished scientists who are not involved in selecting or overseeing HEI studies. During the review process, the investigators have an opportunity to exchange comments with the Review Committee and, as necessary, to revise their report. The Critique reflects the information provided in the final version of the report.

CONTRIBUTORS

HEI RESEARCH COMMITTEE

David A. Savitz (Chair) *Professor of Epidemiology, School of Public Health, and Professor of Obstetrics and Gynecology, Alpert Medical School, Brown University*

Jeffrey R. Brook *Assistant Professor, Occupational & Environmental Health Division, Dalla Lana School of Public Health, University of Toronto, Canada*

Francesca Dominici *Professor of Biostatistics and Senior Associate Dean for Research, Harvard T.H. Chan School of Public Health*

Amy H. Herring *Sara & Charles Ayres Professor of Statistical Science and Global Health, Duke University*

Barbara Hoffmann *Professor of Environmental Epidemiology, Institute for Occupational, Social, and Environmental Medicine, University of Düsseldorf, Germany*

Neil Pearce *Professor of Epidemiology and Biostatistics, London School of Hygiene and Tropical Medicine, United Kingdom*

Allen L. Robinson *Raymond J. Lane Distinguished Professor and Head, Department of Mechanical Engineering, and Professor, Department of Engineering and Public Policy, Carnegie Mellon University*

Ivan Rusyn *Professor, Department of Veterinary Integrative Biosciences, Texas A&M University*

REVIEW COMMITTEE

Melissa Perry, Chair *Professor and Chair, Department of Environmental and Occupational Health, George Washington University Milken Institute School of Public Health*

Kiros Berhane *Professor and Chair, Department of Biostatistics, Mailman School of Public Health, Columbia University*

Michael Jerrett *Professor and Chair, Department of Environmental Health Sciences, Fielding School of Public Health, University of California- Los Angeles*

Frank Kelly *Henry Battcock Chair of Environment and Health and Director of the Environmental Research Group, Imperial College London School of Public Health*

Jana B. Milford *Professor, Department of Mechanical Engineering and Environmental Engineering Program, University of Colorado-Boulder*

Jennifer L. Peel *Professor of Epidemiology, Colorado School of Public Health and Department of Environmental and Radiological Health Sciences, Colorado State University*

Roger D. Peng *Professor of Biostatistics, Johns Hopkins Bloomberg School of Public Health*

AD HOC REVIEWERS

Dr. Bradley Peterson *Chief, Division of Child Psychiatry, University of Southern California, and Chief, Division of Child Psychiatry, Children's Hospital Los Angeles*

Dr. Megan Horton *Associate Professor, Environmental Medicine and Public Health, Icahn School of Medicine at Mount Sinai*

Dr. Eleanor Setton *Co-Director, Spatial Sciences Research Lab, University of Victoria–Geography, British Columbia, Canada*

HEI PROJECT STAFF

Hanna Boogaard *Consulting Principal Scientist*

Carol Moyer *Consulting Editor*

Kristin Eckles *Senior Editorial Manager*

Hope Green *Editorial Project Manager*

HEI STATEMENT

Synopsis of Research Report 209

Air Pollution and Brain Outcomes in Children

BACKGROUND

Although several epidemiological studies have assessed the association between air pollution exposure during early life and child neurological development, it is yet unclear whether brain structural alterations underlie the observed associations. Advances in neuroimaging that allow in vivo investigation of brain structure and function have emerged. Such studies provide additional information about the possible mechanisms and add biological plausibility to the nervous system outcomes reported in epidemiological studies. So far, only a few studies have used magnetic resonance imaging techniques to evaluate the effect of air pollution on the developing brain.

Dr. Mònica Guxens of ISGlobal, a recipient of HEI's 2016 Walter A. Rosenblith New Investigator Award, and colleagues have assessed the possible relationship of early life air pollution exposure with brain outcomes using neuroimaging data in children.

APPROACH

The study by Dr. Guxens assessed the possible relationship of air pollution exposure during pregnancy and childhood with brain outcomes in children. Brain structural and functional measures were studied in Generation R — an existing birth cohort in Rotterdam, the Netherlands. Mother–child pairs were recruited during pregnancy or at birth from 2002–2006 and followed up until 2015.

Dr. Guxens and colleagues used air pollution data and high-resolution neuroimaging data collected in about 800 school-age children and in about 3,100 pre-adolescents. About 400 children underwent imaging at two time points. To increase statistical power in the first round, a potential sampling bias was introduced by deliberately selecting more school children with child behavior problems and with mothers who reported certain exposures during pregnancy (e.g., exposure to drugs, nicotine, alcohol, and psychiatric medication).

Early life exposure was estimated at the residential address level for various air pollutants using existing land-use regression models, mainly from the European ESCAPE project. Those models were based on air pollution measurements between February 2009 and February 2010 at 40 to 80 sites spread across the Netherlands and Belgium. Guxens and colleagues applied single pollutant regression models to assess the association between early life air pollution exposure and brain structural and functional measures corrected for important potential confounders, such as maternal smoking, prepregnancy body mass index, and socioeconomic status. Because

What This Study Adds

- The goal of the study was to assess whether early life air pollution exposure affects brain outcomes using neuroimaging data from an existing birth cohort (Generation R) in Rotterdam, the Netherlands.
- The study focused on brain structural and functional measures in children.
- Strengths of the study were the availability of high-resolution neuroimaging data for a large subset of the cohort, the wealth of individual-level covariate data, and estimation of a large suite of air pollution exposure metrics.
- The study found some evidence of associations between early life air pollution exposure and various measures of brain structural morphology, structural connectivity, and functional connectivity in children. For example, exposure to air pollution during early life was associated with a thinner cortex in various regions of the brain in both school-age children and pre-adolescents. The clinical relevance of the findings remains unclear.
- The results add to the limited evidence of air pollution effects on the developing brain, with only a few MRI studies in children so far.

This Statement, prepared by the Health Effects Institute, summarizes a research project funded by HEI and conducted by Dr. Mònica Guxens at Barcelona Institute for Global Health, Barcelona, Spain, and colleagues. Research Report 209 contains both the detailed Investigators' Report and a Critique of the study prepared by the Institute's Review Committee.

the number of outcome measurements was very large, analyses of most brain outcomes were corrected for multiple comparisons. Additionally, they used multipollutant models using a deletion/substitution/addition approach.

MAIN RESULTS AND INTERPRETATION

In its independent review of the study, the HEI Review Committee thought the research was well motivated and addressed important and novel questions about the potential relationships between air pollution and the developing brain. This type of research is emerging but remains distinctive — with only a few MRI studies in children so far. The availability of high-resolution neuroimaging data for a large subset of the cohort — the largest sample to date — was unprecedented; the wealth of individual-level covariate data and the large suite of air pollution exposure metrics estimated were strengths of the study.

The study documented associations between early life air pollution exposure and various measures of brain structural morphology, structural connectivity, and functional connectivity in children. For example, exposure to air pollution during early life was associated with a thinner cortex in various regions of the brain in both school-age children and pre-adolescents. Moreover, in pre-adolescents, exposure to air pollution during early life was associated with differences in region-specific brain volumes, such as a smaller volume in the hippocampus and corpus callosum. In addition, associations were documented between exposure and white matter microstructure and higher brain functional connectivity among several brain regions. Although the Review Committee broadly agrees with the investigators' conclusions, it noted a few limitations that should be considered when interpreting the results.

The Committee had concerns about the exposure assessment because of the substantial temporal and spatial misalignment of the data. That issue is particularly important when studying the developing brain, which is exceptionally complex with potentially critical time windows of development. Furthermore, all brain outcomes, including brain volume outcomes, should have been corrected for multiple comparisons because of the large number of analyses. The Committee was not convinced that the multipollutant approach added much, because, for example, it remains unclear how stable the identified specific exposure associations in the multipollutant analyses really are. High correlations were noted among many pollutants in the analyses and between prenatal and childhood exposure. Thus, it was not possible to tease out independent pollutant associations and identify a susceptible exposure window during pregnancy and early childhood. Additionally, some study design features affected the generalizability of the findings.

CONCLUSIONS

Overall, the insights drawn from the current study, along with a few other brain imaging studies in children, are noteworthy and should provide impetus for further research. Because the brain has a dynamic structure that is constantly evolving throughout life, longitudinal studies beginning as early as possible are the best means to assess the effect of air pollution on the developmental trajectories of the brain outcomes included in the current cross-sectional analysis. Also, further analyses should be encouraged, for example, to investigate whether children with worse brain outcomes showed poorer cognitive function or other adverse neurological development outcomes. Those analyses would shed light on whether the brain outcome findings are clinically relevant, but this so far remains unclear.

INVESTIGATORS' REPORT

Associations of Air Pollution on the Brain in Children: A Brain Imaging Study

Mònica Guxens[1,2,3,4], Małgorzata J. Lubczyńska[1,2,3,4], Laura Pérez-Crespo[1,2,3], Ryan L. Muetzel[4], Hanan El Marroun[4,5,6], Xavier Basagaña[1,2,3], Gerard Hoek[7], Henning Tiemeier[4,8]

[1]Barcelona Institute for Global Health (ISGlobal), Barcelona, Spain; [2]Pompeu Fabra University, Barcelona, Spain; [3]Spanish Consortium for Research on Epidemiology and Public Health (CIBERESP), Institute of Health Carlos III, Madrid, Spain; [4]Department of Child and Adolescent Psychiatry, Erasmus MC, University Medical Centre, Rotterdam, the Netherlands; [5]Department of Psychology, Education and Child Studies, Erasmus School of Social and Behavioural Sciences, Erasmus University, Rotterdam, the Netherlands; [6]Department of Pediatrics, Erasmus MC, University Medical Centre, Rotterdam, the Netherlands; [7]Institute for Risk Assessment Sciences, Utrecht University, the Netherlands; [8]Department of Social and Behavioral Science, Harvard T.H. Chan School of Public Health, Boston, Massachusetts

ABSTRACT

Introduction Epidemiological studies are highlighting the negative effects of the exposure to air pollution on children's neurodevelopment. However, most studies assessed children's neurodevelopment using neuropsychological tests or questionnaires. Using magnetic resonance imaging (MRI*) to precisely measure global and region-specific brain development would provide details of brain morphology and connectivity. This would help us understand the observed cognitive and behavioral changes related to air pollution exposure. Moreover, most studies assessed only a few air pollutants. This project investigates whether air pollution exposure to many pollutants during pregnancy and childhood is associated with the morphology and connectivity of the brain in school-age children and pre-adolescents.

Methods We used data from the Generation R Study, a population-based birth cohort set up in Rotterdam, the Netherlands in 2002–2006 (n = 9,610). We used land-use regression (LUR) models to estimate the levels of 14 air pollutants at participant's homes during pregnancy and childhood: nitrogen oxides (NO_x), nitrogen dioxide (NO_2), particulate matter with aerodynamic diameter ≤10 µm (PM_{10}) or ≤2.5 µm ($PM_{2.5}$), PM between 10 µm and 2.5 µm (PM_{COARSE}), absorbance of the $PM_{2.5}$ fraction — a measure of soot ($PM_{2.5}$absorbance), the composition of $PM_{2.5}$ such as polycyclic aromatic hydrocarbons (PAHs), organic carbon (OC), copper (Cu), iron (Fe), silicon (Si), zinc (Zn), and the oxidative potential of $PM_{2.5}$ evaluated using two acellular methods: dithiothreitol (OP^{DTT}) and electron spin resonance (OP^{ESR}). We performed MRI measurements of structural morphology (i.e., brain volumes, cortical thickness, and cortical surface area) using T_1-weighted images in 6- to 10-year-old school-age children and 9- to 12-year-old pre-adolescents, structural connectivity (i.e., white matter microstructure) using diffusion tensor imaging (DTI) in pre-adolescents, and functional connectivity (i.e., connectivity score between brain areas) using resting-state functional MRI (rs-fMRI) in pre-adolescents. We assessed cognitive function using the Developmental Neuropsychological Assessment test (NEPSY-II) in school-age children. For each outcome, we ran regression analysis adjusted for several socioeconomic and lifestyle characteristics. We performed single-pollutant analyses followed by multipollutant analyses using the deletion/substitution/addition (DSA) approach.

Results The project has air pollution and brain MRI data for 783 school-age children and 3,857 pre-adolescents.

First, exposure to air pollution during pregnancy or childhood was not associated with global brain volumes (e.g., total brain, cortical gray matter, and cortical white matter) in school-age children or pre-adolescents. However, higher pregnancy or childhood exposure to several air pollutants was associated with a smaller corpus callosum and hippocampus, and a larger amygdala, nucleus accumbens, and cerebellum in pre-adolescents, but not in school-age children.

Second, higher exposure to several air pollutants during pregnancy was associated with a thinner cortex in various regions of the brain in both school-age children and pre-adolescents. Higher exposure to air pollution during childhood was also associated with a thinner cortex in a single region in pre-adolescents. A thinner cortex in two regions mediated the association between higher exposure to air pollution during pregnancy and an impaired inhibitory control in school-age children.

This Investigators' Report is one part of Health Effects Institute Research Report 209, which also includes a Critique by the Review Committee and an HEI Statement about the research project. Correspondence concerning the Investigators' Report may be addressed to Dr. Mònica Guxens, Barcelona Institute for Global Health (ISGlobal), Doctor Aiguader, 88, 08003 Barcelona, Spain; e-mail: monica.guxens@isglobal.org. No potential conflict of interest was reported by the authors.

Although this document was produced with partial funding by the United States Environmental Protection Agency under Assistance Award CR–83467701 to the Health Effects Institute, it has not been subjected to the Agency's peer and administrative review and therefore may not necessarily reflect the views of the Agency, and no official endorsement by it should be inferred. The contents of this document also have not been reviewed by private party institutions, including those that support the Health Effects Institute; therefore, it may not reflect the views or policies of these parties, and no endorsement by them should be inferred.

* A list of abbreviations and other terms appears at the end of this volume.

Third, higher exposure to air pollution during childhood was associated with smaller cortical surface areas in various regions of the brain except in a region where we observed a larger cortical surface area in pre-adolescents.

In relation to brain structural connectivity, higher exposure to air pollution during pregnancy and childhood was associated with an alteration in white matter microstructure in pre-adolescents.

In relation to brain functional connectivity, a higher exposure to air pollution, mainly during pregnancy and early childhood, was associated with a higher brain functional connectivity among several brain regions in pre-adolescents.

Overall, we identified several air pollutants associated with brain structural morphology, structural connectivity, and functional connectivity, such as NO_x, NO_2, PM of various size fractions (i.e., PM_{10}, PM_{COARSE}, and $PM_{2.5}$), $PM_{2.5}$absorbance, PAHs, OC, three elemental components of $PM_{2.5}$ (i.e., Cu, Si, Zn), and the oxidative potential of $PM_{2.5.}$

Conclusions The results of this project suggest that exposure to air pollution during pregnancy and childhood play an adverse role in brain development. We observed this relationship even at levels of exposure that were below the European Union legislations. We acknowledge that identifying the independent effects of specific pollutants was particularly challenging. Most of our conclusions generally refer to traffic-related air pollutants. However, we did identify pollutants specifically originating from brake linings, tire wear, and tailpipe emissions from diesel combustion. The current direction toward innovative solutions for cleaner energy vehicles is a step in the right direction. However, our findings indicate that these measures might not be completely adequate to mitigate health problems attributable to traffic-related air pollution, as we also observed associations with markers of brake linings and tire wear.

INTRODUCTION

More than half of the world's population now lives in cities, and this fraction is projected to increase (United Nations 2018). This makes the urban environment an important determinant of human health and wellbeing (McMichael 2000). Of particular interest is the exposure to air pollution. In the last decades, several regulatory policy measures have been implemented; however, air pollution still remains the biggest environmental health challenge (Cohen et al. 2017). It is the main environmental contributor to the global burden of disease and one of the top preventable causes of disease (Cohen et al. 2017). In 2017, 98% of the cities in low- and middle-income countries and 56% of the cities in high-income countries did not meet the air quality standards established by the World Health Organization (European Environment Agency 2019).

Children are among the most vulnerable groups. Brain structures are forming and growing during fetal development and childhood. Exposure to environmental factors, such as air pollution, may cause permanent damage (Rice and Barone Jr. 2000). Fine particles may deposit in the respiratory tracts of children and pregnant women; soluble components may translocate into the circulation and generate systemic inflammation (U.S. Environmental Protection Agency [U.S. EPA] 2019). In pregnant women, both systemic inflammation and the translocation of the air pollutants might directly affect fetal development by impairing placental function, decreasing transplacental oxygen and nutrient transport, and producing oxidative stress and epigenetic changes in the placenta (Carvalho et al. 2016; Hettfleisch et al. 2017; Saenen et al. 2019; van den Hooven et al. 2012). A recent study showed for the first time that air pollutants can reach the fetal side of the human placenta (Bové et al. 2019). The systemic inflammation and the air pollutants that translocated into the circulation might cross the blood–brain barrier and directly reach the fetal brain. Moreover, in children, fine particles may also deposit on the olfactory epithelium, and soluble components may be directly transported via the olfactory nerve to the olfactory bulb of the brain (U.S. EPA 2019). Air pollution can have a deleterious impact on the central nervous system through chronic neuroinflammation, oxidative stress, microglia activation, chronic activation of the hypothalamic–pituitary–adrenal axis, alterations in myelin sheaths, and neuronal damage (Block et al. 2012; Costa et al. 2017; Thomson 2019; U.S. EPA 2019).

Epidemiological studies are highlighting the negative effects of the exposure to air pollution on children's neurodevelopment (Costa et al. 2019; de Prado Bert et al. 2018; Donzelli et al. 2020; Herting et al. 2019; Pagalan et al. 2019; Suades-González et al. 2015; U.S. EPA 2019). However, most studies assessed children's neurodevelopment using neuropsychological tests or questionnaires. Using MRI to precisely measure global- and region-specific brain development would provide details of brain morphology and connectivity. This would help us understand the observed cognitive and behavioral changes related to air pollution exposure. In children, maturation of the white and gray matter is essential to properly develop cognitive function (Yurgelun-Todd 2007) and underlies the initiation of many psychiatric disorders (Paus et al. 2008). Brain development shows complex patterns of change over the lifespan (Lenroot and Giedd 2006). Interestingly, white and gray matter develop in different ways. The volume and maturation of white matter increase throughout childhood and adolescence, axons and synapses are overproduced during puberty, and extensive pruning of synaptic connectivity in several brain regions is completed in later adolescence (Fuhrmann et al. 2015; Lenroot and Giedd 2006; Paus 2005). In contrast, the volume of gray matter increases from infancy through childhood and then declines throughout adolescence (Fuhrmann et al. 2015; Lenroot and Giedd 2006; Paus 2005).

Recently, animal and human studies investigated the relationship of exposure to air pollution with brain morphology and connectivity. Exposure to air pollution has been related to an alteration of several brain structures at different ages, such as cortical gray matter, cortical white matter, thalamus, caudate, putamen, pallidum, hippocampus, amygdala, corpus callosum, and cerebellum (Allen et al. 2017; Beckwith et al. 2020; Brown et al. 2020; Calderón-Garcidueñas et al. 2008; Casanova et al. 2016; Chen et al. 2017; Cserbik et al. 2020; Erickson et al. 2020; Gale et al. 2020; Hedges et al. 2019; Long et al. 2014; Mortamais et al. 2017, 2019; Peterson et al. 2015; Power et al. 2018; Pujol et al. 2016b; Wilker et al. 2015). Also, in children, it was suggested that exposure to air pollution was associated with brain structural and functional connectivity (Pujol et al. 2016a,b).

However, many unanswered questions remain on the effect of air pollution on children's neurodevelopment. There are still too few studies, most of them with a small sample size, to draw conclusions. Most of these studies analyzed only few pollutants without examining their composition or trying to identify the independent effects of specific pollutants. This knowledge gap impedes identifying the most toxic components and understanding simultaneous exposures. Also, the association between exposure to air pollution and compromised neurodevelopment might be present during both pregnancy and childhood, but previous studies looked at either one period or the other. In this project, we aim to confront these knowledge gaps and to expand the current body of evidence on the effect of air pollution on children's neurodevelopment.

SPECIFIC AIMS

The overarching aim of the project was to investigate whether exposure to air pollution during pregnancy and childhood is associated with the morphology and connectivity of the brain in childhood. To do so, we pursued the following specific aims:

Aim 1 To assess the relationship of exposure to air pollution during pregnancy and childhood with brain structural morphology in 6- to 10-year-old school-age children and 9- to 12-year-old pre-adolescents. Specifically:

- the relationship of exposure to air pollution during pregnancy with brain volumes in school-age children and pre-adolescents,
- the relationship of exposure to air pollution during pregnancy and childhood with brain cortical thickness and cortical surface area in school-age children and pre-adolescents, and
- the mediation role of brain cortical thickness on the association of exposure to air pollution during pregnancy with cognitive function in school-age children.

We hypothesized that exposure to air pollution during pregnancy and childhood was associated with reduced volumes of the global brain and of specific areas, such as the cortical and subcortical gray matter, the total white matter, the corpus callosum, the cerebellum, the thalamus, the pallidum, and the hippocampus. Also, we expected to observe a larger volume for the caudate nucleus, the putamen, the amygdala, and the nucleus accumbens.

We postulated that exposure to air pollution during pregnancy and childhood was associated with lesser cortical thickness and smaller cortical surface area.

We posited that brain cortical thickness mediates the association of exposure to air pollution during pregnancy and impaired cognitive function.

Aim 2 To assess the relationship of exposure to air pollution during pregnancy and childhood with brain structural connectivity in 9- to 12-year-old pre-adolescents.

We hypothesized that exposure to air pollution during pregnancy and childhood was associated with lower fractional anisotropy (FA) and higher mean diffusivity (MD).

Aim 3 To assess the relationship between exposure to air pollution during pregnancy and childhood and brain functional connectivity in 9- to 12-year-old pre-adolescents.

We hypothesized that exposure to air pollution during pregnancy and childhood was associated with altered brain functional connectivity, but we did not have an a priori hypothesis on the direction of the association.

METHODS AND STUDY DESIGN

HUMAN STUDY APPROVAL

The Medical Ethics Committee of the Erasmus Medical Centre in Rotterdam, the Netherlands, granted ethical approval for the Generation R study (no. MEC 198.782/2001/31), which includes the studies described in this report. Mothers provided written informed consent for themselves and their children.

STUDY DESIGN AND POPULATION

We used data from the Generation R Study, a population-based birth cohort from pregnancy onward, set up in the urban area of Rotterdam, the Netherlands (Kooijman et al. 2016). A total of 8,879 women were enrolled during pregnancy, and 899 women were recruited shortly after the delivery. Children were born between April 2002 and January 2006. We included only singleton pregnancies for this research, resulting in 9,610 mother–child pairs. Children were examined at several time points after birth. We gathered data for the Generation R brain MRI substudy. A brain MRI protocol was developed that included brain morphology, DTI, and rs-fMRI.

A select group of children enrolled in the Generation R study, who were between the ages of 6 and 10 years, was recruited for the *first wave* of the brain MRI substudy (White et al. 2013). The whole cohort of children between the ages of 9 and 12 years was recruited for the *second wave* of the brain MRI substudy (White et al. 2018). Due to the logistics of the visits, there was some overlap on the age of the participants between waves.

The first wave included 1,932 children. This was an oversample based on certain maternal exposures during pregnancy, such as cannabis, nicotine, selective serotonin reuptake inhibitors, depressive symptoms, plasma folate levels, and child behavior problems, such as attention deficit hyperactivity disorder, pervasive developmental problems, dysregulation problems, and aggressive problems. Exclusion criteria comprised contradictions for the MRI procedure, severe motor or sensory disorders, neurological disorders, head injuries with loss of consciousness, and claustrophobia. Of the 1,932 children, the invitation call was not answered for 155, participation was refused for 447, and 5 could not participate due to contraindications for the MRI procedure. Of the 1,325 that attended the MRI visit, we excluded twins and children with poor brain MRI data quality and major abnormalities. We had brain MRI measurements available for 1,070 children. Finally, after excluding those without air pollution estimations, we included 783 children in the project.

In the second wave, the brain MRI measurements were offered to all children still involved in the Generation R study who were 9 to 12 years old (n = 8,548) (White et al. 2018). The invitation call was not answered for 911; participation was refused for 244; 1,531 did not visit the research center; and 1,875 did not undergo the MRI procedure. We excluded twins and children with poor brain MRI data quality and major abnormalities. We had brain MRI measurements available for 3,888 children. Finally, after excluding those without air pollution estimations, we included 3,857 children in the project. We obtained brain structural morphology data for 3,133 of them, structural connectivity data for 2,954, and functional connectivity data for 2,197. The reduction in the number of children for which data of each imaging modality were available was due to attrition along the MRI session.

For 387 children, we had information on air pollution and brain imaging data from both waves. However, we did not combine that information because of the small sample size and because the scanners differed between waves.

AIR POLLUTION ASSESSMENT

We used LUR models to estimate the levels of air pollution at all reported home addresses of each participant during the pregnancy and childhood following a standardized procedure in the context of the ESCAPE (European Study of Cohorts for Air Pollution Effects) and the TRANSPHORM (Transport related Air Pollution and Health impacts — Integrated Methodologies for Assessing Particulate Matter) projects (Beelen et al. 2013; Brunekreef 2008; de Hoogh et al. 2013; Eeftens et al. 2012a; Jedynska et al. 2014b; Yang et al. 2015). We performed 2-week measurements of NO_x and NO_2 in three different seasons (i.e., warm, cold, and intermediate). We performed these measurements between February 2009 and February 2010 at 80 sites spread across the Netherlands and Belgium (Appendix Figure A1; see Additional Materials on the HEI website) (Cyrys et al. 2012). Additionally, at 40 of those sites, we carried out measurements of PM_{10} and $PM_{2.5}$ (Eeftens et al. 2012b). We calculated PM mass between 10 and 2.5 µm (PM_{COARSE}) by subtracting $PM_{2.5}$ from PM_{10}. We measured different parameters in the $PM_{2.5}$ filters: $PM_{2.5}$absorbance, the composition of $PM_{2.5}$ including PAHs, OC, Cu, Fe, Si, and Zn, and the oxidative potential of $PM_{2.5}$ (de Hoogh et al. 2013; Jedynska et al. 2014a; Yang et al. 2015). $PM_{2.5}$absorbance is a measure of the reflectance of the $PM_{2.5}$ filter, and it is highly correlated with elemental or black carbon, also referred to as soot (Cyrys et al. 2003). The oxidative potential of $PM_{2.5}$ is a quantification of the potentiality of fine particles to induce oxidative stress (Yang et al. 2015). We evaluated oxidative potential using two acellular methods: OP^{DTT} and OP^{ESR} (Yang et al. 2015).

Measurement sites were selected to represent the anticipated spatial variation of air pollution at the home addresses of subjects in the epidemiological studies set up in the study area. Measurement sites reflected a large diversity of potential sources of air pollution (e.g., population density, traffic intensity, industry, proximity to ports, etc.), selecting regional background, urban background, and street sites. Regional background sites were located outside major urban areas and were not directly influenced by traffic sources. Urban background sites were located inside an urban area, but at least 50 meters from major roads. Street sites were selected at building facades representative for homes, in streets with traffic intensities of 10,000 or more vehicles per day. Street sites were overrepresented compared with the fraction of addresses on major roads, as the goal was to describe spatial variation in the area of which traffic is a main source. Measurements were performed simultaneously in 20 NO_x–NO_2 sites and in 10 NO_x–NO_2–PM sites. Thus, we performed four rounds of 2-week measurements to complete a measurement period for one season (i.e., to complete the measurements in 80 sites for NO_x–NO_2 and 40 sites for PM). Each round included different types of sites, for example, regional, urban background, and traffic sites. To adjust for the temporal variability of concentrations, a centrally located reference site was chosen at a regional background location that was not directly influenced by local sources, and measurements were taken over the entire year. For each round, we applied a temporal correction in two steps: (1) calculating the difference between the concentration for a 2-week specific sampling period and the annual average of the continuous-reference site, and (2) subtracting that difference from each measurement (Beelen et

al. 2013; Brunekreef 2010; de Hoogh et al. 2013; Eeftens et al. 2012a; Jedynska et al. 2014b; Yang et al. 2015). Next, for each pollutant, we averaged the concentrations of the three 2-week corrected measurements resulting in one annual mean concentration.

We assigned to each monitoring site a variety of potential land-use predictors, such as proximity to the nearest road, traffic intensity on the nearest road, and population density. Then, we applied LUR models by using linear regression models to determine which combination of predictors best explained the annual average concentration of each pollutant (Appendix Table A1). The cross-validation R^2 of the LUR model varied between pollutants and ranged between 0.31 for PAHs and 0.89 for $PM_{2.5}$absorbance (Appendix Table A2). We then applied LUR models to each geocoded address where participants lived during the period of interest (i.e., since conception until date of the MRI assessments) to estimate the exposure of each air pollutant at each address (Figures 1 and 2 and Appendix Figure A2). Addresses were geocoded using the cadaster of all buildings of the Netherlands. For the participants who were recruited shortly after birth, we used their birth address for the pregnancy period. We considered the number of days that the participant spent at each address and weighted the pollution exposures accordingly. Then, we calculated the mean exposure of each pollutant for each participant for several time periods: (1) for the entire pregnancy period, (2) from birth until 2 years of age, (3) from 2 until 5 years of age, (4) from 5 until 9 years of age, and (5) for the entire childhood period (i.e., from birth until the date of the second-wave MRI assessment).

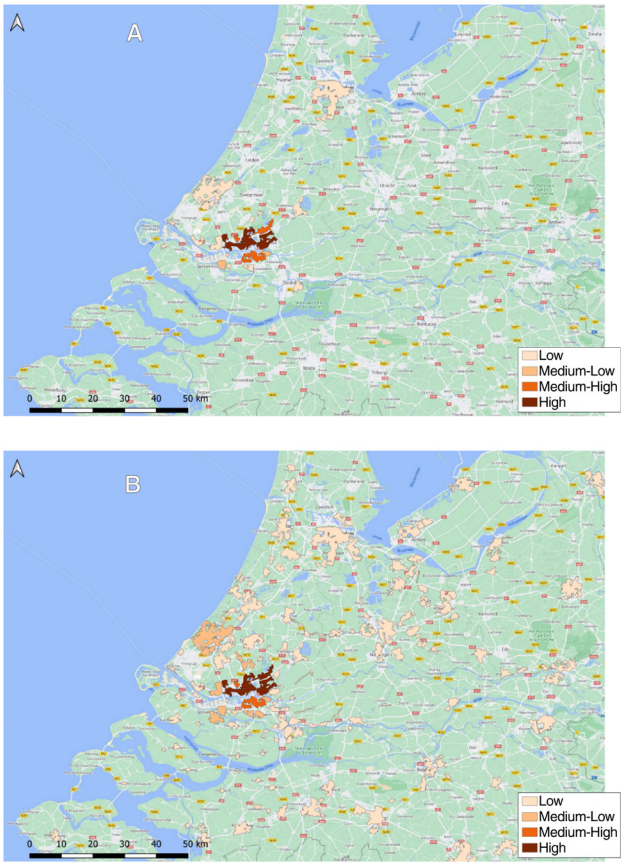

Figure 1. Spatial distribution of density of addresses per municipality across the study area: (A) At recruitment; and (B) At the MRI assessment at 9–12 years. To ensure anonymization, a municipality was not depicted if too few participants lived there (i.e., addresses at the MRI assessment at 9–12 years were also distributed in several other municipalities across the whole study area).

No historical data were available for most of the pollutants. Therefore, we could not perform back and forward extrapolation of the concentrations to match the exact periods of interest. For most analyses, we assumed that the spatial contrast remained constant over time. This assumption was previously demonstrated in the Netherlands for a period up to 8 years (1999–2007) (Eeftens et al. 2011), and in Great Britain for a period up to 18 years (1991–2009) (Gulliver et al. 2013). Exceptionally, in a couple of analyses, we could perform back and forward extrapolation of the concentrations for some pollutants that had historical data available (i.e., NO_x, NO_2, PM_{10}, PM_{COARSE}, $PM_{2.5}$, and $PM_{2.5}$absorbance). To do this, we used daily data from the seven continuous-reference monitoring sites (Brunekreef 2012). We combined the estimated yearly air pollution concentration at each home address *i* (*Cyearly*, *i*) with time-specific measurements from the seven continuous -reference monitoring sites. This was done by averaging the daily concentrations during different periods: (1) the year corresponding to the LUR yearly concentration (*Cyearly*), and (2) each time period *ti* considered (*Cti*). The ratio *Cti*/*Cyearly* constituted the temporal component of the model. For each pollutant, the concentration estimated at the home address *i* (*Cti*, *i*) during each time period was estimated as the product of the temporal (*Cti*/*Cyearly*) and spatial (*Cyearly*, *i*) components. When data from the continuous-reference monitoring sites were unavailable for a given pollutant, we used measurements for another one during the same time period as a replacement. We based the choice of the pollutant used to back and forward extrapolate another one on an extensive study of temporal correlations between pollutants that were simultaneously available. Specifically, we used NO_x when $PM_{2.5}$absorbance was missing and PM_{10} when $PM_{2.5}$ was missing.

BRAIN MRI

In both waves, we wanted participants to be familiarized with the magnetic resonance environment to reduce the possibility of not being able to complete the scanning session. Therefore, each child underwent a half-hour mock scanning session prior to the actual MRI (White et al. 2013, 2018). To limit the movement of the head, we accommodated children by: (1) providing them with a thorough explanation before the scanning session, (2) offering to let them watch a movie or listen to music during the session, and (3) placing cushions around the head to fix it in a comfortable way.

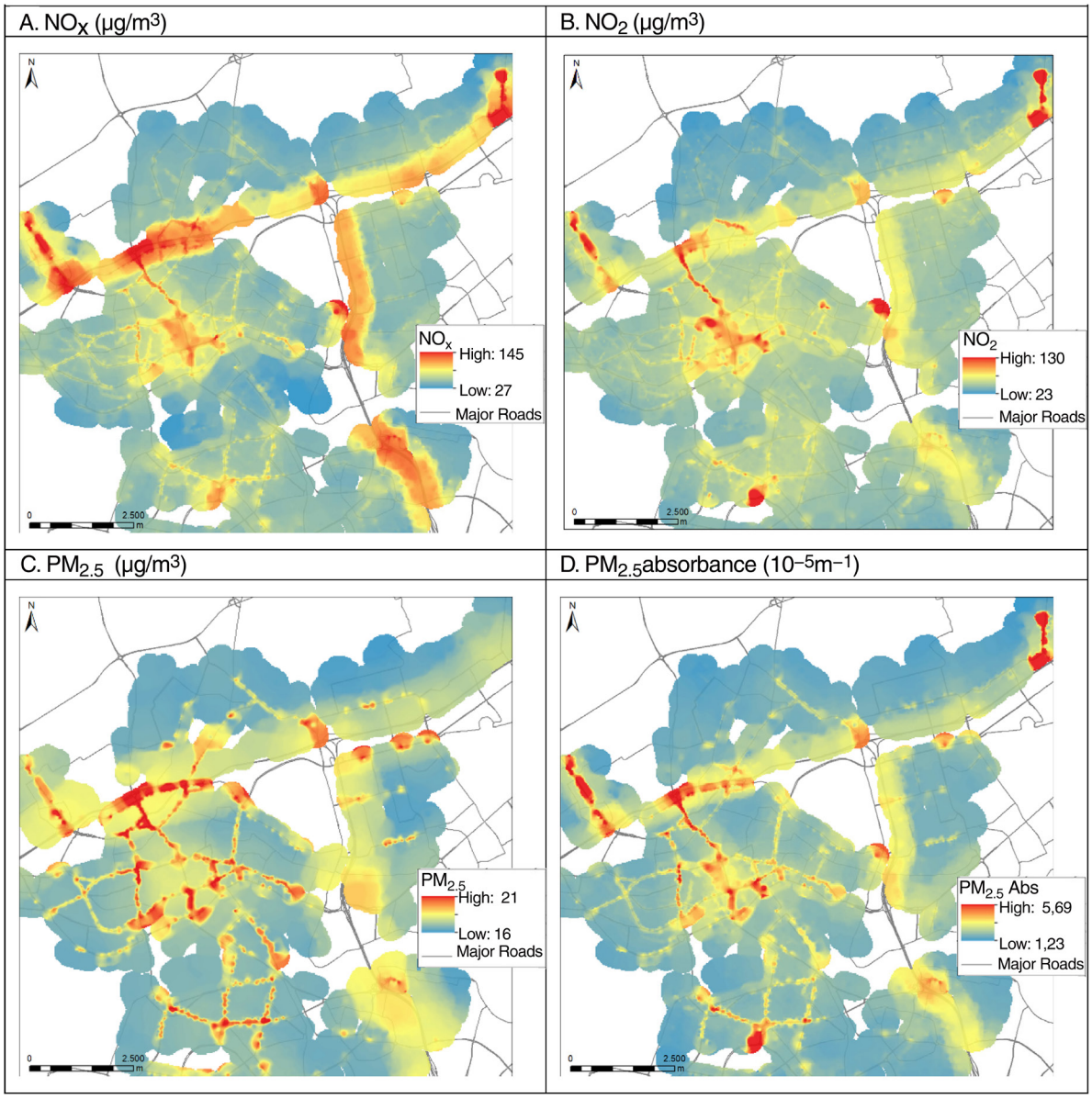

Figure 2. Air pollutant concentrations in Rotterdam where most of the participants lived: (A) NO_x; (B) NO_2; (C) $PM_{2.5}$; and (D) $PM_{2.5}$absorbance.

The brain MRI protocol involved different measurements, such as structural morphology (i.e., brain volumes, cortical thickness, and cortical surface area) using T_1-weighted images, structural connectivity (i.e., white matter microstructure) using DTI, and functional connectivity (i.e., connectivity score between brain areas) using rs-fMRI. In both waves, we used a scanner specifically dedicated for the study. In the first wave, we used a 3 Tesla General Electric scanner (Discovery 750; GE Worldwide, Milwaukee, WI); in the second wave, we used a different 3 Tesla General Electric scanner (Discovery MR750W; GE Worldwide, Milwaukee, WI). Both scanners had an 8-channel head coil. At each wave, the entire session took about 26 minutes. The refined protocol minimized the burden on the participant while allowing for high-quality data collection.

Brain Structural Morphology

In the first wave, we obtained high-resolution T1-weighted images of the whole brain by using the following sequence parameters: repetition time = 10.3 msec, echo time = 4.2 msec, inversion time = 350 msec, flip angle = 16°, in-plane resolution = 0.9 × 0.9 mm, number of slices = 186, and slice thickness = 0.9 mm. In the second wave, we used instead the following sequence parameters: repetition time = 8.77 msec,

echo time = 3.4 msec, inversion time = 600 msec, flip angle = 10°, in-plane resolution = 1 × 1 mm, number of slices = 230, and slice thickness = 1.0 mm (White et al. 2013, 2018).

We then performed cortical reconstruction and volumetric segmentation with FreeSurfer Image Analysis Suite 6.0 (Fischl 2012; Muetzel et al. 2019). We performed automatic parcellation and segmentations protocols using the recon-all stream with preprocessing steps that included the removal of nonbrain tissue, and the normalization of the B1 field in homogeneities. We calculated global brain volumes such as total brain volume, cortical and subcortical gray matter volumes, total white matter volume, corpus callosum volume, and cerebellum volume. We then calculated subcortical brain volumes including the thalamus, caudate nucleus, putamen, pallidum, hippocampus, amygdala, and nucleus accumbens. In the case of bilateral structures, we summed the volumes of the left and right hemispheres. In addition, surface-based morphometric data represented the cortical thickness and cortical surface area at each of the 163,842 vertices per hemisphere. We computed cortical thickness as the shortest distance between white matter and pial surface. We obtained cortical surface area by calculating the average area of the triangles touching the specific vertex. We labeled each vertex in accordance with the Desikan-Killiany atlas (Desikan et al. 2006). For all participants, we coregistered the surface-based maps to a standard stereotaxic space and consequently smoothed with a 10-mm, full-width half-maximum Gaussian (Rosseel 2012) kernel. For every image, we analyzed the accuracy in surface reconstruction through automated and manual methods (Muetzel et al. 2019).

Brain Structural Connectivity

We obtained DTI data with an axial spin echo with 35 noncollinear diffusion direction echo planar imaging sequence by using the following sequence parameters: repetition time = 12.500 msec, echo time = 72 msec, field of view = 240 × 240 mm, acquisition matrix = 120 × 120, acceleration factor = 2, number of slices = 65, slice thickness = 2 mm, and b = 0 and 900 sec/mm^2 (White et al. 2018). The b = 0 sec/mm^2 was acquired 3 times. We preprocessed the data with the FMRIB Software Library, version 5.0.9 (Jenkinson et al. 2012). First, we modified the images to exclude nonbrain tissue. Then we rectified them for artifacts induced by eddy currents, and for translations or rotations that potentially arose from minor movements of the head during the scanning session. The B-table was then rotated considering the rotations calculated and applied to the diffusion data during the eddy current correction step. Next, we fitted a diffusion tensor at each voxel using the RESTORE method from the Camino diffusion MRI toolkit (Cook et al. 2006). Finally, we computed common parameters describing white matter microstructure (i.e., FA and MD). We identified 12 major white matter tracts (i.e., forceps major, forceps minor, and bilateral cingulum bundles, corticospinal tracts, inferior longitudinal fasciculi, superior longitudinal fasciculi, and uncinate fasciculi) via probabilistic tractography with the FMRIB Software Library plugin AutoPtx (de Groot et al. 2015; Muetzel et al. 2018). We then computed the average values per tract of FA and MD, weighted by connectivity distribution. We performed a confirmatory factor analysis with the Lavaan R package (Rosseel 2012) to model a single latent FA and MD measure across the 12 tracts. This represented global FA and MD across the brain (Muetzel et al. 2015). FA indicates the tendency for preferential water diffusion in white matter tracts. It is lower in white matter tracts where axons are less densely packed, and the directionality of the water diffusion is not uniform compared to well-organized tracts. MD describes the magnitude of average water diffusion in all directions within brain tissue, with higher values generally observed in white matter tracts showing a less organized structure.

Brain Functional Connectivity

During the rs-fMRI scan, we instructed children to stay awake with their eyes closed (White et al. 2018). The rs-fMRI technique relies on a phenomenon called intrinsic brain activity (i.e., activity that is not induced by an external stimulus). We used an echo planar imaging sequence sensitive to the blood oxygen level dependent signal with the following parameters: repetition time = 2,000 msec, echo time = 30 msec, flip angle = 85°, number of slices = 37, slice thickness = 4 mm, in-plane resolution = 3.6 × 3.6 mm, and number of volumes = 200. The sequence had a duration of 6 minutes and 2 seconds. This time was long enough to produce stable resting-state networks (White et al. 2014). We processed the data with the standardized fMRIPrep software (Esteban et al. 2019). Then we applied despiking, regressing out of the data the cerebrospinal fluid and white matter signal and the motion parameters (and their temporal derivatives) (Satterthwaite et al. 2013). We included volumes tagged as outliers in subsequent pair-wise correlation estimations (Power et al. 2012). Subsequently, we applied the Human Connectome Project multimodal parcellation to the data for functional connectivity analysis in CIFTI grayordinate space (Glasser et al. 2016). Finally, we computed pair-wise correlation coefficients among the 382 brain areas in the parcellation, excluding two areas for which we lacked data from a high number of children (58.2% and 80.6%). Therefore, the pair-wise correlation coefficients resulted in 72,200 connectivity scores indicating strength and direction of the functional connectivity among the different brain areas. We grouped the brain areas into 31 regions based on location and common properties (e.g., architecture, task-fMRI profiles, or functional connectivity) (Glasse et al. 2016).

COGNITIVE FUNCTION

We assessed the cognitive function of children on the day of the scanning, or shortly after, by using an array of tasks from the Dutch version of the NEPSY-II (Brooks et al. 2010). The tasks were chosen to tap into specific domains, such as: attention

and executive functioning, language, memory and learning, sensorimotor function, and visuospatial processing (White et al. 2013). We individually tested the children in a quiet room by trained investigators. As described in the section *Statistical Methods and Data Analysis*, for the post hoc mediation analysis we selected two specific domains: the attention and executive functioning and the memory and learning domains.

Attention and Executive Functioning Domain

We assessed the attention and executive function of children with two tasks: auditory attention and response set tasks (Brooks et al. 2010; Mous et al. 2017; White et al. 2013). The auditory attention is designed to assess selective auditory attention and the ability to sustain it (vigilance) and it was administered first. Selective attention is the ability to focus on a specific activity while suppressing irrelevant stimuli; sustained attention is the ability to attend to an activity for a long period of time. Children were presented with the recording of a long list of words either referring to colors or other things. Then, they were asked to respond to the word "red" by touching the red circle on the sheet that also contained blue, black, and yellow circles. Touching the red circle within two seconds indicated a correct response.

Afterward, we administered the response set task. This serves to assess response inhibition and working memory. Inhibition is the ability to suppress automatic behavior; whereas working memory is the ability to actively keep information in mind as long as it is needed to complete an activity. Children must respond to the words "red," "yellow," and "blue" by touching the red, the yellow, and the blue circles, respectively. All the other colors or words should be ignored. Touching the correct circle within two seconds indicates a correct response. Touching another color or having a delayed response are incorrect responses.

For each task, we calculated four scores corresponding to the number of correct responses, commission errors (i.e., erroneous answers to a nontarget), omission errors (i.e., failure to respond to a target), and inhibition errors (i.e., inappropriate responses to a color word, indicating failure in inhibiting inappropriate responses).

Memory and Learning Domain

We assessed children's memory and learning with two tasks: memory for faces and memory for faces delayed (Brooks et al. 2010; Mous et al. 2017; White et al. 2013). These are designed to assess encoding of facial features, as well as face discrimination and recognition. The first one serves to assess immediate recall, which is the skill to retrieve information from memory shortly after learning. Children were first presented with multiple series of three faces and asked to look closely at each face for five seconds. They were then immediately provided with another set of three faces and asked which one they had seen before.

The memory for faces delayed task is designed to assess long-term memory for faces. It uses the same process as the previous task, but with a delay of 15 to 25 minutes between the two series of faces. This determines the child's ability to retrieve information after a longer period of time. All presented faces showed a neutral expression.

We calculated a total correct score for each task.

POTENTIAL CONFOUNDING VARIABLES

For each analysis, we defined a priori potential confounding variables, using a direct acyclic graph (e.g., Hernán et al. 2002, Figure A2). We used questionnaires to collect parental characteristics during pregnancy. These characteristics included parental educational levels (primary education or lower, secondary education, higher education), monthly household income (<900€, 900–1,600€, 1,600–2,200€, >2,200€), parental ethnicity (Dutch, other Western, non-Western), parental ages (in years), maternal psychological distress using the Brief Symptom Inventory (De Beurs 2004), maternal smoking use during pregnancy (never, smoking use until pregnancy known, continued smoking use during pregnancy), maternal alcohol use during pregnancy (never, alcohol use until pregnancy known, continued alcohol use during pregnancy), maternal parity (0, ≥1), and family status (married, living together, no partner). Parental weights (kg) and heights (cm) were self-reported or measured in the research center at the first trimester of pregnancy. We then calculated prepregnancy body mass index (kg/m^2). We obtained data about the child's sex (boy, girl) and date of birth from hospital or national registries. We estimated the child's genetics ancestry on the basis of data on genome-wide single nucleotide polymorphism from whole blood at birth, including four principal components of ancestry to better correct for population stratification (Neumann et al. 2017; Price et al. 2006). We finally assessed the maternal intelligence quotient when the child was six years old using the Ravens Advanced Progressive Matrices Test, set I (Prieler 2003). We also annotated the child's age at scanning.

STATISTICAL METHODS AND DATA ANALYSIS

MISSING DATA

For each analysis, we applied multiple imputation using chained equations to impute the missing values of all potential confounding variables among all participants with available data on the exposure and the outcome (Spratt et al. 2010; Sterne et al. 2009). We obtained 25 complete datasets that were analyzed following the standard procedure for multiple imputation. The percentage of missing values of the imputed potential confounding variables was below 30% except for paternal ethnicity, paternal education level, paternal psychological distress, and child genetics ancestry, which had 30%, 38%, 41%, and 36% of missing values, respectively.

The distribution of the imputed values looked plausible and was similar to the distribution of the observed values (data not shown).

NONRESPONSE ANALYSIS

Compared with the study population initially recruited (9,610 children), children who were included in the current analyses were more likely to have parents with a higher education level and a higher household income, from Dutch ethnicity, younger, with lower body mass index, higher height, and lower psychological distress, as well as more likely to have mothers with a partner, nulliparous, who did not smoke during pregnancy, and with higher IQ (data not shown). Selection bias potentially arises when the study includes only the population with available data on exposure and outcome instead of the full initial cohort recruited at pregnancy. To correct such bias, we used inverse probability weighting in each analysis (Weisskopf et al. 2015; Weuve et al. 2012). First, we imputed the missing covariates to all eligible participants recruited at pregnancy. Then, we used all the available information to predict the probability to participate in each analysis. Finally, we used the inverse of those probabilities as weights in the analyses. This way, the results would be representative for the initial population of the cohort.

EXPOSURE–OUTCOME ASSOCIATIONS

Air Pollution Exposure and Brain Structural Morphology

Exposure during pregnancy and childhood — brain volumes in school-age children and pre-adolescents First, we used linear regression models to study the association of the exposure to each air pollutant (i.e., NO_2, PM_{COARSE}, $PM_{2.5}$, and $PM_{2.5}$absorbance temporally adjusted) during pregnancy with each brain volume in school-age children (Table 1).

Second, we again used linear regression models to study the association of the exposure to each air pollutant (i.e., NO_x, NO_2, PM_{10}, PM_{COARSE}, $PM_{2.5}$, $PM_{2.5}$absorbance, PAHs, OC, Cu, Fe, Si, Zn, OP^{DTT}, OP^{ESR} — not temporally adjusted) during pregnancy and childhood separately, with each brain volume in pre-adolescents. All models were adjusted for all potential confounding variables described in the corresponding section. Additionally, corpus callosum volume, cerebellum volume, and subcortical brain volumes were adjusted for intracranial volume to ascertain relativity to the head size. Total brain volume, cortical gray matter volume, and total white matter volume were not adjusted for intracranial volume because of their high correlations (>0.80) with intracranial volume. The assumptions of the linear regression modeling were fulfilled (i.e., normality and homoscedasticity of residuals, linearity between exposure and outcome, and no multicollinearity). We took a hypothesis-based approach, selecting all the brain structures that had previously been associated with exposure to air pollution; thus, we did not correct for multiple testing.

Third, we performed multipollutant analyses using the DSA approach of Sinisi and van der Laan (2004) on each brain volume in pre-adolescents. This algorithm has shown a relatively good compromise between sensitivity and false discovery proportion, in comparison with other similar methods, providing better results than some multiple-testing corrections (Agier et al. 2016). It is an iterative selection method that selects the variables that better predict the outcome by cross-validation. At each iteration, the algorithm allows one to perform three steps: (1) delete a variable, (2) substitute one variable with another one, and (3) add a variable to the pending model. The optimal model represents a combination of variables with the smallest value of root mean square deviation. The exploration of such a model begins with the intercept model and continues with the deletion, substitution, and addition processes, to identify the optimal combination of variables. As the algorithm is based on a cross-validation process, which is subject to random variations, we ran each model 200 times. We then selected the final model using the variables that had been selected in at least 10% of the runs. To ensure the adjustment for all potential confounding variables, these were forced into the model, allowing only the exposures to air pollution to be involved in the selection process. Since PM_{10} showed a correlation of more than 0.90 with $PM_{2.5}$absorbance and $PM_{2.5}$absorbance showed a better LUR performance based on the R^2 of the model, we excluded PM_{10} from the multipollutant analyses. We performed two multipollutant analyses for each brain volume, including all air pollutants either during pregnancy or during childhood. When more than one pollutant was identified in one of these two time periods, we ran a linear regression model mutually adjusting for them.

Fourth, when pollutants were associated with a brain volume in both the pregnancy and the childhood periods, we ran a linear regression model of that brain volume mutually adjusting for those pollutants.

Finally, as a post hoc analysis, we used generalized additive models to assess the relationship between the age at the MRI scanning session and the brain volumes associated with air pollution.

Exposure during pregnancy and childhood — cortical thickness and surface area in school-age children and pre-adolescents First, we used a whole-brain, vertex-wise approach to study the association of the exposure to each air pollutant during pregnancy (i.e., NO_2, PM_{COARSE}, $PM_{2.5}$, and $PM_{2.5}$absorbance — temporally adjusted) with cortical thickness in school-age children (Table 1). We used the FreeSurfer QDEC (Query, Design, Estimate, Contrast) module adjusting for a child's sex and age at scanning. As there are many vertices per hemisphere (~160,000), we corrected the analyses for multiple testing using the built-in Monte Carlo null-Z simulations with 10,000 iterations ($P < 0.01$). There were some limitations in the modeling strategy with the FreeSurfer QDEC module (types of variables, number of

confounding variables, and inability to impute missingness in the latter). Therefore, we imported participant-level data from the regions associated with each air pollutant into Stata version 14 (StataCorp, College Station, TX) for the subsequent analysis. We then used linear regression models to study the association of the exposure to each air pollutant during pregnancy with the cortical thickness of each region. We adjusted all models for all potential confounding variables described in the corresponding section.

Second, we used a whole-brain, vertex-wise approach to study the association of the exposure to each air pollutant (i.e., NO_x, NO_2, PM_{10}, PM_{COARSE}, $PM_{2.5}$, $PM_{2.5}$absorbance, PAHs, OC, Cu, Fe, Si, Zn, OP^{DTT}, OP^{ESR} — not temporally adjusted), during pregnancy and childhood separately, with cortical thickness and cortical surface area in pre-adolescents. We used a QDEC module developed into an in-house R package (*https://github.com/slamballais/QDECR*), so all models were directly adjusted for all potential confounding variables described in the corresponding section. As there are many vertices per hemisphere (~160,000), we corrected the analyses for multiple testing using the built-in Monte Carlo null-Z simulations with 10,000 iterations ($P < 0.001$).

Exposure during pregnancy — cortical thickness and cognitive function in school-age children In school-age children, we identified some brain regions with lesser cortical thickness that were related to exposure to air pollution during pregnancy. On this basis, we selected two specific domains of the NEPSY-II test, the attention and executive functioning and the memory and learning domains. These domains contained tasks that assessed the cognitive processes involved with each region, based on the literature. Specifically, the frontal brain regions and the (pre)cuneus are involved in attention and executive functions (Cavanna and Trimble 2006; Chayer and Freedman 2001), whereas the fusiform gyrus is involved in the face perception, object recognition, and memory (Weiner and Zilles 2016). We assessed whether both exposure to air pollution and the cortical thinness of these regions were associated with the selected cognitive function tasks. For the outcomes of the attention and executive functioning tasks (i.e., total number of correct responses, total number of commission errors, total number of omission errors, total number of inhibition errors) we used adjusted negative binomial models. Instead, for the outcomes of the memory for faces tasks (i.e., memory for faces total score, memory for faces delayed total score) we used linear regression models. We then applied mediation analysis to estimate the natural direct effect (NDE), the natural indirect effect (NIE), and the total effect (Valeri and Vanderweele 2013). We assessed the direct and indirect effects of exposure to air pollution during pregnancy on cognitive function. We tested whether part of the indirect effect was mediated by cortical thinness. We used negative binomial regression for the outcome regression model and linear regression for the mediator regression model. We calculated standard errors using bootstrapping. We adjusted all models for all potential confounding variables described in the corresponding section. The total effect resulted as the product of NDE and NIE. We also calculated the proportion mediated as incidence rate ratio $(IRR)^{NDE}(IRR^{NIE} - 1)/(IRR^{NDE}IRR^{NIE} - 1)$.

Air Pollution Exposure and Brain Structural Connectivity

First, we used linear regression models to assess the association between exposure to each air pollutant (i.e., NO_x, NO_2, PM_{10}, PM_{COARSE}, $PM_{2.5}$, $PM_{2.5}$absorbance, PAHs, OC, Cu, Fe, Si, Zn, OP^{DTT}, OP^{ESR} — not temporally adjusted), during pregnancy and childhood separately, and each global white matter microstructure outcome (i.e., global FA and global MD) (Table 1). We adjusted all models for all potential confounding variables described in the corresponding section. The assumptions of the linear regression modeling were fulfilled (i.e., normality and homoscedasticity of residuals, linearity between exposure and outcome, and no multicollinearity).

Second, we performed multipollutant analyses using the DSA approach (see details in section *Exposure During Pregnancy and Childhood — Brain Volumes in School-Age Children and Pre-adolescents*). In brief, we excluded PM_{10} from the multipollutant analyses because PM_{10} showed a correlation of more than 0.90 with $PM_{2.5}$absorbance, and $PM_{2.5}$absorbance showed a better LUR performance based on the R^2 of the model. We performed two multipollutant analyses for white matter microstructure outcome, including all air pollutants either during pregnancy or during childhood. When more than one pollutant was identified in one of these two time periods, we ran a linear regression model mutually adjusting for them.

Third, when pollutants were associated with a global white matter microstructure outcome in both the pregnancy and childhood time periods, we ran a linear regression model of that global white matter microstructure outcome, mutually adjusting for those pollutants.

Fourth, we ran linear regression models between the pollutants associated with the global white matter microstructure, and the twelve individual white matter microstructure tracts.

Fifth, we used a bootstrap method to quantify the measurement error in the assessment of air pollution (LUR model predictions) and to transfer the resulting uncertainty to the exposure–outcome associations (Szpiro et al. 2011b). This method includes the following iterative steps: (1) simulate a new health outcome variable and the exposure at the monitoring locations on the basis of fitted models and residual errors; (2) build a new LUR model that predicts the simulated exposure; (3) use the new LUR model to predict exposure for the whole cohort; and (4) estimate the exposure–outcome association with the newly generated health outcome variable and predicted exposure. The variance in the estimates result-

Table 1. Summary of Data Included in Each Analysis

Analysis	Exposure			Outcome	Age	*n*
	Pollutants	Temporal Adjustment	Time Periods			
Brain structural morphology	NO_2, PM_{COARSE}, $PM_{2.5}$, $PM_{2.5}$absorbance	Yes	Pregnancy	Volumes Thickness Cognitive function	School-age children	783
	NO_x, NO_2, PM_{10}, PM_{COARSE}, $PM_{2.5}$, $PM_{2.5}$absorbance, PAHs, OC, Cu, Fe, Si, Zn, OP^{DTT}, OP^{ESR}	No	Pregnancy Childhood	Volumes Thickness Surface area	Pre-adolescents	3,133
Brain structural connectivity	NO_x, NO_2, PM_{10}, PM_{COARSE}, $PM_{2.5}$, $PM_{2.5}$absorbance, PAHs, OC, Cu, Fe, Si, Zn, OP^{DTT}, OP^{ESR}	No	Pregnancy Childhood	FA MD	Pre-adolescents	2,954
Brain functional connectivity	NO_x, NO_2, PM_{10}, PM_{COARSE}, $PM_{2.5}$, $PM_{2.5}$absorbance	Yes	Pregnancy 0–2 years 2–5 years 5–9 years	Connectivity scores	Pre-adolescents	2,197

ing from the different iterations is used as the measurement error corrected variance. This variance or, equivalently, the confidence interval (CI), was compared with the variance obtained when measurement error was not considered. As the measurement error is expected to be mostly of Berkson type, bias in exposure–outcome coefficient estimates was not expected and, therefore, it was not corrected (Szpiro et al. 2011b). We quantified the measurement error for the adjusted associations between exposure to each air pollutant (i.e., NO_x, NO_2, PM_{10}, PM_{COARSE}, $PM_{2.5}$, $PM_{2.5}$absorbance, Cu, Fe, Si, and Zn) during pregnancy and childhood separately, and each global white matter microstructure outcome (i.e., global FA and global MD).

Air Pollution Exposure and Brain Functional Connectivity

We used linear regression models to assess the association of exposure to each air pollutant (i.e., NO_x, NO_2, PM_{10}, PM_{COARSE}, $PM_{2.5}$, and $PM_{2.5}$absorbance — temporally adjusted) during pregnancy and for three childhood periods separately (i.e., from birth to 2 years of age, from 2 to 5 years of age, and from 5 to 9 years of age) with each correlation coefficient (Table 1). We adjusted all models for all potential confounding variables described in the corresponding section. In this analysis, we used several periods of exposure during childhood because brain function experiences greater changes in the first years of life, in comparison with brain morphology. The assumptions of the linear regression modeling were fulfilled (i.e., normality and homoscedasticity of residuals, linearity between exposure and outcome, no multicollinearity). As there are many connectivity scores (72,200), we corrected the analyses for multiple testing using a false discovery rating where a new critical *q*-value for each association was obtained.

STATISTICAL PACKAGES

We carried out all analyses with R (versions 3.4.2 and 3.4.3 R Core Team [2017] and version 3.5.3 R Core Team [2018]) using an in-house R package *https://github.com/slamballais/QDECR* and with STATA (versions 13.0 and 14.0; StataCorporation, College Station, TX).

RESULTS

DESCRIPTIVE ANALYSIS

Participants' characteristics at recruitment, at the 1st MRI wave, and at the 2nd MRI wave are shown in Table 2.

Mean air pollution levels during pregnancy were 34.6 μg/m³ for NO_2 (range 21.3–81.2), and 17.0 μg/m³ for $PM_{2.5}$ (range 16.2–21.7) (Table 3). During childhood, mean levels were 32.5 μg/m³ for NO_2 (range 13.9–104.8), and 16.8 μg/m³ for $PM_{2.5}$ (range 10.1–20.3). Spearman correlations of the levels of the air pollutants between the two time periods were generally moderate, ranging between 0.48 for NO_2 and 0.67 for PAHs. Correlations between the levels of the air pollutants within each time period varied considerably depending on the pollutant (Figure 3).

AIR POLLUTION EXPOSURE AND BRAIN STRUCTURAL MORPHOLOGY

Exposure During Pregnancy and Childhood — Brain Volumes in School-Age Children and Pre-adolescents

Exposure to air pollution during pregnancy was not associated with global brain volumes, such as total brain, cortical gray matter, subcortical gray matter, and total white matter volumes, in school-age children and pre-adolescents (Table 4 and Appendix Table A3 [available on the HEI website]). Likewise, exposure to air pollution during childhood was not associated with global brain volumes in pre-adolescents.

While air pollution during pregnancy was not associated with region-specific brain volumes in school-age children (data not shown), exposure to air pollution during pregnancy and childhood was associated with some region-specific brain volumes in pre-adolescents (Table 5). Among the subcortical structures, we observed no association of the exposure to air pollutants during pregnancy or childhood with the volumes of thalamus and caudate nucleus. Higher exposure to PM_{COARSE} during pregnancy was associated with a larger putamen and pallidum in the single-pollutant analysis, although these associations did not remain using the multipollutant approach. We did not find any association of exposure to air pollution during childhood with the volumes of putamen and pallidum. Higher exposure to PAHs and Cu during pregnancy and to PM_{COARSE} and OP^{DTT} during childhood was associated with a smaller hippocampus in the single-pollutant analysis. After the multipollutant approach, we could only confirm the associations of higher exposure to PAHs during pregnancy and to OP^{DTT} during childhood with a smaller hippocampus,

Table 2. Participant Characteristics[a]

	Recruitment (*n* = 9,610)	1st MRI Wave (*n* = 783)	2nd MRI Wave (*n* = 3,857)
Maternal education level			
Primary education	11.3	7.0	7.1
Secondary education	46.0	44.8	41.4
University education	42.7	48.2	51.5
Monthly household income			
<1,200€	20.8	14.1	14.1
1,200€–2,000€	18.5	17.7	16.8
>2,000€	60.7	68.1	69.1
Maternal ethnicity			
Dutch	50.0	65.2	56.8
Other western	8.6	14.5	8.4
Nonwestern	41.4	20.3	34.9
Maternal age (years)	29.9 (5.4)	30.7 (4.9)	31.1 (4.9)
Family status (monoparental)	14.5	13.5	11.4
Maternal parity (multiparous)	44.8	39.5	42.4
Maternal smoking use during pregnancy			
Never	73.5	75.3	77.3
Smoking use until pregnancy known	8.5	6.5	8.8
Continued smoking use during pregnancy	18.0	18.2	13.9
Maternal alcohol use during pregnancy			
Never	49.8	37.6	43.0
Alcohol use until pregnancy known	13.6	14.3	14.7
Continued alcohol use during pregnancy	36.6	48.1	42.3
Maternal prepregnancy body mass index (kg/m²)	23.7 (4.4)	24.6 (4.3)	23.5 (4.2)
Maternal overall psychological distress	0.3 (0.4)	0.3 (0.4)	0.3 (0.4)
Maternal intelligence quotient score	95.7 (15.4)	98.4 (13.9)	97.4 (14.9)

[a] Values are percentages for the categorical variables and mean (standard deviation) for the continuous variables.

Table 3. Air Pollutant Concentrations Without Temporal Adjustment During Pregnancy and Childhood with Spearman Correlations of the Average Concentrations Between the Two Time Periods[a]

Air Pollutant	Pregnancy [Mean (Minimum–Maximum)]	Childhood [Mean (Minimum–Maximum)]	Spearman Correlation
NO_x (μg/m^3)	51.0 (26.4 to 130.6)	46.8 (21.2 to 130.4)	0.55
NO_2 (μg/m^3)	34.6 (21.3 to 81.2)	32.5 (13.9 to 104.8)	0.48
PM_{10} (μg/m^3)	27.1 (24.3 to 38.2)	26.5 (16.0 to 36.0)	0.52
PM_{COARSE} (μg/m^3)	9.9 (7.6 to 14.8)	9.5 (5.0 to 14.8)	0.56
$PM_{2.5}$ (μg/m^3)	17.0 (16.2 to 21.7)	16.8 (10.1 to 20.3)	0.60
$PM_{2.5}$absorbance (10^{-5}/m^{-1})	1.7 (1.2 to 4.2)	1.6 (1.0 to 4.6)	0.53
PAHs (ng/m^3)	1.0 (0.6 to 3.8)	1.0 (0.0 to 2.9)	0.67
OC (μg/m^3)	1.7 (0.5 to 2.8)	1.6 (0.5 to 2.5)	0.59
Cu (ng/m^3)	4.9 (3.5 to 12.2)	4.6 (1.8 to 11.4)	0.54
Fe (ng/m^3)	123.5 (86.6 to 311.8)	116.7 (45.8 to 384.1)	0.52
Si (ng/m^3)	93.1 (81.2 to 279.1)	91.6 (50.8 to 337.1)	0.61
Zn (ng/m^3)	20.1 (12.8 to 43.2)	19.9 (7.4 to 58.0)	0.56
OP^{DTT} (nmol DTT/min/m^3)	1.3 (0.6 to 1.7)	1.3 (0.4 to 1.6)	0.58
OP^{ESR} (units/m^3)	1,080.7 (811.1 to 3,528.9)	1,037.2 (616.7 to 3,746.4)	0.58

[a] Pregnancy = from conception until birth; childhood = from birth until 9–12 years.

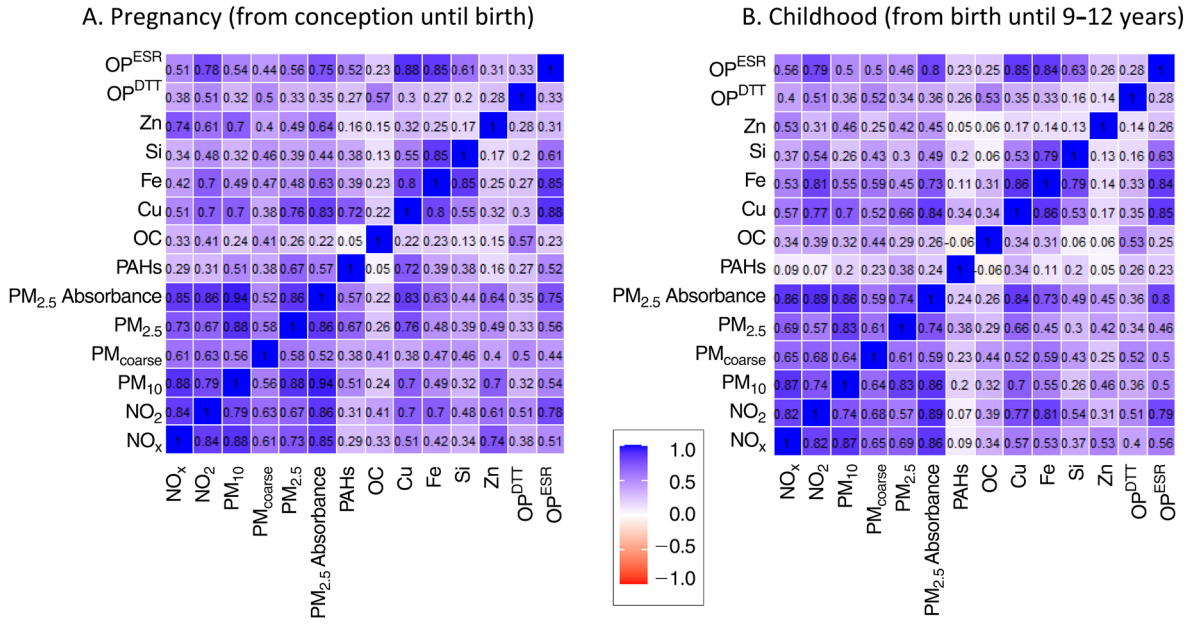

Cu, copper; Fe, iron; NO_2, nitrogen dioxide; NO_x, nitrogen oxides; OC, organic carbon; OP^{DTT}, oxidative potential using dithiothreitol; OP^{ESR} , oxidative potential using electron spin resonance; PAHs, polycyclic aromatic hydrocarbons; $PM_{2.5}$, particulate matter with aerodynamic diameter less than 2.5 μm, $PM_{2.5}$ absorbance, absorbance of $PM_{2.5}$ filters; PM_{10}, particulate matter with aerodynamic diameter less than 10μm; PM_{COARSE}, particulate matter with aerodynamic diameter between 10 μm and 2.5 μm; Si, silicon; Zn, zinc.

*Non-back- and forward-extrapolated levels.

Figure 3. Spearman correlations between air pollutant concentrations without a temporal adjustment: (A) estimated during pregnancy (from conception until birth); and (B) estimated during childhood (from birth until 9–12 years).

Table 4. Adjusted Associations Between Exposure to Air Pollutants During Pregnancy and Childhood and Global Brain Volumes in School-Age Children and Pre-adolescents[a]

Global brain volumes / Air pollutants (per unit of change)	School-Age Children[b] (n = 783)	Pre-adolescents[b,c] (n = 3,133)	
	Pregnancy Exposure Coefficient (95% CI)	Pregnancy Exposure Coefficient (95% CI)	Childhood Exposure Coefficient (95% CI)
Total Brain (mm^3)			
NO_2 (10 $\mu g/m^3$)	124 (−1,118 to 1,135)	5,745 (−767 to 12,257)	−793 (−6,522 to 4,937)
PM_{COARSE} (5 $\mu g/m^3$)	−4,868 (−10,337 to 822)	15,026 (−380 to 30,432)	−2,815 (−19,051 to 13,422)
$PM_{2.5}$ (5 $\mu g/m^3$)	−3,079 (−7,790 to 1,632)	11,437 (−14,435 to 37,309)	−1,604 (−34,765 to 31,557)
$PM_{2.5}$absorbance ($10^{-5}m^{-1}$)	−2,861 (−18,745 to 24,467)	7,715 (−2,923 to 18,353)	1,005 (−10,727 to 12,738)
Cortical Gray Matter (mm^3)			
NO_2 (10 $\mu g/m^3$)	−60 (−853 to 733)	2,288 (−945 to 5,521)	−1,354 (−4,198 to 1,489)
PM_{COARSE} (5 $\mu g/m^3$)	−3,542 (−7,059 to 8)	6,181 (−1,454 to 13,816)	−3,823 (−11,875 to 4,229)
$PM_{2.5}$ (5 $\mu g/m^3$)	−2,598 (−5,583 to 387)	693 (−12,166 to 13,552)	−5,661 (−22,095 to 10,773)
$PM_{2.5}$absorbance ($10^{-5}m^{-1}$)	−2,683 (−16,377 to 11,012)	2,439 (−2,845 to 7,723)	−1,373 (−7,196 to 4,451)
Subcortical Gray Matter (mm^3)			
NO_2 (10 $\mu g/m^3$)	36 (−17 to 89)	95 (−106 to 296)	47 (−129 to 222)
PM_{COARSE} (5 $\mu g/m^3$)	−92 (−325 to 148)	419 (−53 to 892)	87 (−411 to 585)
$PM_{2.5}$ (5 $\mu g/m^3$)	−60 (−258 to 138)	285 (−515 to 1,085)	−31 (−1,052 to 990)
$PM_{2.5}$absorbance ($10^{-5}m^{-1}$)	418 (−497 to 1,334)	53 (−275 to 382)	48 (−313 to 409)
Total White Matter (mm^3)			
NO_2 (10 $\mu g/m^3$)	199 (−287 to 685)	2,045 (−969 to 5,099)	430 (−2,219 to 3,080)
PM_{COARSE} (5 $\mu g/m^3$)	−1,129 (−3,215 to 1,127)	5,097 (−2,036 to 12,231)	−67 (−7,584 to 7,450)
$PM_{2.5}$ (5 $\mu g/m^3$)	−268 (−2,096 to 1,559)	5,569 (−6,428 to 17,567)	−69 (−15,431 to 15,294)
$PM_{2.5}$absorbance ($10^{-5}m^{-1}$)	5,807 (−2,566 to 14,180)	3,009 (−1,922 to 7,939)	1,492 (−3,938 to 6,923)

[a] The expected direction of the associations was higher air pollution exposure during pregnancy and smaller global brain volumes.

[b] Coefficients and 95% confidence intervals from linear regression models were adjusted for maternal and paternal education, ethnicity, age, height, body mass index, and psychological distress during pregnancy; maternal smoking and alcohol use during pregnancy; maternal parity, maternal intelligence quotient, family status, and household income; and child's genetic ancestry, sex, and age at the scanning session.

[c] Subcortical gray matter was additionally adjusted by intracranial volume in the pre-adolescents analysis.

−69 mm^3 (95% CI = −129 to −9) per 1-ng/m^3 increase in PAHs, and −198 mm^3 (95% CI = −371 to −25) per 1-nmol DTT/min/m^3 increase in OP^{DTT} (Appendix Table A4). Higher exposure to Si during pregnancy was associated with a larger amygdala in both the single and multipollutant approaches (111 mm^3 [95% CI = 41 to 181] per 100-ng/m^3 increase in Si). Also, in the multipollutant model, exposure to PAHs and OC during pregnancy was associated with a smaller amygdala. We did not find any association between either exposure to air pollution during childhood and volume of the amygdala or exposure to air pollution during pregnancy and volume of the nucleus accumbens. On the contrary, higher exposure to Zn during childhood was associated with a larger nucleus accumbens, after both the single and multipollutant approaches (17 mm^3 [95% CI = 3 to 30] per 10-ng/m^3 increase in Zn).

Higher exposure to OP^{ESR} during pregnancy and to OC during childhood was associated with smaller corpus callosum in both the single and multipollutant approaches (−101 mm^3 [95% CI = −185 to −16] per 1,000-units/m^3 increase in OP^{ESR}, and −56 mm^3 [95% CI = −97 to −14] per 1-µg/m^3 increase in OC) (Table 5 and Appendix Table A4). In the single-pollutant analysis, higher exposure to PM_{10}, PM_{COARSE},

Table 5. Adjusted Associations Between Exposure to Air Pollutants During Pregnancy and Childhood and Volume of Subcortical Structures, Corpus Callosum, and Cerebellum in Pre-adolescents[a]

Region-Specific Brain Volumes / Air Pollutants (per unit of change)	Pregnancy Exposure[b,c]	Childhood Exposure[b,c]
	Coefficient (95% CI)	Coefficient (95% CI)
Thalamus (mm^3)		
NO_x (20 $\mu g/m^3$)	1 (−42 to 44)	−3 (−50 to 44)
NO_2 (10 $\mu g/m^3$)	−19 (−84 to 46)	−18 (−74 to 39)
PM_{10} (10 $\mu g/m^3$)	5 (−188 to 197)	−49 (−270 to 171)
PM_{COARSE} (5 $\mu g/m^3$)	80 (−73 to 232)	−6 (−166 to 155)
$PM_{2.5}$ (5 $\mu g/m^3$)	40 (−218 to 297)	−88 (−417 to 241)
$PM_{2.5}$absorbance ($10^{-5}m^{-1}$)	−20 (−125 to 86)	−36 (−153 to 80)
PAHs (1 ng/m^3)	− 2 (−91 to 94)	−75 (−185 to 36)
OC (1 $\mu g/m^3$)	−26 (−109 to 58)	−34 (−119 to 51)
Cu (5 ng/m^3)	−111 (−291 to 70)	−102 (−306 to 101)
Fe (100 ng/m^3)	−111 (−267 to 46)	−20 (−166 to 125)
Si (100 ng/m^3)	−102 (−291 to 87)	30 (−163 to 224)
Zn (10 ng/m^3)	−18 (−95 to 60)	−8 (−80 to 64)
OP^{DTT} (1 nmol DTT/min/m^3)	−53 (−317 to 211)	−247 (−513 to 20)
OP^{ESR} (1,000 units/m^3)	−120 (−292 to 52)	−59 (−237 to 119)
Caudate nucleus (mm^3)		
NO_x (20 $\mu g/m^3$)	11 (−28 to 50)	−5 (−47 to 37)
NO_2 (10 $\mu g/m^3$)	42 (−16 to 100)	21 (−30 to 73)
PM_{10} (10 $\mu g/m^3$)	51 (−123 to 225)	−44 (−243 to 155)
PM_{COARSE} (5 $\mu g/m^3$)	82 (−55 to 220)	−17 (−161 to 128)
$PM_{2.5}$ (5 $\mu g/m^3$)	83 (−150 to 315)	−64 (−361 to 233)
$PM_{2.5}$absorbance ($10^{-5}m^{-1}$)	44 (−52 to 139)	26 (−79 to 131)
PAHs (1 ng/m^3)	16 (−68 to 99)	−4 (−104 to 96)
OC (1 $\mu g/m^3$)	−31 (−107 to 44)	−58 (−135 to 18)
Cu (5 ng/m^3)	70 (−92 to 233)	24 (−159 to 207)
Fe (100 ng/m^3)	72 (−69 to 213)	20 (−112 to 151)
Si (100 ng/m^3)	40 (−130 to 210)	−8 (−183 to 167)
Zn (10 ng/m^3)	−6 (−76 to 64)	5 (−60 to 70)
OP^{DTT} (1 nmol DTT/min/m^3)	100 (−138 to 338)	126 (−114 to 366)
OP^{ESR} (1,000 units/m^3)	98 (−57 to 253)	98 (−62 to 258)

(Table continues next page)

[a] The expected direction of the associations was higher air pollution exposure during pregnancy and childhood and smaller thalamus volume, larger caudate nucleus volume, larger putamen volume, smaller pallidum volume, smaller hippocampus volume, larger amygdala volume, larger nucleus accumbens volume, smaller corpus callosum volume, and smaller cerebellum volume.

[b] Coefficients and 95% confidence intervals from linear regression models were adjusted for maternal and paternal education, ethnicity, age, height, body mass index, and psychological distress during pregnancy, maternal smoking and alcohol use during pregnancy, maternal parity, maternal intelligence quotient, family status, household income, and child's genetic ancestry, sex, and age at the scanning session, and intracranial volume.

[c] **Bolded values** indicate P value < 0.05.

[d] The association was identified in the multipollutant approach (see Appendix Table A4). PM_{10} was not included (see Statistical Methods and Data Analysis section).

Table 5 (*Continued*). Adjusted Associations Between Exposure to Air Pollutants During Pregnancy and Childhood and Volume of Subcortical Structures, Corpus Callosum, and Cerebellum in Pre-adolescents[a]

Region-Specific Brain Volumes / Air Pollutants (per unit of change)	Pregnancy Exposure[b,c]	Childhood Exposure[b,c]
	Coefficient (95% CI)	Coefficient (95% CI)
Putamen (mm^3)		
NO_x (20 $\mu g/m^3$)	43 (−3 to 88)	41 (−9 to 91)
NO_2 (10 $\mu g/m^3$)	49 (−20 to 118)	35 (−26 to 95)
PM_{10} (10 $\mu g/m^3$)	156 (−50 to 362)	171 (−64 to 407)
PM_{COARSE} (5 $\mu g/m^3$)	**166 (3 to 329)**	154 (−18 to 326)
$PM_{2.5}$ (5 $\mu g/m^3$)	256 (−19 to 531)	257 (−95 to 608)
$PM_{2.5}$absorbance ($10^{-5}m^{-1}$)	61 (−52 to 174)	59 (−65 to 183)
PAHs (1 ng/m^3)	78 (−21 to 176)	31 (−88 to 149)
OC (1 $\mu g/m^3$)	−16 (−106 to 73)	−12 (−103 to 79)
Cu (5 ng/m^3)	29 (−164 to 221)	−23 (−240 to 195)
Fe (100 ng/m^3)	−12 (−179 to 156)	7 (−149 to 162)
Si (100 ng/m^3)	18 (−184 to 220)	110 (−97 to 317)
Zn (10 ng/m^3)	50 (−34 to 133)	46 (−31 to 123)
OP^{DTT} (1 nmol DTT/min/m^3)	3 (−279 to 286)	−20 (−305 to 265)
OP^{ESR} (1,000 units/m^3)	11 (−173 to 196)	−20 (−210 to 171)
Pallidum (mm^3)		
NO_x (20 $\mu g/m^3$)	−2 (−18 to 15)	−10 (−28 to 8)
NO_2 (10 $\mu g/m^3$)	8 (−17 to 33)	−10 (−32 to 11)
PM_{10} (10 $\mu g/m^3$)	−16 (−91 to 58)	−43 (−128 to 43)
PM_{COARSE} (5 $\mu g/m^3$)	**60 (1 to 119)**	21 (−41 to 82)
$PM_{2.5}$ (5 $\mu g/m^3$)	23 (−77 to 122)	−16 (−143 to 111)
$PM_{2.5}$absorbance ($10^{-5}m^{-1}$)	−7 (−48 to 33)	−36 (−81 to 9)
PAHs (1 ng/m^3)	3 (−32 to 39)	−22 (−65 to 20)
OC (1 $\mu g/m^3$)	7 (−25 to 40)	14 (−19 to 47)
Cu (5 ng/m^3)	4 (−66 to 74)	−31 (−110 to 47)
Fe (100 ng/m^3)	15 (−45 to 76)	2 (−54 to 58)
Si (100 ng/m^3)	16 (−57 to 89)	27 (−48 to 102)
Zn (10 ng/m^3)	−11 (−41 to 19)	−9 (−37 to 19)
OP^{DTT} (1 nmol DTT/min/m^3)	51 (−51 to 153)	−22 (−126 to 81)
OP^{ESR} (1,000 units/m^3)	15 (−52 to 81)	−34 (−103 to 35)

(Table continues next page)

[a] The expected direction of the associations was higher air pollution exposure during pregnancy and childhood and smaller thalamus volume, larger caudate nucleus volume, larger putamen volume, smaller pallidum volume, smaller hippocampus volume, larger amygdala volume, larger nucleus accumbens volume, smaller corpus callosum volume, and smaller cerebellum volume.

[b] Coefficients and 95% confidence intervals from linear regression models were adjusted for maternal and paternal education, ethnicity, age, height, body mass index, and psychological distress during pregnancy, maternal smoking and alcohol use during pregnancy, maternal parity, maternal intelligence quotient, family status, household income, and child's genetic ancestry, sex, and age at the scanning session, and intracranial volume.

[c] **Bolded values** indicate P value < 0.05.

[d] The association was identified in the multipollutant approach (see Appendix Table A4). PM_{10} was not included (see Statistical Methods and Data Analysis section).

Table 5 (*Continued*). Adjusted Associations Between Exposure to Air Pollutants During Pregnancy and Childhood and Volume of Subcortical Structures, Corpus Callosum, and Cerebellum in Pre-adolescents[a]

Region-Specific Brain Volumes / Air Pollutants (per unit of change)	Pregnancy Exposure[b,c]	Childhood Exposure[b,c]
	Coefficient (95% CI)	Coefficient (95% CI)
Hippocampus (mm^3)		
NO_x (20 $\mu g/m^3$)	−16 (−44 to 12)	−7 (−38 to 23)
NO_2 (10 $\mu g/m^3$)	−22 (−64 to 19)	−8 (−45 to 28)
PM_{10} (10 $\mu g/m^3$)	−105 (−230 to 19)	−89 (−232 to 53)
PM_{COARSE} (5 $\mu g/m^3$)	−49 (−147 to 50)	**−107 (−211 to −3)**
$PM_{2.5}$ (5 $\mu g/m^3$)	−158 (−325 to 9)	−184 (−397 to 29)
$PM_{2.5}$absorbance ($10^{-5}m^{-1}$	−57 (−126 to 11)	−13 (−88 to 62)
PAHs (1 ng/m^3)	**−69 (−129 to −9)**[d]	−44 (−116 to 27)
OC (1 $\mu g/m^3$)	40 (−15 to 94)	−1 (−56 to 54)
Cu (5 ng/m^3)	**−121 (−238 to −4)**	−41 (−173 to 91)
Fe (100 ng/m^3)	−73 (−174 to 29)	6 (−88 to 100)
Si (100 ng/m^3)	−80 (−203 to 42)	45 (−80 to 170)
Zn (10 ng/m^3)	−19 (−69 to 31)	−20 (−67 to 27)
OP^{DTT} (1 nmol DTT/min/m^3)	−54 (−226 to 117)	**−198 (−371 to −25)**[d]
OP^{ESR} (1,000 units/m^3)	−90 (−202 to 21)	−2 (−118 to 113)
Amygdala (mm^3)		
NO_x (20 $\mu g/m^3$)	−7 (−21 to 8)	− 3 (−19 to 13)
NO_2 (10 $\mu g/m^3$)	−4 (−26 to 18)	− 7 (−26 to 13)
PM_{10} (10 $\mu g/m^3$)	−41 (−106 to 25)	− 5 (−80 to 70)
PM_{COARSE} (5 $\mu g/m^3$)	−2 (−54 to 50)	−26 (−81 to 29)
$PM_{2.5}$ (5 $\mu g/m^3$)	−56 (−144 to 31)	−19 (−131 to 93)
$PM_{2.5}$absorbance ($10^{-5}m^{-1}$)	−14 (−50 to 22)	− 5 (−45 to 34)
PAHs (1 ng/m^3)	−14 (−46 to 17)[d]	−29 (−66 to 9)
OC (1 $\mu g/m^3$)	**−28 (−57 to 0)**[d]	−22 (−51 to 7)
Cu (5 ng/m^3)	−15 (−77 to 46)	−23 (−92 to 47)
Fe (100 ng/m^3)	38 (−15 to 92)	18 (−31 to 68)
Si (100 ng/m^3)	**72 (8 to 136)**[d]	63 (−3 to 129)
Zn (10 ng/m^3)	3 (−24 to 29)	12 (−12 to 37)
OP^{DTT} (1 nmol DTT/min/m^3)	−35 (−125 to 55)	−77 (−167 to 14)
OP^{ESR} (1,000 units/m^3)	10 (-49 to 68)	−10 (−71 to 51)

(Table continues next page)

[a] The expected direction of the associations was higher air pollution exposure during pregnancy and childhood and smaller thalamus volume, larger caudate nucleus volume, larger putamen volume, smaller pallidum volume, smaller hippocampus volume, larger amygdala volume, larger nucleus accumbens volume, smaller corpus callosum volume, and smaller cerebellum volume.

[b] Coefficients and 95% confidence intervals from linear regression models were adjusted for maternal and paternal education, ethnicity, age, height, body mass index, and psychological distress during pregnancy, maternal smoking and alcohol use during pregnancy, maternal parity, maternal intelligence quotient, family status, household income, and child's genetic ancestry, sex, and age at the scanning session, and intracranial volume.

[c] **Bolded values** indicate P value < 0.05.

[d] The association was identified in the multipollutant approach (see Appendix Table A4). PM_{10} was not included (see Statistical Methods and Data Analysis section).

Table 5 (*Continued*). Adjusted Associations Between Exposure to Air Pollutants During Pregnancy and Childhood and Volume of Subcortical Structures, Corpus Callosum, and Cerebellum in Pre-adolescents[a]

Region-Specific Brain Volumes / Air Pollutants (per unit of change)	Pregnancy Exposure[b,c]	Childhood Exposure[b,c]
	Coefficient (95% CI)	Coefficient (95% CI)
Nucleus accumbens (mm^3)		
NO_x (20 $\mu g/m^3$)	3 (−5 to 11)	5 (−4 to 14)
NO_2 (10 $\mu g/m^3$)	9 (−3 to 21)	8 (−3 to 18)
PM_{10} (10 $\mu g/m^3$)	22 (−13 to 58)	26 (−15 to 67)
PM_{COARSE} (5 $\mu g/m^3$)	16 (−12 to 44)	18 (−12 to 48)
$PM_{2.5}$ (5 $\mu g/m^3$)	32 (−15 to 80)	24 (−37 to 85)
$PM_{2.5}$absorbance ($10^{-5}m^{-1}$)	12 (−8 to 32)	15 (−7 to 37)
PAHs (1 ng/m^3)	4 (−13 to 21)	−5 (−25 to 16)
OC (1 $\mu g/m^3$)	3 (−12 to 19)	−4 (−20 to 11)
Cu (5 ng/m^3)	8 (−25 to 42)	12 (−26 to 50)
Fe (100 ng/m^3)	5 (−24 to 34)	17 (−10 to 44)
Si (100 ng/m^3)	6 (−29 to 41)	18 (−18 to 54)
Zn (10 ng/m^3)	1 (−13 to 16)	**17 (3 to 30)**[d]
OP^{DTT} (1 nmol DTT/min/m^3)	30 (−19 to 79)	36 (−14 to 85)
OP^{ESR} (1,000 units/m^3)	4 (−28 to 35)	23 (−10 to 56)
Corpus callosum (mm^3)		
NO_x (20 $\mu g/m^3$)	−14 (−35 to 7)	−18 (−41 to 5)
NO_2 (10 $\mu g/m^3$)	−28 (−59 to 4)	−14 (−42 to 14)
PM_{10} (10 $\mu g/m^3$)	−31 (−126 to 64)	−52 (−161 to 56)
PM_{COARSE} (5 $\mu g/m^3$)	39 (−36 to 114)	−11 (−90 to 68)
$PM_{2.5}$ (5 $\mu g/m^3$)	31 (−96 to 158)	−98 (−260 to 64)
$PM_{2.5}$absorbance ($10^{-5}m^{-1}$)	−32 (−84 to 20)	−28 (−85 to 30)
PAHs (1 ng/m^3)	14 (−32 to 59)	7 (−47 to 62)
OC (1 $\mu g/m^3$)	−29 (−70 to 12)	**−55 (−97 to −14)**[d]
Cu (5 ng/m^3)	−76 (−164 to 13)	−74 (−174 to 26)
Fe (100 ng/m^3)	−61 (−138 to 16)	−28 (−99 to 44)
Si (100 ng/m^3)	6 (−87 to 99)	31 (−65 to 126)
Zn (10 ng/m^3)	−22 (−60 to 17)	−25 (−61 to 10)
OP^{DTT} (1 nmol DTT/min/m^3)	−50 (−180 to 80)	−84 (−215 to 47)
OP^{ESR} (1,000 units/m^3)	**−101 (−185 to −16)**[d]	−63 (−151 to 24)

(Table continues next page)

[a] The expected direction of the associations was higher air pollution exposure during pregnancy and childhood and smaller thalamus volume, larger caudate nucleus volume, larger putamen volume, smaller pallidum volume, smaller hippocampus volume, larger amygdala volume, larger nucleus accumbens volume, smaller corpus callosum volume, and smaller cerebellum volume.

[b] Coefficients and 95% confidence intervals from linear regression models were adjusted for maternal and paternal education, ethnicity, age, height, body mass index, and psychological distress during pregnancy, maternal smoking and alcohol use during pregnancy, maternal parity, maternal intelligence quotient, family status, household income, and child's genetic ancestry, sex, and age at the scanning session, and intracranial volume.

[c] **Bolded values** indicate P value < 0.05.

[d] The association was identified in the multipollutant approach (see Appendix Table A4). PM_{10} was not included (see Statistical Methods and Data Analysis section).

Table 5 (*Continued*). Adjusted Associations Between Exposure to Air Pollutants During Pregnancy and Childhood and Volume of Subcortical Structures, Corpus Callosum, and Cerebellum in Pre-adolescents[a]

Region-Specific Brain Volumes / Air Pollutants (per unit of change)	Pregnancy Exposure[b,c]	Childhood Exposure[b,c]
	Coefficient (95% CI)	Coefficient (95% CI)
Cerebellum (mm^3)		
NO_x (20 $\mu g/m^3$)	458 (−28 to 944)	263 (−268 to 795)
NO_2 (10 $\mu g/m^3$)	582 (−149 to 1,312)	−15 (−656 to 626)
PM_{10} (10 $\mu g/m^3$)	**2,603 (429 to 4,776)**	1,759 (−741 to 4,259)
PM_{COARSE} (5 $\mu g/m^3$)	**1,891 (168 to 3,613)**[d]	967 (−850 to 2,784)
$PM_{2.5}$ (5 $\mu g/m^3$)	**3,446 (539 to 6,353)**	3,165 (−570 to 6,900)
$PM_{2.5}$absorbance ($10^{-5}m^{-1}$)	**1,242 (48 to 2,436)**	406 (−911 to 1,724)
PAHs (1 ng/m^3)	886 (−154 to 1,927)	756 (−495 to 2,007)
OC (1 $\mu g/m^3$)	−278 (−1,223 to 666)	−486 (−1,440 to 467)
Cu (5 ng/m^3)	1,346 (−685 to 3,378)	−171 (−2,464 to 2,123)
Fe (100 ng/m^3)	626 (−1,141 to 2,392)	−444 (−2,084 to 1,196)
Si (100 ng/m^3)	921 (−1,209 to 3,051)	130 (−2,054 to 2,314)
Zn (10 ng/m^3)	817 (−61 to 1,696)	671 (−148 to 1,489)
OP^{DTT} (1 nmol DTT/min/m^3)	−1,374 (−4,360 to 1,611)[d]	−1,050 (−4,074 to 1,975)
OP^{ESR} (1,000 units/m^3)	889 (−1,051 to 2,829)	−79 (−2,088 to 1,930)

[a] The expected direction of the associations was higher air pollution exposure during pregnancy and childhood and smaller thalamus volume, larger caudate nucleus volume, larger putamen volume, smaller pallidum volume, smaller hippocampus volume, larger amygdala volume, larger nucleus accumbens volume, smaller corpus callosum volume, and smaller cerebellum volume.

[b] Coefficients and 95% confidence intervals from linear regression models were adjusted for maternal and paternal education, ethnicity, age, height, body mass index, and psychological distress during pregnancy, maternal smoking and alcohol use during pregnancy, maternal parity, maternal intelligence quotient, family status, household income, and child's genetic ancestry, sex, and age at the scanning session, and intracranial volume.

[c] **Bolded values** indicate P value < 0.05.

[d] The association was identified in the multipollutant approach (see Appendix Table A4). PM_{10} was not included (see Statistical Methods and Data Analysis section).

$PM_{2.5}$, and $PM_{2.5}$absorbance during pregnancy was associated with a larger cerebellum. Nevertheless, only the association with higher exposure to PM_{COARSE} remained after the multipollutant approach (2,501 mm^3 [95% CI = 447 to 4,555] per 5-$\mu g/m^3$ increase in PM_{COARSE}). In the multipollutant model, exposure to OP^{DTT} during pregnancy was also associated with a smaller cerebellum. No associations were found between exposure to air pollution during childhood and volume of the cerebellum.

By simultaneously analyzing the air pollutants that showed associations with a certain structure during pregnancy or childhood, we found that both higher exposure to PAHs and to OP^{DTT} remained associated with a smaller hippocampus. Moreover, both higher exposure to OP^{ESR} and to OC during childhood remained associated with a smaller corpus callosum (Appendix Table A5).

In the post hoc analysis, we observed that higher age at the MRI scanning session was associated with a larger hippocampus, corpus callosum, and cerebellum but with a smaller amygdala and nucleus accumbens (Appendix Figure A3).

Exposure During Pregnancy and Childhood — Cortical Thickness and Surface Area in School-Age Children and Pre-adolescents

Exposure during pregnancy — cortical thickness in school-age children Higher exposure to PM during pregnancy was associated with thinner cortices in several brain regions in both hemispheres of school-age children (e.g., cerebral cortex of the precuneus region of the right hemisphere was 0.045 mm thinner [95% CI = −0.062 to −0.028] per 5-$\mu g/m^3$ increase in $PM_{2.5}$) (Figure 4 and Table 6). These regions had a mean size between 532 and 2,995 mm^2 and a mean thickness between

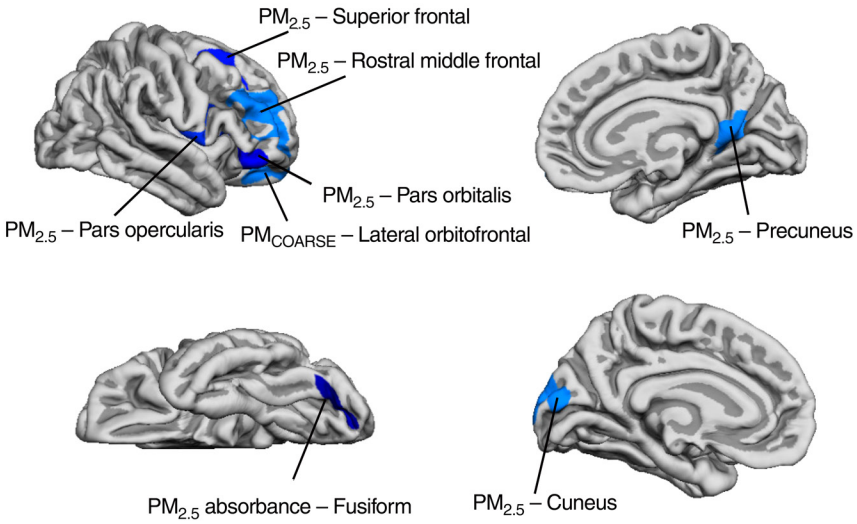

Figure 4. Brain regions identified on the adjusted associations between exposure to $PM_{2.5}$, PM_{COARSE}, and $PM_{2.5}$absorbance during pregnancy and cortical thickness (mm) in school-age children. Blue indicates negative coefficients; a darker blue color indicates a stronger association. Associations from linear regression models were adjusted for maternal and paternal education, ethnicity, age, height, body mass index, and psychological distress during pregnancy, maternal smoking and alcohol use during pregnancy, maternal parity, maternal intelligence quotient, family status, household income, and child's genetic ancestry, sex, and age at the scanning session. All brain regions survived the correction for multiple testing (built-in Monte Carlo null-Z simulation with 10,000 iterations, $P < 0.01$). The expected direction of the association was higher air pollution exposure during pregnancy and smaller cortical thickness.

2.31 and 3.17 mm^2 (with a minimum of 1.61 to 2.23 mm^2 and a maximum of 3.23 to 3.97 mm^2) (data not shown).

Exposure during pregnancy and childhood — cortical thickness and surface area in pre-adolescents Higher exposure to OC, $PM_{2.5}$absorbance, and Cu during pregnancy, and to OP^{DTT} during childhood was associated with thinner cortices in three brain regions in pre-adolescents (e.g., cerebral cortex of the postcentral gyrus of the right hemisphere was 0.06 mm thinner [95% CI = −0.11 to −0.01] per 1-μg/m^3 increase in OC) (Figure 5 and Table 7). These regions had a mean size between 164 and 198 mm^2.

Higher exposure to Zn and OP^{ESR} during childhood was associated with a larger cortical surface area in three brain regions (e.g., cortical surface area of the precentral gyrus of the right hemisphere was 0.01 mm^2 larger [95% CI = 0.00 to 0.02] per 10-ng/m^3 increase in Zn). Higher exposure to PM_{COARSE} during childhood, instead, was associated with a smaller cortical surface area in one brain region (cortical surface area of the pars triangularis of the right hemisphere was 0.10 mm^2 smaller [95% CI –0.18 to –0.02] per 5-μg/m^3 increase in PM_{COARSE}) (Figure 5 and Table 7). These regions had a mean surface area between 157 and 289 mm^2.

Exposure During Pregnancy — Cortical Thickness and Cognitive Function in School-Age Children

Higher exposure to $PM_{2.5}$ during pregnancy was associated with a higher number of inhibition errors in the response set task for school-age children (IRR 1.07 [95% CI = 1.01 to 1.14] per 5-μg/m^3 increase in $PM_{2.5}$). No significant associations were observed for the other cognitive outcomes (data not shown). A thinner cortex in the precuneus region and in the rostral middle frontal region was also associated with a higher number of inhibition errors (IRR 1.32 [95% CI = 1.00 to 1.77] per 1-mm decrease in the cortex of the precuneus region and IRR 1.69 [95% CI = 1.09 to 2.61]) per 1-mm decrease in the cortex of the rostral middle frontal region).

The reduced cortical thickness in the precuneus and rostral middle frontal regions partially mediated the association between exposure to $PM_{2.5}$ during pregnancy and the increased number of inhibition errors (NIE: IRR 1.01 [95% CI = 1.00 to 1.02]) per 1-mm decrease in the cortex of the precuneus and the rostral middle frontal regions). We estimated that the proportion mediated through the reduced cortical thickness in each of the regions was 15%.

AIR POLLUTION EXPOSURE AND BRAIN STRUCTURAL CONNECTIVITY

Exposure during Pregnancy and Childhood — Global FA

In the single-pollutant analysis, higher exposure to NO_x, PM_{10}, $PM_{2.5}$, and $PM_{2.5}$absorbance during pregnancy was associated with lower global FA in pre-adolescents (Table 8). After the multipollutant approach, higher exposure to $PM_{2.5}$ during pregnancy was associated with lower global FA (–0.71 [95% CI = –1.26 to –0.16] per 5-μg/m^3 increase in $PM_{2.5}$). When exposure to PAHs during pregnancy was simultaneously included in the model with $PM_{2.5}$, we observed an inverse

Table 6. Adjusted Associations Between Exposure to Air Pollutants During Pregnancy and Cortical Thickness (mm) in School-Age Children[a]

Brain Region – Hemisphere	Air Pollutant (per unit of change)	Region Size (mm^2)	Coefficient (95% CI)[b] (mm)
Precuneus – Right	$PM_{2.5}$ (5 μg/m^3)	936	−0.045 (−0.062 to −0.028)
Pars opercularis – Right	$PM_{2.5}$ (5 μg/m^3)	753	−0.024 (−0.033 to −0.014)
Pars orbitalis – Right	$PM_{2.5}$ (5 μg/m^3)	651	−0.028 (−0.043 to −0.012)
Rostral middle frontal – Right	$PM_{2.5}$ (5 μg/m^3)	2,995	−0.029 (−0.041 to −0.018)
Superior frontal – Right	$PM_{2.5}$ (5 μg/m^3)	722	−0.029 (−0.043 to −0.016)
Lateral orbitofrontal – Right	PM_{COARSE} (5 μg/m^3)	565	−0.037 (−0.059 to −0.016)
Cuneus – Left	$PM_{2.5}$ (5 μg/m^3)	843	−0.022 (−0.035 to −0.009)
Fusiform – Left	$PM_{2.5}$absorbance ($10^{-5}m^{-1}$)	532	−0.105 (−0.160 to −0.049)

[a] The expected direction of the association was higher air pollution exposure during pregnancy and smaller cortical thickness.

[b] Coefficients and 95% confidence intervals from linear regression models were adjusted for maternal and paternal education, ethnicity, age, height, body mass index, and psychological distress during pregnancy; maternal smoking and alcohol use during pregnancy; maternal parity, maternal intelligence quotient, family status, household income; and child's genetic ancestry, sex, and age at the scanning session. All brain regions survived the correction for multiple testing (built-in Monte Carlo null-Z simulation with 10,000 iteration, P value < 0.01).

and positive association with global FA (0.33 higher global FA [95% CI = 0.06 to 0.60] per 1-ng/m^3 increase in PAHs) (Appendix Table A6).

In the single-pollutant analysis, higher exposure to NO_x, NO_2, $PM_{2.5}$absorbance, and OC during childhood was associated with lower global FA. After the multipollutant approach, only higher exposure to NO_x during childhood was associated with lower global FA (–0.14 [95% CI = –0.23 to –0.04] per 20-μg/m^3 increase in NO_x) (Appendix Table A6).

When exposures to $PM_{2.5}$ during pregnancy and NO_x during childhood were simultaneously added in the same model, none remained associated with global FA (Appendix Table A7).

Exposure During Pregnancy and Childhood — Global MD

In the single-pollutant analysis, higher exposure to NO_x, NO_2, PM_{10}, $PM_{2.5}$, $PM_{2.5}$absorbance, Cu, Fe, Si, and OP^{ESR} during pregnancy was associated with higher global MD in pre-adolescents (Table 8). After the multipollutant approach, only higher exposure to Si during pregnancy remained associated with higher global MD (0.06 [95% CI = 0.01 to 0.11] per 100-ng/m^3 increase in Si) (Appendix Table A6).

In the single-pollutant analysis, higher exposure to NO_x, NO_2, PM_{10}, PM_{COARSE}, $PM_{2.5}$, $PM_{2.5}$absorbance, Si, Zn, and OP^{DTT} during childhood was associated with higher global MD (Table 8). After the multipollutant approach, only higher exposure to Zn and OP^{DTT} was associated with higher global MD (0.03 [95% CI = 0.01 to 0.04] per 10-ng/m^3 increase in Zn, and 0.07 [95% CI = 0.00 to 0.14) per 1-nmol DTT/min/m^3 increase in OP^{DTT}) (Appendix Table A6).

When we simultaneously added in the same model exposures to Si during pregnancy, Zn during childhood, and OP^{DTT} during childhood, only Si and Zn remained associated with global MD (Appendix Table A7).

Exposure During Pregnancy and Childhood — Specific FA and MD Tracts

Higher exposure to $PM_{2.5}$ during pregnancy was associated with four FA tracts in pre-adolescents (i.e., superior longitudinal fasciculus tract of the right hemisphere, forceps minor tract, and corticospinal tracts of the left and right hemispheres) (Figure 6 and Appendix Table A8). Higher exposure to NO_x during childhood was associated with five FA tracts (i.e., uncinated fasciculus tracts of the left and right hemispheres, superior longitudinal fasciculus tract of the right hemisphere, inferior longitudinal fasciculus tract of the right hemisphere, and corticospinal tract of the left hemisphere).

Higher exposure to Si during pregnancy was associated with five MD tracts (i.e., cingulate gyrus part of the cingulum tracts of the left and right hemispheres, superior longitudinal fasciculus tract of the left hemisphere, forceps minor tract, and inferior longitudinal fasciculus tract of the left hemisphere) (Figure 6 and Appendix Table A9). Higher exposure to Zn during childhood was associated with nine MD tracts (i.e., uncinated fasciculus tracts of the left and right hemispheres, cingulate gyrus part of the cingulum tracts of the left and right hemispheres, superior longitudinal fasciculus tracts of the left and right hemispheres, forceps minor tract, and inferior longitudinal fasciculus tracts of the left and right hemispheres). Higher exposure to OP^{DTT} during childhood

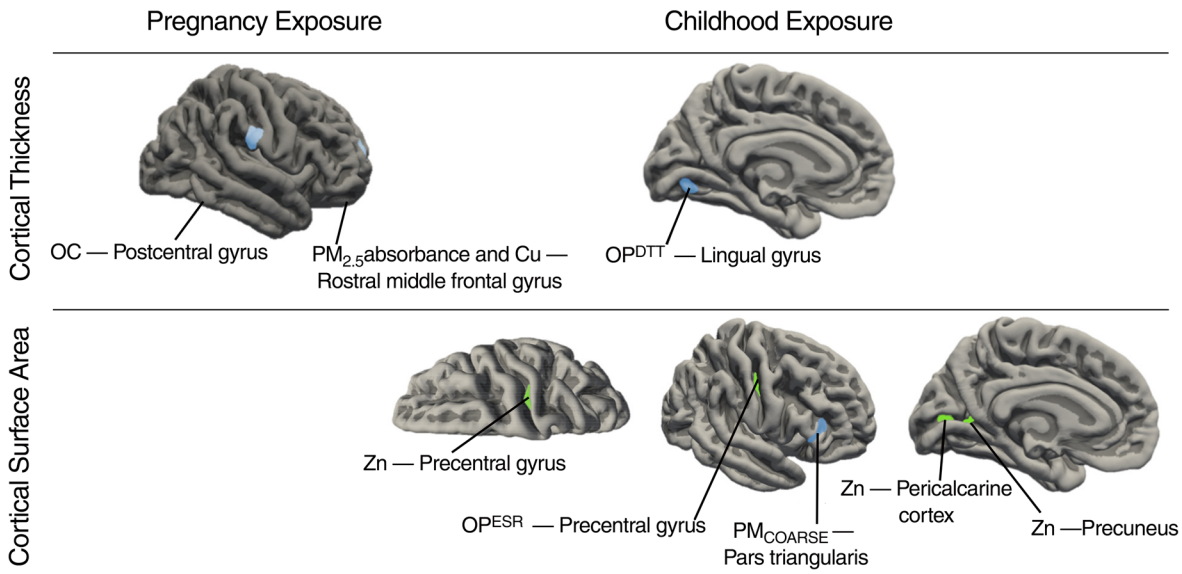

Figure 5. Brain regions identified on the adjusted associations between exposure to OC, $PM_{2.5}$absorbance, and Cu during pregnancy and cortical thickness (mm), OP^{DTT} during childhood and cortical thickness (mm), and Zn, OP^{ESR}, and PM_{COARSE} and cortical surface area (mm^2) in pre-adolescents. Blue indicates negative coefficients and green indicates positive coefficients. Associations from linear regression models were adjusted for maternal and paternal education, ethnicity, age, height, body mass index, and psychological distress during pregnancy, maternal smoking and alcohol use during pregnancy, maternal parity, maternal intelligence quotient, family status, household income, and child's genetic ancestry, sex, and age at the scanning session. All brain regions survived the correction for multiple testing (built-in Monte Carlo null-Z simulation with 10,000 iterations, $P < 0.001$). The expected direction of the association was higher air pollution exposure during pregnancy and childhood and smaller cortical thickness and smaller cortical surface area.

was associated with one MD tract (i.e., cingulate gyrus part of the cingulum tract of the left hemisphere).

Quantification of the Measurement Error

Accounting for measurement error only slightly increased the standard errors and did not alter the main conclusions (Appendix Table A10).

AIR POLLUTION EXPOSURE AND BRAIN FUNCTIONAL CONNECTIVITY

Higher exposure to NO_x from birth to 2 years of age and from 2 to 5 years of age was related to 10 and 5 higher correlation coefficients between brain areas, respectively (e.g., 0.06 higher correlation coefficient between left STSd posterior area and left ventral diencephalon area [95% CI = 0.04 to 0.09]) per 20-μg/m^3 increase in NO_x, from birth to 2 years of age (Figure 7 and Appendix Table A11). Most of the brain connections associated with the exposure from birth to 2 years of age were interhemispheric. However, with exposure at 2 to 5 years of age, connections mainly occurred between brain regions of the same hemisphere. The identified regions for the two exposure windows were predominantly located in the auditory association, premotor, orbital and polar frontal, inferior parietal, and posterior cingulate cortices, in the ventral diencephalon, and in the MT+ Complex and Neighboring Visual Areas.

Higher exposure to NO_2 during pregnancy and from birth to 2 years of age was related to 12 and 8 higher correlation coefficients among brain areas, respectively (e.g., 0.08 higher correlation coefficient between left prostriate area and left V3A area [95% CI = 0.04 to 0.11] per 10-μg/m^3 increase in NO_2 during pregnancy) (Figure 7 and Appendix Table A11). Most brain connections during pregnancy occurred between brain regions of the same brain hemisphere. The identified regions were predominantly located in the auditory association, dorsolateral prefrontal, somatosensory and motor, anterior cingulate and medial prefrontal, dorsal stream visual, and insular and frontal opercular cortices.

Higher exposure to PM_{COARSE} from 2 to 5 years of age and from 5 to 9 years of age was related to a higher brain correlation coefficient only between 2 brain areas in both time periods. From 2 to 5 years of age, connectivity between the right lateral occipital 1 area and the right s32 area was 0.25 higher (95% CI = 0.15 to 0.34) per 5-μg/m^3 increase in PM_{COARSE}. From 5 to 9 years of age, connectivity was 0.23 higher (95% CI = 0.14 to 0.33) per 5-μg/m^3 increase in PM_{COARSE} (Figure 7 and Appendix Table A11). The identified regions were located in the anterior cingulate and medial prefrontal cortices and in the MT+ Complex and Neighboring Visual Areas region.

Higher exposure to $PM_{2.5}$absorbance from birth to 2 years of age and from 2 to 5 years of age was related to 70 and 13 higher correlation coefficients among brain areas, respectively

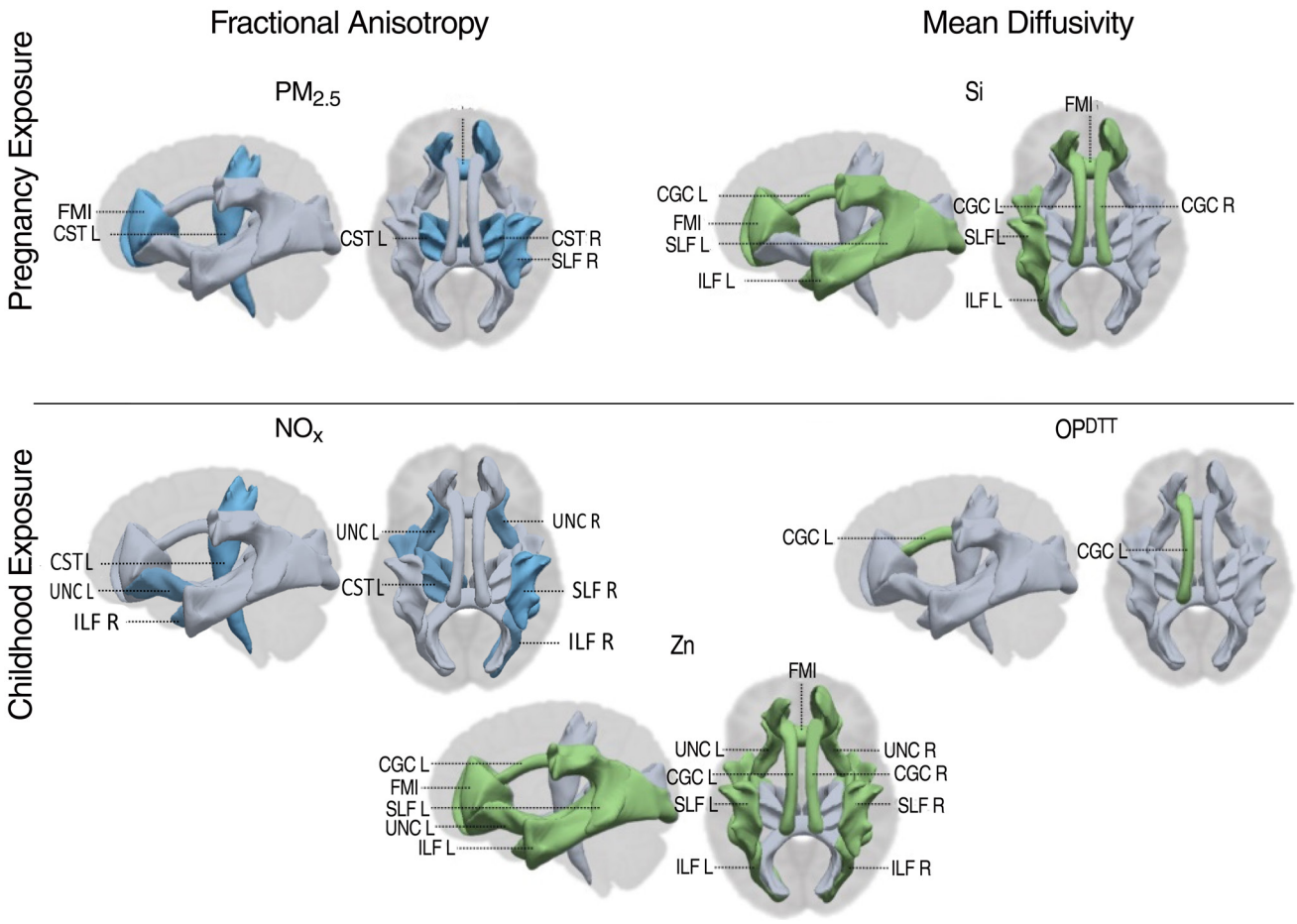

Figure 6. Adjusted associations in the twelve individual white matter tracts in pre-adolescents. Blue indicates negative coefficients and green indicates positive coefficients. Associations from linear regression models were adjusted for maternal and paternal education, ethnicity, age, height, body mass index, and psychological distress during pregnancy, maternal smoking and alcohol use during pregnancy, maternal parity, maternal intelligence quotient, family status, household income, and child's genetic ancestry, sex, and age at the scanning session. The expected direction of the association was higher air pollution exposure during pregnancy and childhood and lower global fractional anisotropy and higher global mean diffusivity. CGC-L = cingulum bundle left; CGC-R = cingulum bundle right; CST-L = corticospinal tract left; CST-R = corticospinal tract right; FMI = forceps minor; ILF-L = inferior longitudinal fasciculus left; ILF-R = inferior longitudinal fasciculus right SLF-L = superior longitudinal fasciculus left hemisphere; SLF-R = superior longitudinal fasciculus right hemisphere; UNC-L = uncinated fasciculus left hemisphere; UNC-R = uncinated fasciculus right hemisphere.

(e.g., 0.14 higher connectivity between left primary motor cortex and left auditory 4 complex [95% CI = 0.07 to 0.21] per each $10^{-5}m^{-1}$ increase of $PM_{2.5}$absorbance, from birth to 2 years of age) (Figure 7 and Appendix Table A11). Most brain connections using the exposure window from birth to 2 years of age group were interhemispheric. However, connections using the exposure window from 2 to 5 years of age mainly occurred between brain regions of the same brain hemisphere. The identified regions were predominantly located in the insular and frontal opercular, auditory association, lateral temporal, somatosensory and motor, anterior cingulate and medial prefrontal, and posterior cingulate cortices, and in the MT+ Complex and Neighboring Visual Areas.

Exposure to PM_{10} and $PM_{2.5}$ was not associated with brain functional connectivity.

DISCUSSION

MAIN FINDINGS

Air Pollution Exposure and Brain Structural Morphology

Exposure during pregnancy and childhood — brain volumes in school-age children and pre-adolescents We found that exposure to air pollution during pregnancy or childhood was not associated with global brain volumes in 6- to 10-year-old

Table 7. Adjusted Associations Between Exposure to Air Pollutants During Pregnancy and Childhood and Cortical Thickness and Cortical Surface in Pre-adolescents[a]

	Pregnancy Exposure[b]		Childhood Exposure[b]	
Brain Region – Hemisphere / Air Pollutant (per unit of change)	Region Size (mm^2)	Coefficient (95% CI)	Region Size (mm^2)	Coefficient (95% CI)
Cortical thickness (mm)				
Postcentral gyrus – Right				
OC (1 $\mu g/m^3$)	164	−0.06 (−0.11 to −0.01)	—	—
Rostral middle frontal gyrus — Right				
$PM_{2.5}$absorbance ($10^{-5}m^{-1}$)	174	−0.07 (−0.13 to −0.01)	—	—
Cu (5 ng/m^3)	198	−0.12 (−0.21 to −0.03)	—	—
Lingual gyrus – Left				
OP^{DTT} (1 nmol DTT/min/m^3)	—	—	177	−0.15 (−0.28 to −0.03)
Cortical surface (mm^2)				
Precentral gyrus – Right				
Zn (10 ng/m^3)	—	—	240	**0.01 (0.00 to 0.02)**
OP^{ESR} (1,000 units/m^3)	—	—	157	**0.02 (0.00 to 0.04)**
Pars triangularis – Right				
PM_{COARSE} (5 $\mu g/m^3$)	—	—	180	−0.10 (−0.18 to −0.02)
Precuneus – Left				
Zn (10 ng/m^3)	—	—	177	0.02 (0.01 to 0.04)
Pericalcarine cortex – Left				
Zn (10 ng/m^3)	—	—	289	0.02 (0.01 to 0.03)

[a] The expected direction of the association was higher air pollution exposure during pregnancy and childhood and smaller cortical thickness and smaller cortical surface area. — = not significant.

[b] Coefficients and 95% confidence intervals from linear regression models were adjusted for maternal and paternal education, ethnicity, age, height, body mass index, and psychological distress during pregnancy; maternal smoking and alcohol use during pregnancy; maternal parity, maternal intelligence quotient, family status, and household income; and child's genetic ancestry, sex, and age at the scanning session. All brain regions survived the correction for multiple testing (built-in Monte Carlo null-Z simulation with 10,000 iteration, P value < 0.001).

children and 9- to 12-year-old pre-adolescents. However, higher pregnancy or childhood exposures to several air pollutants were associated with a smaller corpus callosum and hippocampus and a larger amygdala, nucleus accumbens, and cerebellum in pre-adolescents, but not in school-age children (Table 9).

Corpus callosum, the largest white matter structure of the brain, is crucial for proper brain functional connectivity and cognitive processing (Hinkley et al. 2012). The volume of corpus callosum increases during the entire childhood (Durston et al. 2001), as we confirmed within our study population. We found that a higher exposure to the oxidative potential of $PM_{2.5}$ during pregnancy and to OC during childhood was associated with a smaller volume of the corpus callosum in pre-adolescents. In line with our results, a recent study found the same association between exposure to $PM_{2.5}$ during pregnancy and the corpus callosum in 8- to 12-year-old children (Mortamais et al. 2019). Another study in adults showed that cumulative exposure to $PM_{2.5}$, but not to diesel PM, was also associated with a smaller volume of the corpus callosum in women of approximately 70 years of age (Chen et al. 2017). Results from experimental studies support these findings (Allen et al. 2017; Klocke et al. 2017; Morris-Schaffer et al. 2019). They demonstrate that exposure to air pollution was associated with an increase in inflammatory reactions in the corpus callosum. Moreover, these inflammatory responses were paired with alterations in the size of the structure. It has also been shown that exposure to air pollution activates the hypothalamic–pituitary–

Table 8. Adjusted Associations Between Exposure to Air Pollutants During Pregnancy and Childhood and Global Fractional Anisotropy and Mean Diffusivity in Pre-adolescents[a]

Air Pollutant (per unit of change)	Global FA		Global MD	
	Pregnancy Exposure[b,c] Coefficient (95% CI)	Childhood Exposure[b,c] Coefficient (95% CI)	Pregnancy Exposure[b,c] Coefficient (95% CI)	Childhood Exposure[b,c] Coefficient (95% CI)
NO_x (20 μg/m^3)	**−0.11 (−0.20; −0.02)**	**−0.14 (−0.23;−0.04)**[d]	**0.01 (0.00; 0.02)**	**0.02 (0.01; 0.03)**
NO_2 (10 μg/m^3)	−0.11 (−0.25; 0.03)	**−0.13 (−0.25; −0.01)**	**0.02 (0.00; 0.04)**	**0.02 (0.00; 0.03)**
PM_{10} (10 μg/m^3)	**−0.49 (−0.90; −0.08)**	−0.45 (−0.91; 0.01)	**0.05 (0.00; 0.10)**	**0.07 (0.01; 0.12)**
PM_{COARSE} (5 μg/m^3)	−0.05 (−0.37; 0.27)	−0.29 (−0.63; 0.04)	0.03 (−0.01; 0.07)	**0.04 (0.00; 0.09)**
$PM_{2.5}$ (5 μg/m^3)	**−0.71 (−1.26; −0.16)**[d]	−0.46 (−1.14; 0.21)	**0.09 (0.02; 0.15)**	**0.11 (0.03; 0.20)**
$PM_{2.5}$absorbance ($10^{-5}m^{-1}$)	**−0.29 (−0.51; −0.07)**	**−0.27 (−0.51; −0.02)**	**0.04 (0.01; 0.06)**	**0.04 (0.01; 0.07)**
PAHs (1 ng/m^3)	0.01 (−0.19; 0.21)[d]	0.15 (−0.09; 0.38)	0.01 (−0.01; 0.04)	0.01 (−0.02; 0.04)
OC (1 μg/m^3)	−0.12 (−0.29; 0.05)	**−0.20 (−0.38; −0.03)**	0.02 (−0.01; 0.04)	0.02 (−0.00; 0.04)
Cu (5 ng/m^3)	−0.32 (−0.71; 0.06)	−0.22 (−0.65; 0.21)	**0.05 (0.01; 0.10)**	0.03 (−0.02; 0.09)
Fe (100 ng/m^3)	−0.20 (−0.54; 0.14)	−0.22 (−0.53; 0.09)	**0.05 (0.01; 0.09)**	0.03 (−0.01; 0.07)
Si (100 ng/m^3)	−0.28 (−0.70; 0.15)	−0.24 (−0.66; 0.19)	**0.07 (0.02; 0.12)**[d]	**0.05 (0.00; 0.11)**
Zn (10 ng/m^3)	−0.12 (−0.28; 0.04)	−0.13 (−0.27; 0.02)	0.01 (−0.01; 0.03)	**0.03 (0.01; 0.05)**[d]
OP^{DTT}(1nmol DTT/min/m^3)	0.21 (−0.34; 0.75)	−0.14 (−0.69; 0.42)	0.06 (−0.00; 0.13)	**0.09 (0.02; 0.16)**[d]
OP^{ESR} (1,000 units/m^3)	−0.19 (−0.55; 0.17)	−0.21 (−0.57; 0.16)	**0.04 (0.00; 0.09)**	0.04 (−0.00; 0.09)

[a] The expected direction of the association was higher air pollution exposure during pregnancy and childhood and lower global FA and higher global MD.

[b] Coefficients and 95% confidence intervals from linear regression models were adjusted for maternal and paternal education, ethnicity, age, height, body mass index, and psychological distress during pregnancy; maternal smoking and alcohol use during pregnancy; maternal parity, maternal intelligence quotient, family status, and household income; and child's genetic ancestry, sex, and age at the scanning session

[c] **Bolded values** indicate $P < 0.05$.

[d] The association was identified in the multipollutant approach (see Appendix Table A6). PM_{10} was not included (see Statistical Methods and Data Analysis) section.

adrenal axis and the neuroendocrine stress response (Thomson 2019), and that early life stress is associated with reductions in corpus callosum size in both experimental (Jackowski et al. 2011) and epidemiological studies (Teicher et al. 2004).

Higher exposure to PAHs during pregnancy and to the oxidative potential of $PM_{2.5}$ during childhood showed associations with a smaller volume of the hippocampus, while higher exposure to Si during pregnancy was associated with a larger volume of the amygdala in pre-adolescents. A previous epidemiological study in adults also found an association between a higher exposure to $PM_{2.5}$ and a smaller volume of the hippocampus (Hedges et al. 2019). Moreover, an experimental study showed that a higher exposure to ultrafine particles was related to alterations of the amygdala (Allen et al. 2017). The hippocampus increases in volume during childhood (Durston et al. 2001), and we confirmed this trend in our study population. A larger volume of the amygdala has previously been associated with behavior problems in pre-adolescents (Jones et al. 2019). The hippocampus and the amygdala are two subcortical structures from the limbic system and are involved in emotional regulation and encoding of emotional memories (Richardson et al. 2004). They are particularly sensitive to the effects of stress hormones and are subject to developmental programming by early life stress. Specifically, early life stress has been associated with a smaller volume of the hippocampus (Coe et al. 2003) and a larger volume of the amygdala (Salm et al. 2004) in animal models. These findings are consistent with epidemiological associations (Buss et al. 2012; Humphreys et al. 2019; Lupien et al. 2011). Finally, in the multipollutant model, higher exposure to PAHs and to OC during pregnancy was associated with a smaller volume of the amygdala, although these associations were not statistically significant in the single-pollutant analyses. One explanation for this unexpected result is that it could be a chance finding due to negative residual confounding of correlated exposures.

We observed an association between a higher exposure to Zn during childhood and a larger volume of the nucleus accumbens in pre-adolescents. The nucleus accumbens plays a key role in integrating cognitive and affective information (Floresco 2015), and its volume decreases across childhood (Wierenga et al.

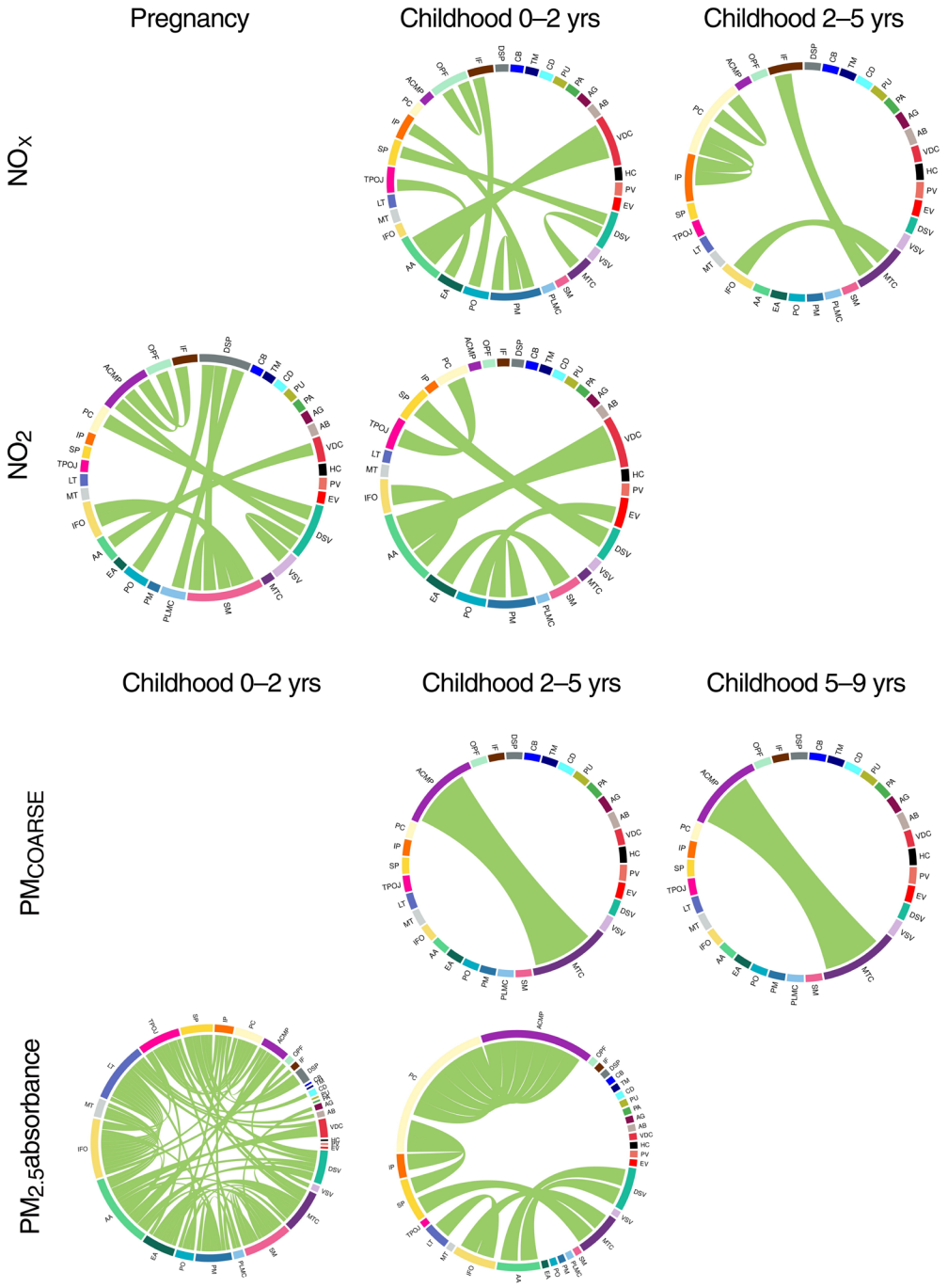

Figure 7. Adjusted associations between exposure to air pollutants during each time period and brain functional connectivity in pre-adolescents. Green indicates positive coefficients; thickness of the connection represents the strengths of the association. Associations from linear regression models were adjusted for maternal and paternal education, ethnicity, age, height, body mass index, and psychological distress during pregnancy, maternal smoking and alcohol use during pregnancy, maternal parity, maternal intelligence quotient, family status, household income, and child's genetic ancestry, sex, and age at the scanning session. All brain regions survived the correction for multiple testing using a false discovery rating. AA = auditory association; AB = nucleus accumbens; ACMP = anterior cingulate and medial prefrontal; AG = amygdala; CB = cerebellum; CD = caudate; DSP = dorsolateral prefrontal; DSV = dorsal stream visual; EA = early auditory; EV = early visual; HC = hippocampus; IF = inferior frontal; IFO = insular and frontal opercular; IP = inferior parietal; LT = lateral temporal; MT = medial temporal; MTC = MT+ complex and neighboring visual areas; OPF = orbital and polar frontal; PA = pallidum; PC = posterior cingulate; PLMC = paracentral lobular and mid cingulate; PM = premotor; PO = posterior opercular; PU = putamen; PV = primary visual; SM = somatosensory and motor; SP = superior parietal; TPOJ = temporo-parieto-occipital junction; TM = thalamus; VDC = ventral diencephalon; VSV = ventral stream visual.

Table 9. Summary Table of the Key Findings on the Associations of Exposure to Air Pollutants During Pregnancy and Childhood with Brain Structural Morphology, Structural Connectivity, and Functional Connectivity in School-Age Children and Pre-adolescents

	Direction of Association			Pollutant Analysis	
Outcome	Expected	Observed	Period	Single Pollutant	Multipollutant
Structural morphology					
Corpus callosum volume	−	−	Pregnancy	OP^{ESR}	OP^{ESR}
	−	−	Childhood	OC	OC
Putamen volume	+	+	Pregnancy	PM_{COARSE}	—
Pallidum volume	−	+	Pregnancy	PM_{COARSE}	—
Hippocampus volume	−	−	Pregnancy	PAHs, Cu	PAHs
	−	−	Childhood	PM_{COARSE}, OP^{DTT}	OP^{DTT}
Amygdala volume	+	+	Pregnancy	Si	Si
Nucleus accumbens volume	+	+	Childhood	Zn	Zn
Cerebellum volume	−	+	Pregnancy	PM_{10}, PM_{COARSE}, $PM_{2.5}$, $PM_{2.5}$absorbance	PM_{COARSE}
Cortical thickness	−	−	Pregnancy	$PM_{2.5}$, PM_{COARSE}, $PM_{2.5}$absorbance, OC, Cu	NA
	−	−	Childhood	OP^{DTT}	NA
Cortical surface area	−	+	Pregnancy	Zn, OPESR	NA
	−	−	Childhood	PM_{COARSE}	NA
Structural connectivity					
Fractional anisotropy	−	−	Pregnancy	NO_x, PM_{10}, $PM_{2.5}$, $PM_{2.5}$absorbance	$PM_{2.5}$
	−	−	Childhood	NO_x, NO_2, $PM_{2.5}$absorbance, OC	NO_x
Mean diffusivity	+	+	Pregnancy	NO_x, NO_2, PM_{10}, $PM_{2.5}$, $PM_{2.5}$absorbance, Cu, Fe, Si, OP^{ESR}	Si
	+	+	Childhood	NO_x, NO_2, PM_{10}, PM_{COARSE}, $PM_{2.5}$, $PM_{2.5}$absorbance, Si, Zn, OP^{DTT}	Zn, OP^{DTT}
Functional connectivity					
	?	+	Pregnancy	NO_2	NA
	?	+	Childhood	NO_x, NO_2, PM_{COARSE}, $PM_{2.5}$absorbance	NA

[a] NA = not applicable (correction for multiple testing applied in the single-pollutant analysis due to the large number of suboutcomes analyzed (~140,000–320,000 depending on the outcome).

2018), as we confirmed in our study population. The nucleus accumbens is also strongly impacted by stress signaling, receiving inputs from key stress-impacted regions of the brain, including the hippocampus and amygdala. Chronic stress has been associated with structural changes in experimental models (Bessa et al. 2013; Campioni et al. 2009; Muhammad et al. 2012) and with increased volume in individuals with major depressive disorder (Abdallah et al. 2017). A recent study has also found a cross-sectional association between exposure to $PM_{2.5}$ and a larger volume of the left nucleus accumbens (Cserbik et al. 2020). Moreover, animal studies suggested that exposure to air pollution produces neurotoxicity, oxidative stress, and inflammation in the nucleus accumbens and the striatum (Cory-Slechta et al. 2019; Kim et al. 2018).

We found an association between exposure to PM_{COARSE} during pregnancy and a larger volume of the cerebellum in pre-adolescents. This finding was unexpected considering that the volume of the cerebellum increases during childhood and starts decreasing between the ages of 7 and 12 in girls, and around 15.5 years in boys (Tiemeier et al. 2010; Wierenga et al. 2014). Early exposure to stress has been associated with a number of functional and structural changes in the cerebellum (Moreno-Rius 2019). In a controlled experimental study examining the impacts of early life stress, rhesus monkeys raised by peers instead of by their mothers had an enlarged cerebellar vermis (Spinelli et al. 2009). Several animal studies support a potential effect of exposure to air pollution on the cerebellum through oxidative stress and inflammation (Fagundes et al. 2015; Kim et al. 2018). Contrary to our findings, a recent study found an association between a higher exposure to $PM_{2.5}$ during the first year of life and a smaller volume of the cerebellum in 12-year-old children (Beckwith et al. 2020). In the multipollutant model, a higher exposure to the oxidative potential of $PM_{2.5}$ during pregnancy was associated with a smaller volume of the cerebellum. However, this association was not statistically significant in the single-pollutant analysis; thus, this result was most probably a chance finding due to negative residual confounding of correlated exposures.

We did not observe any associations of exposure to air pollution during pregnancy and childhood with global brain volumes in school-age children and pre-adolescents. However, other studies found associations with global brain measures both in children and adults (Beckwith et al. 2020; Calderón-Garcidueñas et al. 2008; Casanova et al. 2016; Chen et al. 2017; Erickson et al. 2020; Gale et al. 2020; Peterson et al. 2015; Wilker et al. 2015). Similarly, we did not find associations with any of the main basal ganglia structures (i.e., thalamus, caudate nucleus, putamen, pallidum), despite previous literature demonstrating such associations in human and animal studies (Brown et al. 2020; Casanova et al. 2016; Cserbik et al. 2020; Long et al. 2014; Mortamais et al. 2017; Power et al. 2018; Pujol et al. 2016a).

Exposure during pregnancy and childhood — cortical thickness and surface area in school-age children and pre-adolescents A higher exposure to several air pollutants, such as $PM_{2.5}$, PM_{COARSE}, $PM_{2.5}$absorbance, OC, and Cu, during pregnancy was associated with a thinner cortex in various regions of the brain in 6- to 10-year-old children and 9- to 12-year-old pre-adolescents (Table 9). A higher exposure to the oxidative potential of $PM_{2.5}$ during childhood was also associated with a thinner cortex in one region in pre-adolescents. Moreover, a higher exposure to air pollution, such as Zn and the oxidative potential of $PM_{2.5}$, during childhood was associated with a smaller surface area of the cortex in various regions of the brain in pre-adolescents. An exception was represented by a region where a higher exposure to PM_{COARSE} was associated with a larger surface area of the cortex in pre-adolescents.

Regions with a thinner cortex showed an overlap between school-age children and pre-adolescents. They were located in the anterior and middle regions of the right hemisphere and in the posterior region of the left hemisphere. The sizes of the identified areas in our study were rather small in pre-adolescents in particular, compared with school-age children, because of the less stringent correction for multiple testing in the latter. Another study also demonstrated that higher exposure to $PM_{2.5}$ during the first year of life was related with lesser cortical thickness in pre-adolescents (Beckwith et al. 2020). The identified cortical regions involved partially overlapped the regions identified in our study. However, a recent study found cross-sectional associations between higher exposure to $PM_{2.5}$ and both lesser and greater cortical thickness in pre-adolescents (Cserbik et al. 2020). Moreover, one study did not find an association between personal exposure to PAHs during the third trimester of pregnancy and any measure of cortical thickness (Peterson et al. 2015). In summary, although different studies present contradictory results, it seems that exposure to air pollution affects the gray matter of specific regions of the brain instead of having a more widespread effect. This could be due to the different timing of the developmental process of each brain region across childhood. For example, the cortical volume of the frontal lobe showed a relatively stable trajectory in late childhood and an accelerated thinning in adolescence (Tamnes et al. 2017). However, the cortical thickness of the parietal and occipital lobes showed a decelerating thinning with increasing age.

In pre-adolescents, a higher exposure to Zn and the oxidative potential of $PM_{2.5}$ during childhood was associated with a larger surface area of the precentral gyrus of the right hemisphere and of the precuneus and pericalcarine regions of the left hemisphere. However, a higher exposure to PM_{COARSE} during childhood was related to a smaller surface area of the pars triangularis of the right hemisphere. Another study found cross-sectional associations of a higher exposure to $PM_{2.5}$ with both larger and smaller surface areas in other brain regions of pre-adolescents (Cserbik et al. 2020). The observed discordant region-specific associations of air pollution with larger and smaller surface areas could reflect regional variations of the neurodevelopmental trajectories across early life.

A thinner cortex is generally considered a marker of impaired cortical structure, often being associated with neuropsychological disorders such as depression or schizophrenia (Marrus et al. 2015; van Erp et al. 2018). Nevertheless, the clinical implications of a larger or smaller surface area of the cortex in children are unclear. In the first years of life, an increase in the surface area of the brain is generally associated with healthy development. However, some patterns of brain maturation that take place between childhood and adolescence involve dynamic changes in both gray and white matter, with the surface area showing steady decreases (Houston et al. 2014; Lenroot and Giedd 2006; Tamnes et al. 2017). Thus, a larger surface area of the cortex could be a sign of a delayed maturation of the brain or inadequate synaptic pruning, rather than of healthy development in pre-adolescents. Nevertheless, many of the differences in brain structures observed at this age range could be of a transient nature (Sudre et al. 2018). Further studies will require repeated assessments of neuroimaging across childhood and adolescence.

Exposure during pregnancy — cortical thickness and cognitive function in school-age children This was the first study showing that a higher exposure to $PM_{2.5}$ during pregnancy was associated with an impaired inhibitory control, and that a thinner cortex in the precuneus and the rostral middle frontal regions partially mediated this association in 6- to 10-year-old children. Inhibitory control, a key component of executive functions, regulates the ability to resist temptations and impulsive actions and to perform attention-demanding tasks (i.e., selective attention) (Diamond and Ling 2016). Impaired inhibitory control has been related to several mental health problems such as addictive behaviors or attention deficit hyperactivity disorder (Jentsch and Pennington 2014; Ma et al. 2016). A previous study found that the white matter disruption partially mediated the association between a higher exposure to PAHs during pregnancy and a slower speed of information processing in children (Peterson et al. 2015). We hypothesize that exposure to air pollution exposure during pregnancy could lead to brain structural changes, and therefore, to specific cognitive delays. Unfortunately, we did not collect cognitive function assessments in pre-adolescents to test this hypothesis at later ages when more imaging parameters were available.

Air Pollution Exposure and Brain Structural Connectivity

We observed associations of a higher exposure to $PM_{2.5}$ and Si during pregnancy and to NO_x, Zn, and the oxidative potential of $PM_{2.5}$ during childhood with the white matter microstructure of 9- to 12-year-old pre-adolescents. We also observed associations of these air pollutants with projection, commissural, and association fibers of the FA tracts and with limbic, commissural, and association fibers of the MD tracts (Table 9).

Generally, the development of normal white matter microstructure is characterized by gradually increasing FA and decreasing MD. Therefore, the opposite is considered an indicator for atypical development and it has previously been associated with a number of psychiatric and neurological disorders (Aoki et al. 2017; van Ewijk et al. 2012; White et al. 2008). FA describes the propensity for enhanced water diffusion in the white matter tracts; whereas MD expresses the average water diffusion in every direction within brain tissue (Alexander et al. 2007). A lower FA and higher MD can be a result of several determining factors, such as lower packing and disturbance of internal structure of axons, higher permeability of the membrane, and decreased myelination (Lebel et al. 2019).

To our knowledge, there has been only one previous epidemiological study of associations between air pollution and white matter microstructure (Pujol et al. 2016a). In that study, exposure to higher concentrations of Cu at school was associated with higher FA in regions adjacent to the caudate nucleus in 8- to 12-year-old children. Similar to Zn, Cu reflects air pollution due to brake linings (Viana et al. 2008). In our study, we did not find a significant association between exposure to Cu during pregnancy or childhood and FA. The discrepancies in the results between the study of Pujol and colleagues and ours might be attributable to differences in various aspects: (1) an assessment of the exposure with respect to location and timing (school levels at 8 to 10 years of age vs. residential levels during pregnancy and from birth until 9 to 12 years of age); (2) Cu concentrations (8.7 ng/m^3 vs. 4.7 ng/m^3); and (3) sample size (263 vs. 2,954 children).

In the multipollutant model, a higher exposure to PAHs during pregnancy was associated with a higher FA, although this association was not statistically significant in the single-pollutant analyses. This unexpected result is most probably a chance finding due to negative residual confounding of correlated exposures.

Air Pollution Exposure and Brain Functional Connectivity

A higher exposure to NO_2 during pregnancy, to NO_x, NO_2, and $PM_{2.5}$absorbance from birth to 2 years of age, to NO_2, PM_{COARSE}, and $PM_{2.5}$absorbance from 2 to 5 years of age, and to PM_{COARSE} from 5 to 9 years of age were associated with higher brain functional connectivity among several brain areas in 9- to 12-year-old pre-adolescents (Table 9).

Areas with higher connectivity were located in regions that are part of the task negative, task positive, and somatosensory/motor networks. On one hand, the task negative network is highly active in inner mental processes and is negatively correlated to networks participating in attention-demanding tasks (Fox et al. 2005). In line with these findings, some previous studies also found an association of exposure to air pollution with impaired attentional function and inhibitory

control, which was measured using neuropsychological or computer tests (Basagaña et al. 2016; Chiu et al. 2013; Guxens et al. 2018; Pujol et al. 2016a; Sentís et al. 2017; Sunyer et al. 2015, 2017). The task positive network is activated during tasks that demands external attention and deactivated in the resting state, and it is negatively correlated with the task negative network (Blumenfeld 2016). The task positive and task negative networks should have an opposite relationship (i.e., the activation of one network would inhibit the other, to avoid the other's interference in the coordination of a neural process) (Cheng et al. 2020). Therefore, increased connectivity of the task positive network during resting conditions could be an indicator of functional brain connectivity impairment.

The somatosensory/motor network is activated during motor tasks, such as finger tapping, indicating that the regions of this network may involve a premediated state that readies the brain to perform or coordinate a motor task (Biswal et al. 1995). Consistent with these results, an association between exposure to air pollution and an impaired psychomotor function, in particular fine motor function, measured using neuropsychological tests or questionnaires, has been previously reported (Binter et al. [in review]; Guxens et al. 2014; Lubczyńska et al. 2017).

To our knowledge, previous evidence of an association between exposure to air pollution and brain functional connectivity has been limited to a single study that obtained results similar to ours (Pujol et al. 2016b). Higher exposure to NO_2 and elemental carbon at school was associated with higher functional connectivity between regions close in space, indicating a lower network segregation. Also, they were related to lower deactivation in the supplemental motor area and somatosensory cortex.

We have identified pregnancy and the first years of life as sensitive periods of exposure to air pollution for brain functional connectivity. Consistent findings from both fetal and neonatal rs-fMRI studies suggested that the foundations of resting-state networks are already laid down before birth, with rapid neural growth in the last trimester of pregnancy (Doria et al. 2010). However, some networks appear to be more developed than others. For example, functional connectivity of the visual and auditory networks is relatively mature, in comparison with other networks. Additionally, changes in network size, represented by the percentage change in brain volume, have been observed during the first years of life (Lin et al. 2008). Moreover, several resting-state networks exhibited a significant increase in functional connectivity and cerebral volumes of cortical connectivity. The development of connectivity networks during the early years of life could explain why exposures to air pollution during pregnancy and early childhood were related to more changes in brain functional connectivity during the rs-fMRI scan. From the age of two years onward, neurodevelopment is characterized by a gain in higher-order cognitive abilities, such as attention and memory; networks supporting these abilities show differences, reflecting a process of maturation (de Bie et al. 2012). Finally, it has been demonstrated that the interhemispheric functional connectivity between brain regions exists in healthy human fetuses from the last trimester of pregnancy (Thomason et al. 2013). This could explain why we found more interhemispheric connections in relation to exposure to air pollution during early childhood than during pregnancy.

Air Pollutants Related to Impaired Brain Development

In this project, we estimated the exposure to several air pollutants, and we applied a multipollutant approach with the aim to identify which air pollutants were related to impaired brain development in pre-adolescents. We observed that brain structural morphology, structural connectivity, or functional connectivity was associated with exposure to several air pollutants: NO_x, NO_2, PM of various size fractions (i.e., PM_{10}, PM_{COARSE}, and $PM_{2.5}$), $PM_{2.5}$absorbance, PAHs, OC, three elemental components of $PM_{2.5}$ (i.e., Cu, Si, Zn), and the oxidative potential of $PM_{2.5}$.

In Europe, the predominant source of NO_x and NO_2 gasses in the air is an incomplete combustion of hydrocarbons, manly originating from diesel fuel (Le et al. 2010). Higher exposure to diesel exhaust has been linked to numerous adverse health effects, such as an increased risk of neuroinflammation (Block et al. 2012).

PM is comprised of components that are directly emitted or formed through atmospheric chemical reactions involving gaseous precursors (U.S. EPA 2019). Within an urban environment, most PM emissions are from anthropogenic sources and include a combination of industrial activities, motor vehicles, cooking, and fuel combustion (U.S. EPA 2019). A higher exposure to PM of various size fractions has been associated with health effects in neurological and neuropsychological domains, among many others (U.S. EPA 2019). Higher exposure to $PM_{2.5}$ has been related to oxidative stress and neuroinflammation (Block et al. 2012; U.S. EPA 2019); whereas higher exposure to PM_{COARSE} has been associated with an activated hypothalamic–pituitary–adrenal stress axis and altered gene expressions in the brain (U.S. EPA 2019).

$PM_{2.5}$absorbance is a measure of the reflectance of the $PM_{2.5}$ filter, and it is highly correlated with elemental or black carbon, also referred to as "soot" (Cyrys et al. 2003). In urban settings, the main sources of $PM_{2.5}$absorbance are combustion engines (especially diesel) and residential wood burning (Janssen et al. 2012). Soot was one of the first air pollutants for which health effects were recognized (Bell and Davis 2001). In the last years, higher exposure to $PM_{2.5}$absorbance, or a related measure, have been related to several health effects, including neurodevelopment (Janssen et al. 2012; Suades-González et al. 2015).

PAHs are formed as a byproduct during an incomplete combustion of fossil fuels or other organic materials and have been linked to various acute and chronic health effects,

including neurological disorders (de Prado Bert et al. 2018; Kim et al. 2013; Suades-González et al. 2015).

OC is formed by incomplete combustion of diesel fuel and has been related to brain oxidative stress and cell inflammation (Manzo et al. 2010; Wilhelm et al. 2011).

Cu reflects air pollution due to brake linings (Viana et al. 2008). Although this element is necessary for cellular metabolism, abnormal Cu levels lead to relevant brain impairment (Scheiber et al. 2014). The deleterious effect of an excess of Cu is well-known from Wilson disease, an inherited metabolic disorder affecting the basal ganglia (Bandmann et al. 2015).

Si has not been documented as a potential neurotoxin to date. However, Si may be a marker of exposure to resuspended road dust (Viana et al. 2008). Associations with Si may therefore reflect associations with exposure to high traffic, rather than exposure to Si specifically.

Zn reflects air pollution due to brake linings and tire wear (Viana et al. 2008). Zn is a vital trace element for proper brain development and brain function later in life (Gower-Winter and Levenson 2012). However, its accumulation in the brain can cause excitotoxicity, oxidative stress, and impair cellular energy generation (Gower-Winter and Levenson 2012).

The oxidative potential of $PM_{2.5}$ is a quantification of the potentiality of fine particles to induce oxidative stress (Yang et al. 2015). The brain is an organ with a high oxygen depletion rate; it primarily comprises lipids, specifically in the white matter (O'Brien et al. 1964). Lipids are easily oxidized; moreover, because the brain lacks the solid defenses of antioxidants, it is vulnerable to lesions induced by oxidative stress (Salim 2017).

While understanding the health effects of exposure to an isolated pollutant is necessary and important, it is also clear that such a scenario does not reflect the actual outdoor conditions. Rather, humans are exposed to a mixture of pollutants, highlighting the importance of multipollutant approaches. Also, single-pollutant analyses may be affected by a high proportion of false-positive findings. However, multipollutant approaches also lead to methodological considerations that need to be addressed. The LUR models used in this project were developed using land-use predictors mainly related to traffic, such as distance to major roads and number of vehicles per time unit (Beelen et al. 2013; de Hoogh et al. 2013; Eeftens et al. 2012a; Jedynska et al. 2014b; Montagne et al. 2015; Yang et al. 2015). Therefore, to a large degree, the modeled estimates of exposure represent pollutants from traffic as their main source of origin. This results in high, and occasionally remarkably high, correlations between pollutants, which hinders the ability to identify the independent effects of specific pollutants in a complex mixture. Moreover, high correlations between pollutants increase the likelihood of collinearity when they are simultaneously analyzed. Collinearity has the tendency to increase the variance of one or more estimated regression coefficients (Vatcheva and Lee 2016). This might result in regression coefficients switching signs. To overcome this limitation, we applied the DSA algorithm as a multipollutant approach. This method is based on a relatively good trade-off between sensitivity and false discovery proportion, in comparison with other methods (Agier et al. 2016). It is an iterative selection method, which selects the exposures that are most predictive of the outcome by cross-validation, considering the correlation matrix of air pollutants, and simultaneously correcting for multiple testing. However, several limitations arose. First, when two variables are competing as predictors in a regression model, the variable estimated with a lower measurement error will be selected, even if the other is the one causally related to the outcome (Zidek et al. 1996). Second, this algorithm is based on a cross-validation process that is subjected to random variations. We ran each model 200 times and selected the final model based on the variables selected in at least 10% of the runs. However, these results might not be robust and stable, and the percentage of times a variable was selected should be considered when interpreting the results. Third, collinearity might still not be completely controlled, as we observed in some of our findings. Overall, our results might be less prone to false-positive findings, but they should be interpreted with caution and need to be replicated. Also, further research must apply other multipollutant approaches that consider interactions between air pollutants (Barrera-Gómez et al. 2017), evaluate the joint effect of the entire pollutant mixture (Keil et al. 2019), or apply other selection methods.

LIMITATIONS

All the research presented in this report was based on a prospective population-based birth cohort with a follow-up from the fetal period onward. The prospective nature of birth cohorts allows one to adequately assess the relationship between early life exposures and long-term health effects. Therefore, this is a highly valuable study design in environmental epidemiology. Nevertheless, we also encountered several limitations.

Air Pollution Exposure Assessment

Epidemiological studies require accurate data on exposure to correctly assess the relationships between exposure and health outcomes. In studies addressing health problems associated with air pollution, the exposure is often modeled to represent personal levels of the study population based on central measurements. Surely, personal monitoring of air pollution would be a more precise method to assess individual levels of exposure (Nieuwenhuijsen 2004). However, in cohort studies with many participants, the use of personal monitors would be highly labor-intensive and expensive (Nieuwenhuijsen 2004). Furthermore, since personal monitors are carried only for short periods of time, they could be less representative of long-term exposure, in comparison

with estimations of individual exposure through appropriate models. Additionally, personal measurements may have an inaccurate reflectance of exposures to outdoor sources, due to the time participants spent indoors exposed to indoor sources (Weisskopf and Webster 2017). Also, the levels of air pollution from outdoor exposures are regulated, so their potential effects on health are the ones truly relevant from a public health and policy perspective. Nevertheless, modeled exposure to air pollution is more likely to be prone to misclassification. In our project, we modeled air pollution to the individual level of home addresses of each participant, using LUR models based on validated measurements (Beelen et al. 2013; de Hoogh et al. 2013; Eeftens et al. 2012a; Jedynska et al. 2014b; Montagne et al. 2015; Yang et al. 2015). However, the temporal and spatial density of the sampling sites was quite limited. This could have impaired the accuracy of the estimates calculated from LUR models and may have led to over-smooth the prediction surfaces, particularly for some of the primary metals that likely have fine-scale variations. Also, LUR models were not fit using methods such as V-fold cross-validation to avoid overfitting and poor predictions at the home addresses of the participants. Another limitation was that sampling campaigns were carried out when children were between 3 and 8 years old. In most of the analysis, we did not perform temporal adjustments because we did not have historical pollutant data available. Therefore, we assumed that the spatial contrast of air pollution remained stable over time, although absolute levels may differ. This assumption was based on previous research supporting stability of spatial contrast in air pollution for periods up to 18 years (Eeftens et al. 2011; Gulliver et al. 2013). However, this assumption could lead to exposure misclassification. Also, for the analysis in which we extrapolated the levels to the specific periods of interest, an exposure error could have been introduced. Another source of misclassification emerged when a participant spent time away from home during hours of the day when air pollution levels were higher (e.g., at work during pregnancy, at school during childhood, and in commuting routes). Overall, our findings could be affected by nondifferential misclassification, resulting in a possible underestimation or dilution of the true association (Pollack et al. 2013). Lastly, Rotterdam hosts one of the largest seaports in the world with associated refineries located upwind of the study population. This could have had an impact on the pollution levels and mixtures. Nevertheless, LUR models were mainly built to capture pollutants deriving from road traffic sources. Therefore, they might have failed to accurately estimate the levels of air pollutants that were more affected by the emissions from the port.

Overall, one main limitation for the correct assessment for the exposure to air pollution is the possibility of introducing measurement error in the air pollution exposure estimates (Szpiro et al. 2011a). Measurement error is introduced when the modeled exposures are different from the actual measured exposures and comprises classical-like and Berkson-like error. Classical-like error arises from the uncertainty related to selection of the parameters of the estimation model for exposure, in our case the LUR model, and it may bias the estimates of the health effect. Also, it could potentially inflate the standard error of the health effect estimates. The Berkson-like error arises from smoothing the exposure surface. While it causes little to no bias in the measurements, it may inflate the standard error of the health effect estimates (Szpiro et al. 2011b). We investigated to what extent the measurement error affected the health effect estimates that we obtained from the association of exposure to air pollution during pregnancy and childhood with white matter microstructure. We took advantage of the availability of the actual measurements of most of the air pollutants to quantify the error in the LUR models that we used to estimate individual levels of exposure. This way, we quantified the uncertainty in the exposure–outcome association (Szpiro et al. 2011b). We observed that the bias introduced in the estimated standard errors was small. However, these results may be influenced by the relatively small number of measurement sites included in our project.

Single Time Point for Outcome Data

One main limitation of our project is the lack of repeated measures. We performed two MRI waves, one at school-age and one at pre-adolescence, but information from both waves was only available for 387 children. Moreover, the use of a different scanner in each wave made the comparison between the measurements difficult. Repeated MRI measurements would have allowed us to analyze changes in brain morphology and connectivity related to the exposure over time; therefore, it would have increased the feasibility of causal inference (Rothman and Greenland 2005). The ongoing Generation R study just finished a third wave of MRI measurements on the same children who are now 13–17 years old, using the same scanner. This will allow us to pursue longitudinal analyses in the near future.

We aimed to establish a temporal relationship between exposure and outcome to represent exposures during pregnancy and during childhood prior to the MRI assessment. Moreover, we performed mediation analysis to understand whether the observed brain alterations could partially explain the association between exposure to air pollution and cognitive function in school-age children. Nevertheless, such approaches were insufficient to infer causality, as the dynamic processes of the brain could not be modeled. Therefore, we cannot discard that the alterations observed in our study were already present at earlier ages.

Confounding

The prospective nature of birth cohorts allows one to generate a rich database of potential confounding variables,

including various socioeconomic and lifestyle characteristics of children and parents. In turn, this allows one to adjust the final models accordingly. Despite the availability of many potential confounding variables in our studies, we cannot discard the possibility of residual confounding. There might be variables that we either did not consider, or that we considered but were unable to include because of poor measurement or lack of measurement. For example, we may not have a perfect control on the socioeconomic status, and on the genetic and family factors related to brain development. Therefore, residual confounding could have introduced bias, finally leading to incorrectly estimate the main associations and to further hinder causal inference (Weisskopf et al. 2018). Also, although we performed multiple imputation of the missing potential confounding variables, some of them had a high level of missingness (30% to 50%). The validity of results from multiple imputation data relies on using appropriate models to impute the missing values. Therefore, we carefully generated the imputation models, using as predictors variables that were moderately to strongly correlated with the missing potential confounding variables. Moreover, we performed appropriate checks of the imputation models.

Generalizability

A goal of research in public health is to apply the results to the target population (i.e., the original population from which the study sample is selected). However, in most epidemiological studies, the study sample is not randomly chosen from the target population, and this limits the generalizability of the results. In the Generation R study, the overall response rate at recruitment was 61% (Jaddoe et al. 2006). Educational level and house income of the participating mothers was higher in comparison to the target population, whereas ethnic distribution only moderately differed (Jaddoe et al. 2006). In our project, we included two study samples, one selected among school-age children and one among pre-adolescents. None of them was randomly chosen from the population initially recruited in the cohort. The population of school-age children was oversampled based on certain maternal exposures during pregnancy and children's behavior problems. The population of pre-adolescents was represented by the families that agreed to participate in the brain MRI substudy. The resulting samples presented slightly different characteristics from the initial population; in particular, children were more likely to have parents who were older, had a higher education level, a higher household income, and Dutch ethnicity. However, school-age children included in the first sample did not differ from the initial population for characteristics like maternal smoking during pregnancy and psychological distress, thanks to the oversampling. On the contrary, pre-adolescents included in the second sample differed in these same characteristics because of an attrition effect toward a healthier population. We applied inverse probability weighting to correct for selection bias and estimate unbiased inferences for the initial population in the cohort. However, we applied inverse probability weighting using the data collected in the study, and therefore it remains unknown whether we have fully eliminated this type of bias. Also, we were not able to calculate inverse probability weights considering the target population characteristics. This limited the generalizability of our results slightly.

CONCLUSIONS

We identified several air pollutants associated with brain structural morphology, structural connectivity, and functional connectivity. These pollutants included NO_x, NO_2, PM of various size fractions (i.e., PM_{10}, PM_{COARSE}, and $PM_{2.5}$), $PM_{2.5}$absorbance, PAHs, OC, three elemental components of $PM_{2.5}$ (i.e., Cu, Si, Zn), and the oxidative potential of $PM_{2.5}$.

In relation to brain structural morphology, we observed that exposure to air pollution during pregnancy or childhood was not associated with global brain volumes, neither in school-age children nor in pre-adolescents. However, it was related to alterations in region-specific volumes in pre-adolescents. We also found that exposure to air pollution during pregnancy or childhood was associated with a thinner cortex in both school-age children and pre-adolescents and with alterations of the cortical surface area in pre-adolescents. A thinner cortex mediated the association between exposure to air pollution during pregnancy and an impaired inhibitory control in school-age children.

In relation to brain structural connectivity, we observed associations of exposure to air pollution during pregnancy and childhood with white matter microstructure in pre-adolescents. Finally, in relation to brain functional connectivity, we observed associations of exposure to air pollution mainly during pregnancy and early childhood with higher brain functional connectivity among several brain regions in pre-adolescents.

IMPLICATIONS OF FINDINGS

The results of this project suggest that exposure to air pollution during pregnancy and childhood plays an adverse role in brain development. We observed this relationship even at levels of exposure that were below the European Union legislations, such as the levels of exposure for $PM_{2.5}$ in most of our study population. Considering the ubiquity of air pollution and the involuntary nature of the exposure to it, policy makers should lower the current legislated standards and, above all, strive to lower the levels of air pollution.

Moreover, the air pollutants analyzed in this project originate mainly from traffic-related sources that are highly ubiquitous in urban areas and that put a large number of children at risk. We acknowledge that identifying the effects of specific

pollutants was particularly challenging in our study setting. Also, most of our conclusions generally refer to traffic-related air pollutants. However, we did identify pollutants specifically originating from brake linings, tire wear, and tailpipe emissions from diesel combustion. The current direction toward innovative solutions for cleaner energy vehicles is a step in the right direction. However, our findings indicate that these measures might not be completely adequate to mitigate health problems attributable to traffic-related air pollution, as we also observed associations with markers of brake linings and tire wear.

ACKNOWLEDGEMENTS

The Generation R Study is conducted by the Erasmus Medical Center in close collaboration with the School of Law and Faculty of Social Sciences of the Erasmus University Rotterdam, the Municipal Health Service Rotterdam area, Rotterdam, the Rotterdam Homecare Foundation, Rotterdam and the Stichting Trombosedienst & Artsenlaboratorium Rijnmond (STAR-MDC), Rotterdam. We gratefully acknowledge the contribution of children and parents, general practitioners, hospitals, midwives, and pharmacies in Rotterdam. The general design of Generation R Study is made possible by financial support from the Erasmus Medical Center, Rotterdam, the Erasmus University Rotterdam, the Netherlands Organization for Health Research and Development (ZonMw), the Netherlands Organization for Scientific Research (NWO), and the Ministry of Health, Welfare and Sport. Air pollution exposure assessment was possible by funding from the European Community's Seventh Framework Program (GA#211250, GA#243406). In addition, the study was made possible by financial support from the Netherlands Organization for Health Research and Development (ZonMW Geestkracht Program 10.000.1003 & ZonMw TOP 40-00812-98-11021). The neuroimaging infrastructure was funded via TOP project number 91211021 to Tonya White and supercomputing computations for imaging processing were supported by the NWO Physical Sciences Division (Exacte Wetenschappen) and SURFsara (Lisa compute cluster, *www.surfsara.nl*). Henning Tiemeier received funding from the Netherlands Organization for Health Research and Development (NWO-grant 016.VICI.170.200). Hanan El Marroun received funding from the European Union's Horizon 2020 research and innovation programme under grant agreement No. 633595 (DynaHEALTH) and No. 733206 (LifeCycle). The Erasmus University Rotterdam granted Hanan El Marroun a personal fellowship (EUR Fellow 2014) and supported this work financially. Mònica Guxens is funded by a Miguel Servet fellowship (MS13/00054, CP13/00054, CPII18/00018) awarded by the Spanish Institute of Health Carlos III. We acknowledge support from the Spanish Ministry of Science and Innovation and State Research Agency through the "Centro de Excelencia Severo Ochoa 2019–2023" Program (CEX2018-000806-S) and support from the Generalitat de Catalunya through the CERCA Program.

REFERENCES

Abdallah CG, Jackowski A, Salas R, Gupta S, Sato JR, Mao X, et al. 2017. The nucleus accumbens and ketamine treatment in major depressive disorder. Neuropsychopharmacology 42:1739–1746; doi:10.1038/npp.2017.49.

Agier L, Portengen L, Hyam MC, Basagaña X, Allemand LG, Siroux V, et al. 2016. A systematic comparison of linear regression–based statistical methods to assess exposome-health associations. Environ Health Perspect 124:1848–1856; doi:10.1289/EHP172.

Alexander AL, Lee JE, Lazar M, Field AS. 2007. Diffusion tensor imaging of the brain. Neurotherapeutics 4:316–329; doi:10.1016/j.nurt.2007.05.011.

Allen JL, Oberdorster G, Morris-Schaffer K, Wong C, Klocke C, Sobolewski M, et al. 2017. Developmental neurotoxicity of inhaled ambient ultrafine particle air pollution: Parallels with neuropathological and behavioral features of autism and other neurodevelopmental disorders. Neurotoxicology 59:140–154; doi:10.1016/j.neuro.2015.12.014.

Aoki Y, Yoncheva YN, Chen B, Nath T, Sharp D, Lazar M, et al. 2017. Association of white matter structure with autism spectrum disorder and attention-deficit/hyperactivity disorder. JAMA Psychiatry 74:1120–1128; doi:10.1001/jamapsychiatry.2017.2573.

Bandmann O, Weiss KH, Kaler SG. 2015. Wilson's disease and other neurological copper disorders. Lancet Neurol 14:103–113; doi:10.1016/S1474-4422(14)70190-5.

Barrera-Gómez J, Agier L, Portengen L, Chadeau-Hyam M, Giorgis-Allemand L, Siroux V, et al. 2017. A systematic comparison of statistical methods to detect interactions in exposome-health associations. Environ Heal 16; doi:10.1186/s12940-017-0277-6.

Basagaña X, Esnaola M, Rivas I, Amato F, Alvarez-Pedrerol M, Forns J, et al. 2016. Neurodevelopmental deceleration by urban fine particles from different emission sources: A longitudinal observational study. Environ Health Perspect 124:1630–1636; doi:10.1289/EHP209.

Beckwith T, Cecil K, Altaye M, Severs R, Wolfe C, Percy Z, et al. 2020. Reduced gray matter volume and cortical thickness associated with traffic-related air pollution in a longitudinally studied pediatric cohort. PLoS One 15; doi:10.1371/journal.pone.0228092.

Beelen R, Hoek G, Vienneau D, Eeftens M, Dimakopoulou K, Pedeli X, et al. 2013. Development of NO_2 and NO_x land use regression models for estimating air pollution exposure in 36 study areas in Europe - The ESCAPE project. Atmos Environ 72:10–23.

Bell ML, Davis DL. 2001. Reassessment of the lethal London fog of 1952: Novel indicators of acute and chronic conse-

quences of acute exposure to air pollution. Environ Health Perspect 109:389–394; doi:10.1289/ehp.01109s3389.

Bessa JM, Morais M, Marques F, Pinto L, Palha JA, Almeida OFX, et al. 2013. Stress-induced anhedonia is associated with hypertrophy of medium spiny neurons of the nucleus accumbens. Transl Psychiatry 3; doi:10.1038/tp.2013.39.

Binter A, Bernard JY, Mon-Williams M, Andiarena A, González-Safont L, Vafeiadi, M, et al. 2021. Urban environment and cognitive and motor function in children from four European birth cohorts. Environ Int 158:106933.

Biswal B, Yetkin FZ, Haughton VM, Hyde JS. 1995. Functional connectivity in the motor cortex of resting human brain using echo–planar MRI. Magn Reson Med 34:537–541; doi:10.1002/mrm.1910340409.

Block ML, Elder A, Auten RL, Bilbo SD, Chen H, Chen JC, et al. 2012. The outdoor air pollution and brain health workshop. Neurotoxicology 33:972–984.

Blumenfeld H. 2016. Neuroanatomical basis of consciousness. In: The Neurology of Consciousness, Second Edition (Laureys S, Gosseries O, Tononi G, eds). Cambridge, MA:Academic Press, 3–29.

Bové H, Bongaerts E, Slenders E, Bijnens EM, Saenen ND, Gyselaers W, et al. 2019. Ambient black carbon particles reach the fetal side of human placenta. Nat Commun 10:3866.

Brooks BL, Sherman EMS, Strauss E. 2010. NEPSY-II: A Developmental neuropsychological assessment, second edition. Child Neuropsychol 16:80–101; doi:10.1080/09297040903146966.

Brown BL, Hedges DW, Erickson LD, Gale SD, Anderson JE. 2020. Association between exposure to air pollution and thalamus volume in adults: A cross-sectional study. PLoS One 15; doi:10.1371/journal.pone.0230829.

Brunekreef B. 2008. ESCAPE Study Manual. Available: *http://www.escapeproject.eu/manuals/ESCAPE-Study-manual_x007E_final.pdf* [accessed 4 April 2020].

Brunekreef B. 2010. ESCAPE Exposure Assessment Manual. Available: *http://www.escapeproject.eu/manuals/ESCAPE_Exposure-manualv9.pdf* [accessed 4 April 2020].

Brunekreef B. 2012. ESCAPE Procedure for Extrapolation Back in Time. Available: *http://www.escapeproject.eu/manuals/Procedure_for_extrapolation_back_in_time.pdf* [accessed 4 April 2020].

Buss C, Davis EP, Shahbaba B, Pruessner JC, Head K, Sandman CA. 2012. Maternal cortisol over the course of pregnancy and subsequent child amygdala and hippocampus volumes and affective problems. Proc Natl Acad Sci U S A 109; doi:10.1073/pnas.1201295109.

Calderón-Garcidueñ L, Mora-Tiscareño A, Ontiveros E, Gómez-Garza G, Barragán-Mejía G, Broadway J, et al. 2008. Air pollution, cognitive deficits and brain abnormalities: A pilot study with children and dogs. Brain Cogn 68:117–127; doi:10.1016/j.bandc.2008.04.008.

Campioni MR, Xu M, McGehee DS. 2009. Stress-induced changes in nucleus accumbens glutamate synaptic plasticity. J Neurophysiol 101:3192–3198; doi:10.1152/jn.91111.2008.

Carvalho MA, Bernardes LS, Hettfleisch K, Pastro LDM, Vieira SE, Saldiva SRDM, et al. 2016. Associations of maternal personal exposure to air pollution on fetal weight and fetoplacental Doppler: A prospective cohort study. Reprod Toxicol 62:9–17; doi:10.1016/j.reprotox.2016.04.013.

Casanova R, Wang X, Reyes J, Akita Y, Serre ML, Vizuete W, et al. 2016. A voxel-based morphometry study reveals local brain structural alterations associated with ambient fine particles in older women. Front Hum Neurosci 10; doi:10.3389/fnhum.2016.00495.

Cavanna AE, Trimble MR. 2006. The precuneus: A review of its functional anatomy and behavioural correlates. Brain 129:564–583; doi:10.1093/brain/awl004.

Chayer C, Freedman M. 2001. Frontal lobe functions. Curr Neurol Neurosci Rep 1:547–552; doi:10.1007/s11910-001-0060-4.

Chen J-C, Wang X, Serre M, Cen S, Franklin M, Espeland M. 2017. Particulate air pollutants, brain structure, and neurocognitive disorders in older women. Research Report 193. Boston, MA:Health Effects Institute.

Cheng X, Yuan Y, Wang Y, Wang R. 2020. Neural antagonistic mechanism between default-mode and task-positive networks. Neurocomputing 417:74–85; doi:10.1016/j.neucom.2020.07.079.

Chiu YHM, Bellinger DC, Coull BA, Anderson S, Barber R, Wright RO, et al. 2013. Associations between traffic-related black carbon exposure and attention in a prospective birth cohort of urban children. Environ Health Perspect 121:859–864; doi:10.1289/ehp.1205940.

Coe CL, Kramer M, Czéh B, Gould E, Reeves AJ, Kirschbaum C, et al. 2003. Prenatal stress diminishes neurogenesis in the dentate gyrus of juvenile Rhesus monkeys. Biol Psychiatry 54:1025–1034; doi:10.1016/S0006-3223(03)00698-X.

Cohen AJ, Brauer M, Burnett R, Anderson HR, Frostad J, Estep K, et al. 2017. Estimates and 25-year trends of the global burden of disease attributable to ambient air pollution: An analysis of data from the Global Burden of Diseases Study 2015. Lancet 389:1907–1918; doi:10.1016/S0140-6736(17)30505-6.

Cook PA, Bai Y, Nedjati-Gilani S, Seunarine KK, Hall MG, Parker GJ, et al. 2006. Camino: Open-source diffusion-MRI reconstruction and processing. Proc Intl Soc Mag Reson Med 14:2759.

Cory-Slechta DA, Sobolewski M, Marvin E, Conrad K, Merrill A, Anderson T, et al. 2019. The impact of inhaled ambient

ultrafine particulate matter on developing brain: Potential importance of elemental contaminants. Toxicol Pathol 47:976–992; doi:10.1177/0192623319878400.

Costa LG, Cole TB, Coburn J, Chang YC, Dao K, Roqué PJ. 2017. Neurotoxicity of traffic-related air pollution. Neurotoxicology 59:133–139; doi:10.1016/j.neuro.2015.11.008.

Costa LG, Cole TB, Dao K, Chang YC, Garrick JM. 2019. Developmental impact of air pollution on brain function. Neurochem Int 131:104580; doi:10.1016/j.neuint.2019.104580.

Cserbik D, Chen JC, McConnell R, Berhane K, Sowell ER, Schwartz J, et al. 2020. Fine particulate matter exposure during childhood relates to hemispheric-specific differences in brain structure. Environ Int 143; doi:10.1016/j.envint.2020.105933.

Cyrys J, Eeftens M, Heinrich J, Ampe C, Armengaud A, Beelen R, et al. 2012. Variation of NO_2 and NO_x concentrations between and within 36 European study areas: Results from the ESCAPE study. Atmos Environ 62:374–390; doi:10.1016/j.atmosenv.2012.07.080.

Cyrys J, Heinrich J, Hoek G, Meliefste K, Lewné M, Gehring U, et al. 2003. Comparison between different traffic-related particle indicators: Elemental carbon (EC), $PM_{2.5}$ mass, and absorbance. J Expo Anal Environ Epidemiol 13:134–143; doi:10.1038/sj.jea.7500262.

De Beurs E. 2004. Brief Symptom Inventory, handleiding [in Dutch]. Leiden, the Netherlands;PITS B.V.

de Bie HMA, Boersma M, Adriaanse S, Veltman DJ, Wink AM, Roosendaal SD, et al. 2012. Resting-state networks in awake five- to eight-year old children. Hum Brain Mapp 33:1189–1201; doi:10.1002/hbm.21280.

de Groot M, Ikram MA, Akoudad S, Krestin GP, Hofman A, van der Lugt A, et al. 2015. Tract-specific white matter degeneration in aging: the Rotterdam Study. Alzheimers Dement 11:321–330; doi:10.1016/j.jalz.2014.06.011.

de Hoogh K, Wang M, Adam M, Badaloni C, Beelen R, Birk M, et al. 2013. Development of land use regression models for particle composition in twenty study areas in Europe. Environ Sci Technol 47:5778–5786; doi:10.1021/es400156t.

de Prado Bert P, Mercader EMH, Pujol J, Sunyer J, Mortamais M. 2018. The effects of air pollution on the brain: A review of studies interfacing environmental epidemiology and neuroimaging. Curr Environ Heal Rep 5:351–364; doi:10.1007/s40572-018-0209-9.

Desikan RS, Ségonne F, Fischl B, Quinn BT, Dickerson BC, Blacker D, et al. 2006. An automated labeling system for subdividing the human cerebral cortex on MRI scans into gyral based regions of interest. Neuroimage 31:968–980; doi:10.1016/j.neuroimage.2006.01.021.

Diamond A, Ling DS. 2016. Conclusions about interventions, programs, and approaches for improving executive functions that appear justified and those that, despite much hype, do not. Dev Cogn Neurosci 18:34–48; doi:10.1016/j.dcn.2015.11.005.

Donzelli G, Llopis-Gonzalez A, Llopis-Morales A, Cioni L, Morales-Suárez-varela M. 2020. Particulate matter exposure and attention-deficit/hyperactivity disorder in children: A systematic review of epidemiological studies. Int J Environ Res Public Health 17:pii:E67; doi:10.3390/ijerph17010067.

Doria V, Beckmann CF, Arichi T, Merchant N, Groppo M, Turkheimer FE, et al. 2010. Emergence of resting state networks in the preterm human brain. Proc Natl Acad Sci U S A 107:20015–20020; doi:10.1073/pnas.1007921107.

Durston S, Hulshoff Pol HE, Casey BJ, Giedd JN, Buitelaar JK, Van Engeland H. 2001. Anatomical MRI of the developing human brain: What have we learned? J Am Acad Child Adolesc Psychiatry 40:1012–1020; doi:10.1097/00004583-200109000-00009.

Eeftens M, Beelen R, De Hoogh K, Bellander T, Cesaroni G, Cirach M, et al. 2012a. Development of land use regression models for $PM_{2.5}$, $PM_{2.5}$absorbance, PM_{10} and PM_{COARSE} in 20 European study areas; Results of the ESCAPE project. Environ Sci Technol 46:11195–11205; doi:10.1021/es301948k.

Eeftens M, Beelen R, Fischer P, Brunekreef B, Meliefste K, Hoek G. 2011. Stability of measured and modelled spatial contrasts in NO_2 over time. Occup Environ Med 68:765–770; doi:10.1136/oem.2010.061135.

Eeftens M, Tsai MY, Ampe C, Anwander B, Beelen R, Bellander T, et al. 2012b. Spatial variation of $PM_{2.5}$, PM_{10}, $PM_{2.5}$absorbance and PM_{COARSE} concentrations between and within 20 European study areas and the relationship with NO_2 — Results of the ESCAPE project. Atmos Environ 62:303–317; doi:10.1016/j.atmosenv.2012.08.038.

Erickson LD, Gale SD, Anderson JE, Brown BL, Hedges DW. 2020. Association between exposure to air pollution and total gray matter and total white matter volumes in adults: A cross-sectional study. Brain Sci 10; doi:10.3390/brainsci10030164.

Esteban O, Markiewicz CJ, Blair RW, Moodie CA, Isik AI, Erramuzpe A, et al. 2019. fMRIPrep: A robust preprocessing pipeline for functional MRI. Nat Methods 16:111–116; doi:10.1038/s41592-018-0235-4.

European Environment Agency. 2019. Air quality in Europe: 2019 report. EEA Report No 10/2019. Available: *https://www.eea.europa.eu/publications/air-quality-in-europe-2019* [accessed 15 June 2021].

Fagundes LS, Fleck ADS, Zanchi AC, Saldiva PHN, Rhoden CR. 2015. Direct contact with particulate matter increases oxidative stress in different brain structures. Inhal Toxicol 27:462–467; doi:10.3109/08958378.2015.1060278.

Fischl B. 2012. FreeSurfer. Neuroimage 62:774–781; doi:10.1016/j.neuroimage.2012.01.021.

Floresco SB. 2015. The Nucleus Accumbens: An Interface Between Cognition, Emotion, and Action. Annu Rev Psychol 66:25–52; doi:10.1146/annurev-psych-010213-115159.

Fox MD, Snyder AZ, Vincent JL, Corbetta M, Van Essen DC, Raichle ME. 2005. The human brain is intrinsically organized into dynamic, anticorrelated functional networks. Proc Natl Acad Sci U S A 102:9673–9678; doi:10.1073/pnas.0504136102.

Fuhrmann D, Knoll LJ, Blakemore SJ. 2015. Adolescence as a sensitive period of brain development. Trends Cogn Sci 19:558–566; doi:10.1016/j.tics.2015.07.008.

Gale SD, Erickson LD, Anderson JE, Brown BL, Hedges DW. 2020. Association between exposure to air pollution and prefrontal cortical volume in adults: A cross-sectional study from the UK biobank. Environ Res 185; doi:10.1016/j.envres.2020.109365.

Glasser MF, Coalson TS, Robinson EC, Hacker CD, Harwell J, Yacoub E, et al. 2016. A multi-modal parcellation of human cerebral cortex. Nature 536:171–178; doi:10.1038/nature18933.

Gower-Winter SD, Levenson CW. 2012. Zinc in the central nervous system: From molecules to behavior. BioFactors 38:186–193; doi:10.1002/biof.1012.

Gulliver J, De Hoogh K, Hansell A, Vienneau D. 2013. Development and back-extrapolation of NO_2 land use regression models for historic exposure assessment in Great Britain. Environ Sci Technol 47:7804–7811; doi:10.1021/es4008849.

Guxens M, Garcia-Esteban R, Giorgis-Allemand L, Forns J, Badaloni C, Ballester F, et al. 2014. Air pollution during pregnancy and childhood cognitive and psychomotor development: Six European birth cohorts. Epidemiology 25:636–647; doi:10.1097/EDE.0000000000000133.

Guxens M, Lubczyńska MJ, Muetzel RL, Dalmau-Bueno A, Jaddoe VWV, Hoek G, et al. 2018. Air pollution exposure during fetal life, brain morphology, and cognitive function in school-age children. Biol Psychiatry 84:295–303; doi:10.1016/j.biopsych.2018.01.016.

Hedges DW, Erickson LD, Kunzelman J, Brown BL, Gale SD. 2019. Association between exposure to air pollution and hippocampal volume in adults in the UK Biobank. Neurotoxicology 74:108–120; doi:10.1016/j.neuro.2019.06.005.

Hernán MA, Hernández-Diaz S, Werler MM, Mitchell AA. 2002. Causal knowledge as a prerequisite for confounding evaluation: An application to birth defects epidemiology. Am J Epidemiol 155:176–184; doi:10.1093/aje/155.2.176.

Herting MM, Younan D, Campbell CE, Chen J-C. 2019. Outdoor air pollution and brain structure and function from across childhood to young adulthood: A methodological review of brain MRI studies. Front Public Heal 7:332; doi:10.3389/fpubh.2019.00332.

Hettfleisch K, Bernardes LS, Carvalho MA, Pastro LDM, Vieira SE, Saldiva SRDM, et al. 2017. Short-term exposure to urban air pollution and influences on placental vascularization indexes. Environ Health Perspect 125:753–759; doi:10.1289/EHP300.

Hinkley LBN, Marco EJ, Findlay AM, Honma S, Jeremy RJ, Strominger Z, et al. 2012. The role of corpus callosum development in functional connectivity and cognitive processing. PLoS One 7; doi:10.1371/journal.pone.0039804.

Houston SM, Herting MM, Sowell ER. 2014. The neurobiology of childhood structural brain development: Conception through adulthood. Curr Top Behav Neurosci 16:3–17; doi:10.1007/7854_2013_265.

Humphreys KL, King LS, Sacchet MD, Camacho MC, Colich NL, Ordaz SJ, et al. 2019. Evidence for a sensitive period in the effects of early life stress on hippocampal volume. Dev Sci 22; doi:10.1111/desc.12775.

Jackowski A, Perera TD, Abdallah CG, Garrido G, Tang CY, Martinez J, et al. 2011. Early life stress, corpus callosum development, hippocampal volumetrics, and anxious behavior in male nonhuman primates. Psychiatry Res - Neuroimaging 192:37–44; doi:10.1016/j.pscychresns.2010.11.006.

Jaddoe VWV, Mackenbach JP, Moll HA, Steegers EAP, Tiemeier H, Verhulst FA, et al. 2006. The Geenration R Study: Design and cohort profile. Eur J Epidemiol 21:475–484; doi:10.1007/s10654-006-9022-0

Janssen NA, Gerlofs-Nijland ME, Lanki T, Salonen RO, Cassee F, Hoek G, et al. 2012. Health effects of black carbon. Available: *https://www.euro.who.int/__data/assets/pdf_file/0004/162535/e96541.pdf.* Copenhagen, Denmark:World Health Organization.

Jedynska A, Hoek G, Eeftens M, Cyrys J, Keuken M, Ampe C, et al. 2014a. Spatial variations of PAH, hopanes/steranes and EC/OC concentrations within and between European study areas. Atmos Environ 87:239–248; doi:10.1016/j.atmosenv.2014.01.026.

Jedynska A, Hoek G, Wang M, Eeftens M, Cyrys J, Keuken M, et al. 2014b. Development of land use regression models for elemental, organic carbon, PAH, and hopanes/steranes in 10 ESCAPE/TRANSPHORM European study areas. Environ Sci Technol 48:14435–14444; doi:10.1021/es502568z.

Jenkinson M, Beckmann CF, Behrens TEJ, Woolrich MW, Smith SM. 2012. FSL. Neuroimage 62:782–790; doi:10.1016/j.neuroimage.2011.09.015.

Jentsch JD, Pennington ZT. 2014. Reward, interrupted: Inhibitory control and its relevance to addictions. Neuropharmacology 76:479–486; doi:10.1016/j.neuropharm.2013.05.022.

Jones SL, Dufoix R, Laplante DP, Elgbeili G, Patel R, Chakravarty MM, et al. 2019. Larger amygdala volume mediates the association between prenatal maternal stress and higher levels of externalizing behaviors: Sex specific effects in project ice storm. Front Hum Neurosci 13; doi:10.3389/fnhum.2019.00144.

Keil AP, Buckley JP, OBrien KM, Ferguson KK, Zhao S, White AJ. 2019. A quantile-based g-computation approach to addressing the effects of exposure mixtures. Environ Health Perspect 128(4):047004; doi:10.1289/EHP5838.

Kim KH, Jahan SA, Kabir E, Brown RJC. 2013. A review of airborne polycyclic aromatic hydrocarbons (PAHs) and their human health effects. Environ Int 60:71–80; doi:10.1016/j.envint.2013.07.019.

Kim SY, Kim JK, Park SH, Kim BG, Jang AS, Oh SH, et al. 2018. Effects of inhaled particulate matter on the central nervous system in mice. Neurotoxicology 67:169–177; doi:10.1016/j.neuro.2018.06.001.

Klocke C, Allen JL, Sobolewski M, Mayer-Pröschel M, Blum JL, Lauterstein D, et al. 2017. Neuropathological consequences of gestational exposure to concentrated ambient fine and ultrafine particles in the mouse. Toxicol Sci 156:492–508; doi:10.1093/toxsci/kfx010.

Kooijman MN, Kruithof CJ, van Duijn CM, Duijts L, Franco OH, van IJzendoorn MH, et al. 2016. The Generation R Study: Design and cohort update 2017. Eur J Epidemiol 31:1243–1264; doi:10.1007/s10654-016-0224-9.

Le ND, Sun L, Zidek J V. 2010. Air pollution. Chronic Dis Can 29:144–163; doi:10.7748/phc.27.2.13.s14.

Lebel C, Treit S, Beaulieu C. 2019. A review of diffusion MRI of typical white matter development from early childhood to young adulthood. NMR Biomed 32; doi:10.1002/nbm.3778.

Lenroot RK, Giedd JN. 2006. Brain development in children and adolescents: Insights from anatomical magnetic resonance imaging. Neurosci Biobehav Rev 30:718–729; doi:10.1016/j.neubiorev.2006.06.001.

Lin W, Zhu Q, Gao W, Chen Y, Toh CH, Styner M, et al. 2008. Functional connectivity MR imaging reveals cortical functional connectivity in the developing brain. Am J Neuroradiol 29:1883–1889; doi:10.3174/ajnr.A1256.

Long Z, Jiang YM, Li XR, Fadel W, Xu J, Yeh CL, et al. 2014. Vulnerability of welders to manganese exposure — A neuroimaging study. Neurotoxicology 45:285–292; doi:10.1016/j.neuro.2014.03.007.

Lubczyńska MJ, Sunyer J, Tiemeier H, Porta D, Kasper-Sonnenberg M, Jaddoe VWV, et al. 2017. Exposure to elemental composition of outdoor $PM_{2.5}$ at birth and cognitive and psychomotor function in childhood in four European birth cohorts. Environ Int 109:170–180; doi:10.1016/j.envint.2017.09.015.

Lupien SJ, Parent S, Evans AC, Tremblay RE, Zelazo PD, Corbo V, et al. 2011. Larger amygdala but no change in hippocampal volume in 10-year-old children exposed to maternal depressive symptomatology since birth. Proc Natl Acad Sci U S A 108:14324–14329; doi:10.1073/pnas.1105371108.

Ma I, van Duijvenvoorde A, Scheres A. 2016. The interaction between reinforcement and inhibitory control in ADHD: A review and research guidelines. Clin Psychol Rev 44:94–111; doi:10.1016/j.cpr.2016.01.001.

Manzo ND, Slade R, Richards JH, McGee JK, Martin LD, Dye JA. 2010. Susceptibility of inflamed alveolar and airway epithelial cells to injury induced by diesel exhaust particles of varying organic carbon content. J Toxicol Environ Heal - Part A Curr Issues 73:565–580; doi:10.1080/15287390903566625.

Marrus N, Belden A, Nishino T, Handler T, Ratnanather JT, Miller M, et al. 2015. Ventromedial prefrontal cortex thinning in preschool-onset depression. J Affect Disord 180:79–86; doi:10.1016/j.jad.2015.03.033.

McMichael AJ. 2000. The urban environment and health in a world of increasing globalization: Issues for developing countries. Bull World Health Organ 78:1117–1126; doi:10.1590/S0042-96862000000900007.

Montagne DR, Hoek G, Klompmaker JO, Wang M, Meliefste K, Brunekreef B. 2015. Land use regression models for ultrafine particles and black carbon based on short-term monitoring predict past spatial variation. Environ Sci Technol 49:8712–8720; doi:10.1021/es505791g.

Moreno-Rius J. 2019. The cerebellum under stress. Front Neuroendocrinol 54; doi:10.1016/j.yfrne.2019.100774.

Morris-Schaffer K, Merrill AK, Wong C, Jew K, Sobolewski M, Cory-Slechta DA. 2019. Limited developmental neurotoxicity from neonatal inhalation exposure to diesel exhaust particles in C57BL/6 mice. Part Fibre Toxicol 16; doi:10.1186/s12989-018-0287-8.

Mortamais M, Pujol J, Martínez-Vilavella G, Fenoll R, Reynes C, Sabatier R, et al. 2019. Effects of prenatal exposure to particulate matter air pollution on corpus callosum and behavioral problems in children. Environ Res 178; doi:10.1016/j.envres.2019.108734.

Mortamais M, Pujol J, van Drooge BL, Macià D, Martínez-Vilavella G, Reynes C, et al. 2017. Effect of exposure to polycyclic aromatic hydrocarbons on basal ganglia and attention-deficit hyperactivity disorder symptoms in primary school children. Environ Int 105:12–19; doi:10.1016/j.envint.2017.04.011.

Mous SE, Schoemaker NK, Blanken LME, Thijssen S, van der Ende J, Polderman TJC, et al. 2017. The association of gender, age, and intelligence with neuropsychological functioning in young typically developing children: The Generation R study. Appl Neuropsychol Child 6:22–40; doi:10.1080/21622965.2015.1067214.

Muetzel RL, Blanken LME, van der Ende J, El Marroun H, Shaw P, Sudre G, et al. 2018. Tracking brain development and dimensional psychiatric symptoms in children: A longitudinal population-based neuroimaging study. Am J Psychiatry 175:54–62; doi:10.1176/appi.ajp.2017.16070813.

Muetzel RL, Mous SE, van der Ende J, Blanken LME, van der Lugt A, Jaddoe VWV, et al. 2015. White matter integrity and cognitive performance in school-age children: A population-based neuroimaging study. Neuroimage 119:119–128; doi:10.1016/j.neuroimage.2015.06.014.

Muetzel RL, Mulder RH, Lamballais S, Cortes Hidalgo AP, Jansen P, Güroğlu B, et al. 2019. Frequent bullying involvement and brain morphology in children. Front Psychiatry 10:696; doi:10.3389/fpsyt.2019.00696.

Muhammad A, Carroll C, Kolb B. 2012. Stress during development alters dendritic morphology in the nucleus accumbens and prefrontal cortex. Neuroscience 216:103–109; doi:10.1016/j.neuroscience.2012.04.041.

Neumann A, Noppe G, Liu F, Kayser M, Verhulst FC, Jaddoe VWV, et al. 2017. Predicting hair cortisol levels with hair pigmentation genes: A possible hair pigmentation bias. Sci Rep 7:8529; doi:10.1038/s41598-017-07034-w.

Nieuwenhuijsen M (Editor). 2004. Exposure Assessment in Occupational and Environmental Epidemiology. Oxford, England:Oxford University Press.

O'Brien JS, Fillerup DL, Mead JF. 1964. Brain lipids: I. Quantification and fatty acid composition of cerebroside sulfate in human cerebral gray and white matter. J Lipid Res 5:109–116.

Pagalan L, Bickford C, Weikum W, Lanphear B, Brauer M, Lanphear N, et al. 2019. Association of prenatal exposure to air pollution with Autism Spectrum Disorder. JAMA Pediatr 173:86–92; doi:10.1001/jamapediatrics.2018.3101.

Paus T. 2005. Mapping brain maturation and cognitive development during adolescence. Trends Cogn Sci 9:60–68; doi:10.1016/j.tics.2004.12.008.

Paus T, Keshavan M, Giedd JN. 2008. Why do many psychiatric disorders emerge during adolescence? Nat Rev Neurosci 9:947–957; doi:10.1038/nrn2513.

Peterson BS, Rauh VA, Bansal R, Hao X, Toth Z, Nati G, et al. 2015. Effects of prenatal exposure to air pollutants (polycyclic aromatic hydrocarbons) on the development of brain white matter, cognition, and behavior in later childhood. JAMA Psychiatry 72:531–540; doi:10.1001/jamapsychiatry.2015.57.

Pollack AZ, Perkins NJ, Mumford SL, Ye A, Schisterman EF. 2013. Correlated biomarker measurement error: An important threat to inference in environmental epidemiology. Am J Epidemiol 177:84–92; doi:10.1093/aje/kws209.

Power JD, Barnes KA, Snyder AZ, Schlaggar BL, Petersen SE. 2012. Spurious but systematic correlations in functional connectivity MRI networks arise from subject motion. Neuroimage 59:2142–2154; doi:10.1016/j.neuroimage.2011.10.018.

Power MC, Lamichhane AP, Liao D, Xu X, Jack CR, Gottesman RF, et al. 2018. The association of long-term exposure to particulate matter air pollution with brain MRI findings: The ARIC study. Environ Health Perspect 126; doi:10.1289/EHP2152.

Price AL, Patterson NJ, Plenge RM, Weinblatt ME, Shadick NA, Reich D. 2006. Principal components analysis corrects for stratification in genome-wide association studies. Nat Genet 38:904–909; doi:10.1038/ng1847.

Prieler J. 2003. Raven's Advanced Progressive Matrices. Mödling, Austria:Schuhfrieda.

Pujol J, Fenoll R, Macià D, Martínez-Vilavella G, Alvarez-Pedrerol M, Rivas I, et al. 2016a. Airborne copper exposure in school environments associated with poorer motor performance and altered basal ganglia. Brain Behav 6; doi:10.1002/brb3.467.

Pujol J, Martínez-Vilavella G, Macià D, Fenoll R, Alvarez-Pedrerol M, Rivas I, et al. 2016b. Traffic pollution exposure is associated with altered brain connectivity in school children. Neuroimage 129:175–184; doi:10.1016/j.neuroimage.2016.01.036.

Rice D, Barone Jr S. 2000. Critical periods of vulnerability-for the developing nervous system: Evidence from humans and animal models. Environ Health Perspect 108:511–533; doi:10.1289/ehp.00108s3511.

Richardson MP, Strange BA, Dolan RJ. 2004. Encoding of emotional memories depends on amygdala and hippocampus and their interactions. Nat Neurosci 7:278–285; doi:10.1038/nn1190.

Rosseel Y. 2012. Lavaan: An R package for structural equation modeling. J Stat Softw 48:1–36; doi:10.18637/jss.v048.i02.

Rothman KJ, Greenland S. 2005. Causation and causal inference in epidemiology. Am J Public Health 95; doi:10.2105/AJPH.2004.059204.

Saenen ND, Martens DS, Neven KY, Alfano R, Bové H, Janssen BG, et al. 2019. Air pollution-induced placental alterations: An interplay of oxidative stress, epigenetics, and the aging phenotype? Clin Epigenetics 11; doi:10.1186/s13148-019-0688-z.

Salim S. 2017. Oxidative stress and the central nervous system. J Pharmacol Exp Ther 360:201–205; doi:10.1124/jpet.116.237503.

Salm AK, Pavelko M, Krouse EM, Webster W, Kraszpulski M, Birkle DL. 2004. Lateral amygdaloid nucleus expansion in adult rats is associated with exposure to pre-

natal stress. Dev Brain Res 148:159–167; doi:10.1016/j.devbrainres.2003.11.005.

Satterthwaite TD, Elliott MA, Gerraty RT, Ruparel K, Loughead J, Calkins ME, et al. 2013. An improved framework for confound regression and filtering for control of motion artifact in the preprocessing of resting-state functional connectivity data. Neuroimage 64:240–256; doi:10.1016/j.neuroimage.2012.08.052.

Scheiber IF, Mercer JFB, Dringen R. 2014. Metabolism and functions of copper in brain. Prog Neurobiol 116:33–57; doi:10.1016/j.pneurobio.2014.01.002.

Sentís A, Sunyer J, Dalmau-Bueno A, Andiarena A, Ballester F, Cirach M, et al. 2017. Prenatal and postnatal exposure to NO_2 and child attentional function at 4–5 years of age. Environ Int 106:170–177; doi:10.1016/j.envint.2017.05.021.

Sinisi SE, van der Laan MJ. 2004. Loss-based cross-validated Deletion/Substitution/Addition algorithms in estimation. UC Berkeley Division of Biostatistics Working Paper Series. Working Paper 143. Available: *https://biostats.bepress.com/ucbbiostat/paper143*.

Spinelli S, Chefer S, Suomi SJ, Higley JD, Barr CS, Stein E. 2009. Early life stress induces long-term morphologic changes in primate brain. Arch Gen Psychiatry 66:658–665; doi:10.1001/archgenpsychiatry.2009.52.

Spratt M, Carpenter J, Sterne JAC, Carlin JB, Heron J, Henderson J, et al. 2010. Strategies for multiple imputation in longitudinal studies. Am J Epidemiol 172:478–487; doi:10.1093/aje/kwq137.

Sterne JAC, White IR, Carlin JB, Spratt M, Royston P, Kenward MG, et al. 2009. Multiple imputation for missing data in epidemiological and clinical research: Potential and pitfalls. BMJ 339:157–160; doi:10.1136/bmj.b2393.

Suades-González E, Gascon M, Guxens M, Sunyer J. 2015. Air pollution and neuropsychological development: A review of the latest evidence. Endocrinology 156:3473–3482; doi:10.1210/en.2015-1403.

Sudre G, Mangalmurti A, Shaw P. 2018. Growing out of attention deficit hyperactivity disorder: Insights from the 'remitted' brain. Neurosci Biobehav Rev 94:198–209; doi:10.1016/j.neubiorev.2018.08.010.

Sunyer J, Esnaola M, Alvarez-Pedrerol M, Forns J, Rivas I, López-Vicente M, et al. 2015. Association between traffic-related air pollution in schools and cognitive development in primary school children: A Prospective Cohort Study. PLoS Med 12; doi:10.1371/journal.pmed.1001792.

Sunyer J, Suades-González E, García-Esteban R, Rivas I, Pujol J, Alvarez-Pedrerol M, et al. 2017. Traffic-related air pollution and attention in primary school children. Epidemiology 28:181–189; doi:10.1097/EDE.0000000000000603.

Szpiro A, Sheppard L, Lumley T. 2011a. Measurement error in air pollution cohort studies. Epidemiology 22:S32; doi:10.1097/01.ede.0000391757.71204.b9.

Szpiro AA, Sheppard L, Lumley T. 2011b. Efficient measurement error correction with spatially misaligned data. Biostatistics 12:610–623; doi:10.1093/biostatistics/kxq083.

Tamnes CK, Herting MM, Goddings AL, Meuwese R, Blakemore SJ, Dahl RE, et al. 2017. Development of the cerebral cortex across adolescence: A multisample study of inter-related longitudinal changes in cortical volume, surface area, and thickness. J Neurosci 37:3402–3412; doi:10.1523/JNEUROSCI.3302-16.2017.

Teicher MH, Dumont NL, Ito Y, Vaituzis C, Giedd JN, Andersen SL. 2004. Childhood neglect is associated with reduced corpus callosum area. Biol Psychiatry 56:80–85; doi:10.1016/j.biopsych.2004.03.016.

Thomason ME, Dassanayake MT, Shen S, Katkuri Y, Alexis M, Anderson AL, et al. 2013. Cross-hemispheric functional connectivity in the human fetal brain. Sci Transl Med 5; doi:10.1126/scitranslmed.3004978.

Thomson EM. 2019. Air Pollution, Stress, and Allostatic Load: Linking Systemic and Central Nervous System Impacts. J Alzheimer's Dis 69:597–614; doi:10.3233/JAD-190015.

Tiemeier H, Lenroot RK, Greenstein DK, Tran L, Pierson R, Giedd JN. 2010. Cerebellum development during childhood and adolescence: A longitudinal morphometric MRI study. Neuroimage 49:63–70; doi:10.1016/j.neuroimage.2009.08.016.

United Nations, Department of Economic and Social Affairs. 2018. World Urbanization Prospects The 2018 Revision. New York:United Nations.

U.S. Environmental Protection Agency. 2019. Integrated Science Assessment (ISA) for Particulate Matter (Final Report, 2019) Washington, DC:EPA/600/R-19/188.

Valeri L, Vanderweele TJ. 2013. Mediation analysis allowing for exposure-mediator interactions and causal interpretation: theoretical assumptions and implementation with SAS and SPSS macros. Psychol Methods 18:137–150; doi:10.1037/a0031034.

van den Hooven EH, Pierik FH, de Kluizenaar Y, Willemsen SP, Hofman A, van Ratingen SW, et al. 2012. Air pollution exposure during pregnancy, ultrasound measures of fetal growth, and adverse birth outcomes: A prospective cohort study. Environ Health Perspect 120:150–156; doi:10.1289/ehp.1003316.

van Erp TGM, Walton E, Hibar DP, Schmaal L, Jiang W, Glahn DC, et al. 2018. Cortical brain abnormalities in 4474 individuals with schizophrenia and 5098 control subjects via the Enhancing Neuro Imaging Genetics Through Meta Analysis (ENIGMA) Consortium. Biol Psychiatry 84:644–654; doi:10.1016/j.biopsych.2018.04.023.

van Ewijk H, Heslenfeld DJ, Zwiers MP, Buitelaar JK, Oosterlaan J. 2012. Diffusion tensor imaging in attention deficit/hyperactivity disorder: A systematic review and meta-analysis. Neurosci Biobehav Rev 36:1093–1106; doi:10.1016/j.neubiorev.2012.01.003.

Vatcheva K, Lee M. 2016. Multicollinearity in regression analyses conducted in epidemiologic studies. Epidemiol Open Access 06; doi:10.4172/2161-1165.1000227.

Viana M, Kuhlbusch TAJ, Querol X, Alastuey A, Harrison RM, Hopke PK, et al. 2008. Source apportionment of particulate matter in Europe: A review of methods and results. J Aerosol Sci 39:827–849; doi:10.1016/j.jaerosci.2008.05.007.

Weiner KS, Zilles K. 2016. The anatomical and functional specialization of the fusiform gyrus. Neuropsychologia 83:48–62; doi:10.1016/j.neuropsychologia.2015.06.033.

Weisskopf MG, Seals RM, Webster TF. 2018. Bias amplification in epidemiologic analysis of exposure to mixtures. Environ Health Perspect 126:047003-1-047003; doi:10.1289/EHP2450. PMID: 29624292; PMCID: PMC6071813.

Weisskopf MG, Sparrow D, Hu H, Power MC. 2015. Biased exposure-health effect estimates from selection in cohort studies: Are environmental studies at particular risk? Environ Health Perspect 123:1113–1122; doi:10.1289/ehp.1408888.

Weisskopf MG, Webster TF. 2017. Trade-offs of personal versus more proxy exposure measures in environmental epidemiology. Epidemiology 28:635–643; doi:10.1097/EDE.0000000000000686.

Weuve J, Tchetgen Tchetgen EJ, Glymour MM, Beck TL, Aggarwal NT, Wilson RS, et al. 2012. Accounting for bias due to selective attrition: the example of smoking and cognitive decline. Epidemiology 23:119–128; doi:10.1097/EDE.0b013e318230e861.

White T, El Marroun H, Nijs I, Schmidt M, Van Der Lugt A, Wielopolki PA, et al. 2013. Pediatric population-based neuroimaging and the Generation R Study: The intersection of developmental neuroscience and epidemiology. Eur J Epidemiol 28:99–111; doi:10.1007/s10654-013-9768-0.

White T, Muetzel RL, El Marroun H, Blanken LME, Jansen P, Bolhuis K, et al. 2018. Paediatric population neuroimaging and the Generation R Study: The second wave. Eur J Epidemiol 33:99–125; doi:10.1007/s10654-017-0319-y.

White T, Muetzel R, Schmidt M, Langeslag SJE, Jaddoe V, Hofman A, et al. 2014. Time of acquisition and network stability in pediatric resting-state functional magnetic resonance imaging. Brain Connect 4:417–427; doi:10.1089/brain.2013.0195.

White T, Nelson M, Lim KO. 2008. Diffusion tensor imaging in psychiatric disorders. Top Magn Reson Imaging 19:97–106; doi:10.1097/RMR.0b013e3181809f1e.

Wierenga LM, Bos MGN, Schreuders E, vd Kamp F, Peper JS, Tamnes CK, et al. 2018. Unraveling age, puberty and testosterone effects on subcortical brain development across adolescence. Psychoneuroendocrinology 91:105–114; doi:10.1016/j.psyneuen.2018.02.034.

Wierenga L, Langen M, Ambrosino S, van Dijk S, Oranje B, Durston S. 2014. Typical development of basal ganglia, hippocampus, amygdala and cerebellum from age 7 to 24. Neuroimage 96:67–72; doi:10.1016/j.neuroimage.2014.03.072.

Wilhelm M, Ghosh JK, Su J, Cockburn M, Jerrett M, Ritz B. 2011. Traffic-related air toxics and preterm birth: A population-based case-control study in Los Angeles county, California. Environ Heal 10; doi:10.1186/1476-069X-10-89.

Wilker EH, Preis SR, Beiser AS, Wolf PA, Au R, Kloog I, et al. 2015. Long-term exposure to fine particulate matter, residential proximity to major roads and measures of brain structure. Stroke 46:1161–1166; doi:10.1161/STROKEAHA.114.008348.

Yang A, Wang M, Eeftens M, Beelen R, Dons E, Leseman DLAC, et al. 2015. Spatial variation and land use regression modeling of the oxidative potential of fine particles. Environ Health Perspect 123:1187–1192; doi:10.1289/ehp.1408916.

Yurgelun-Todd D. 2007. Emotional and cognitive changes during adolescence. Curr Opin Neurobiol 17:251–257; doi:10.1016/j.conb.2007.03.009.

Zidek JV, Wong H, Le ND, Burnett R. 1996. Causality, measurement error, and multicollinearity in epidemilology. Environmetrics 7:441–451; doi:10.1002/(SICI)1099-095X(199607)7:4<441::AID-ENV226>3.0.CO;2-V.

HEI QUALITY ASSURANCE STATEMENT

The conduct of this study was subjected to independent audits by RTI International staff members Dr. Linda Brown and Dr. Prakash Doraiswamy. These staff members are experienced in quality assurance (QA) oversight for air quality monitoring, chemical transport modeling, use of satellite data, and epidemiological methods and analysis. The RTI QA oversight team also included statistician Dr. David Wilson who reviewed the codes for the exposure and epidemiological statistical models.

The QA oversight program consisted of an initial onsite audit of the research study at ISGlobal for conformance to the study protocol and standard operating procedures and a final remote audit of the final report and the data processing steps. The onsite audit was performed by Drs. Brown and Doraiswamy. The final remote audit was performed by Drs. Brown, Doraiswamy, and Wilson. The dates of the audits and reviews are listed below.

Onsite Audit at ISGlobal, Barcelona, July 8–9, 2019

The auditors conducted an onsite audit in Spain at the Barcelona Institute for Global Health (ISGlobal). The audit

reviewed the following study components: progress reports, personnel and staff, internal quality assurance procedures, air quality data processing and documentation, health data processing and quality checks, and backup procedures. Program codes were inspected to verify proper documentation. The audit included an observation of the scripts, file tree structure on the server, and model diagnostics. No errors were noted, but recommendations were made for updating the study plan and expanding the quality plan, documenting codes, and documenting procedures and assumptions related to model developmentand QA/QC.

Final Remote Audit, August–October 2021

The final remote audit consisted of two parts: (1) review of the final project report, and (2) audit of data processing steps. The review of the final report focused on ensuring that methods are well documented, that the report is easy to understand, and that it highlighted key study findings and limitations. In addition, this review provided guidance on specific aspects of the data processing sequence that could be reviewed remotely. The data audit included (1) a remote live demonstration of selected data processing codes, and (2) the review of the codes for data reduction, processing and analysis, and model development. This specific portion of the audit was restricted to the key components of the study and associated findings. Selected scripts (in R/STATA) for exposure estimation and epidemiological model development were sent to RTI. No data were sent to RTI due to data confidentiality restrictions. Therefore, data inputs to the codes were not available.

The codes were reviewed at RTI to verify, to the extent feasible, linkages between the various scripts, confirmation of the models reported and verification of key tables. The codes appear tobe consistent with the models and tables described in the report and followed the overall model development procedure described; the values themselves could not be generated at RTI due to unavailability of the input data. However, review of selected output files sent to RTI showedagreement with the values in the report, except for minor round-off differences.

The remote live demonstration included a real-time execution of selected codes generating key tables in the report. Demonstration was restricted predominantly to the adolescent population for which data were available at ISGlobal. Values generated by the codes during the real-time demonstration in general matched with the values in the report when rounded off to the respective digit, except for few minor round-off discrepancies that do not impact the conclusions. No major quality-related issues were identified from the review of the codes and the report.

Minor editorial comments and recommendations were made for improved clarity.

A written report was provided to HEI. The QA oversight audit demonstrated that the study was conducted according to the study protocol. The final report, except as noted in the comments, appears to be representative of the study conducted.

Linda Morris Brown, MPH, DrPH, Epidemiologist, Quality Assurance Auditor

Prakash Doraiswamy, PhD, Air Quality Specialist, Quality Assurance Auditor

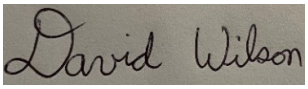

David Wilson, PhD, Statistician, Quality Assurance Auditor

November 18, 2021

MATERIALS AVAILABLE ON THE HEI WEBSITE

Additional Materials 1 contains an appendix with supplemental figures and tables not included in the main report. It is available on the HEI website at *www.healtheffects.org/publications.*

ABOUT THE AUTHORS

Mònica Guxens is an associate research professor at ISGlobal, Spain, and at the Department of Child and Adolescent Psychiatry, Erasmus MC, University Medical Center in Rotterdam, the Netherlands, a lecturer at the Pompeu Fabra University in Barcelona, Spain, and is affiliated with the Spanish Consortium for Research on Epidemiology and Public Health (CIBERESP), Institute of Health Carlos III, Madrid, Spain. She received her medical degree from the Autonomous University of Barcelona, Spain, specializing in Preventive Medicine and Public Health, her MPH from the Pompeu Fabra University in Barcelona, Spain, and her PhD in Public Health and Biomedical Research from the Autonomous University of Barcelona, Spain. Her research interests are focused on the role of several environmental factors, mainly air pollution, noise, light, electromagnetic fields, and persistent and nonpersistent chemicals, and on children's growth and development — in particular, brain development and sleep.

Małgorzata J. Lubczyńska has recently obtained a joint PhD degree from ISGlobal in association with the Pompeu Fabra

University in Barcelona, Spain, and at the Erasmus Medical Center in association with Erasmus University Rotterdam, the Netherlands, under the supervision of Dr. Mònica Guxens and Dr. Henning Tiemeier. She is also affiliated with the Spanish Consortium for Research on Epidemiology and Public Health (CIBERESP), Institute of Health Carlos III, Madrid, Spain. Her doctoral thesis was focused on the association between early life exposure to air pollution and children's brain development, which was assessed with neuropsychological tests and MRI data. Her main research interests are air pollution and the implications thereof on human health, particularly on mental health.

Laura Pérez-Crespo is a PhD candidate at ISGlobal in association with the Pompeu Fabra University in Barcelona, Spain, under the supervision of Dr. Mònica Guxens. She is also affiliated with the Spanish Consortium for Research on Epidemiology and Public Health (CIBERESP), Institute of Health Carlos III, Madrid, Spain. She obtained a degree in human biology and an MPH from the Pompeu Fabra University in Barcelona, Spain. Her research interests are focused on the effects of several environmental factors on the neurodevelopment in children.

Ryan L. Muetzel is an assistant professor at the Department of Child and Adolescent Psychiatry, Erasmus MC, University Medical Center in Rotterdam, the Netherlands. He codirects the Generation R Neuroimaging initiative, one of the world's largest studies of brain development in children and adolescents. His work is primarily centered on population neuroscience, with a particular focus on using MRI to better understand typical and atypical development during childhood and adolescence.

Hanan El Marroun is an assistant professor at the Departments of Child and Adolescent Psychiatry and Pediatrics, Erasmus MC, University Medical Center in Rotterdam, the Netherlands, as well as at the Department of Psychology, Education and Child Studies at the Erasmus School of Social and Behavioural Sciences, Erasmus University Rotterdam, the Netherlands. Her background is in both epidemiology and neuroscience, and her research line focuses on maternal health and child brain development. She teaches bachelor and master students of medicine and psychology about substance use, addiction, and neuropsychology. She collaborates intensively with national and international researchers and clinicians through multidisciplinary consortia.

Xavier Basagaña is an associate research professor at ISGlobal. He is also affiliated with Pompeu Fabra University, Barcelona, Spain, and the Spanish Consortium for Research on Epidemiology and Public Health (CIBERESP), Institute of Health Carlos III, Madrid, Spain. He has a PhD in Biostatistics from Harvard University. His lines of research include the development of statistical methods for environmental epidemiology, the relationship between air pollution exposure and health, and the relationship between extreme temperatures and health.

Gerard Hoek is an associate professor at the Institute for Risk Assessment Sciences, Utrecht University, the Netherlands. His research focuses on methods for improved exposure assessment to environmental stressors, with a focus on outdoor air pollution. His research also involves the application of these exposure estimates in epidemiological studies. In recent years, he worked on mobile monitoring campaigns, application of sensors, exposome, health effects of low-level air pollution, and the combined health effects of different environmental stressors, including air pollution, noise, and green space.

Henning Tiemeier is trained as a medical doctor and sociologist. He is professor of psychiatric epidemiology in the Department of Child and Adolescent Psychiatry, Erasmus MC, University Medical Center in Rotterdam, the Netherlands, and professor of social epidemiology at the Department of Social and Behavioral Science, Harvard T.H. Chan School of Public Health. His expertise is in child psychiatric assessment and developmental studies. Much of his current work focusses on neurodevelopment as assessed by imaging, cognitive testing, or motor assessment; he combines diverse disciplines such as epidemiology, neuroscience, family studies, and child development.

OTHER PUBLICATIONS RESULTING FROM THIS RESEARCH

Lubczyńska MJ, Muetzel RL, El Marroun H, Hoek G, Kooter IM, Thomson EM, et al. 2020. Air pollution exposure during pregnancy and childhood and brain morphology in preadolescents. Environ Res 2020:110446.

Lubczyńska MJ, Muetzel RL, El Marroun H, Basagaña X, Stark M, Denault W, et al. 2020. Exposure to air pollution during pregnancy and childhood, and white matter microstructure in preadolescents. Environ Health Perspect 128:027005.

Guxens M, Lubczyńska MJ, Muetzel RL, Dalmau-Bueno A, Jaddoe VWV, Hoek G, et al. 2018. Air pollution exposure during fetal life, brain morphology, and cognitive function in school-age children. Biol Psychiatry 84:295–303.

Research Report 209, *Associations of Air Pollution on the Brain in Children: A Brain Imaging Study*, M. Guxens et al.

INTRODUCTION

Interest in understanding the association between air pollution and nervous system outcomes has been rapidly growing over the past several decades. It has long been known that inhaling pollutants, such as manganese and lead, can cause brain damage and can lead to severe neurotoxic symptoms similar to those of Parkinson disease in welders and to developmental delays and loss of IQ in children (Landrigan 2002; Levy and Nassetta 2003). The recent U.S. Environmental Protection Agency (U.S. EPA*) Integrated Science Assessment (ISA) for particulate matter (PM) classified long-term $PM_{2.5}$ exposure (PM with aerodynamic diameter ≤2.5 µm) as "likely to be causal" for nervous system outcomes, and "suggestive" for PM_{COARSE} (PM with aerodynamic diameter between 10 µm and 2.5 µm) and ultrafine particles (PM with aerodynamic diameter ≤0.1 µm.) (U.S. EPA 2019). Nervous system outcomes considered were brain inflammation and oxidative stress, morphalogical changes in the brain, cognitive and behavioral outcomes, neurodegenerative diseases, and neurodevelopmental outcomes. It is worth noting that the evidence from studies of neurodevelopmental outcomes did not substantially contribute to the causality determination for nervous system effects (U.S. EPA 2019). A determination of "inadequate" was reached in the ISA of nitrogen dioxide (NO_2) in 2016 for postnatal development (U.S. EPA 2016).

Mechanistic and animal studies have provided some biological plausibility for effects of PM on the brain. These studies have reported the occurrence of inflammation and oxidative stress that could affect the central nervous system by inducing neuronal death and synaptic toxicity. Increased concentrations of circulating cytokines due to systemic inflammation after a pro-inflammatory response in the lung might also have a peripheral effect on the brain. Furthermore, PM might also reach the brain after crossing the blood–brain barrier or more directly via the olfactory bulb and could itself be pro-inflammatory (U.S. EPA 2019). Regarding the prenatal period specifically, PM air pollution might translocate across the placenta (Bongaerts et al. 2020) and impair the placenta function (Saenen et al. 2019; van den Hooven et al. 2012), and thus disrupt neurodevelopment.

Although several epidemiological studies have assessed the association between air pollution exposure during early life and child neurodevelopment (de Prado Bert et al. 2018; Herting et al. 2019; Lopuszanska and Samardakiewicz 2020), it is yet unclear whether brain structural alterations underlie the observed associations. Advances in neuroimaging that allow in vivo investigation of brain structure and function have emerged. Such studies provide additional information about the possible mechanisms and add biological plausibility to the nervous system outcomes reported in epidemiological studies. So far only a few studies have used magnetic resonance imaging (MRI) techniques to evaluate the effect of air pollution on the brain in children, sampled from three cohorts in Spain, Mexico, and the United States (Alemany et al. 2018; Calderón-Garcidueñas et al. 2011, 2012; Mortamais et al. 2017, 2019; Peterson et al. 2015; Pujol et al. 2016a,b).

In response to Request for Applications 15-1 "Walter A. Rosenblith New Investigator Award," Dr. Monica Guxens of Barcelona Institute for Global Health (ISGlobal) submitted a proposal titled "Air Pollution, Autism Spectrum Disorders, and Brain Imaging Amongst Children in Europe." Dr. Guxens proposed to assess the association between air pollution exposure at different time windows and the development of autism spectrum disorders and brain structural and functional measures in children. She proposed two studies. One study would use an existing population-based birth cohort in Rotterdam, the Netherlands (Generation R), in which brain structural and functional imaging in children was conducted. The second study would be a new population-based case–control study on autism spectrum disorders in Catalunya, Spain. The HEI Research Committee recommended Dr. Guxens' application for funding because there had been few studies of air pollution and neurodevelopmental effects, and the use of MRI data was considered novel. In addition, evidence for a possible link between air pollution and autism was inconclusive.

Dr. Mònica Guxens' 3-year study, "Air Pollution, Autism Spectrum Disorders, and Brain Imaging Amongst Children in Europe" began in February 2017. Total expenditures were $474,850. The draft Investigators' Report from Guxens and colleagues was received for review in September 2020. A revised report, received in February 2021, was accepted for publication in February 2021. During the review process, the HEI Review Committee and the investigators had the opportunity to exchange comments and to clarify issues in both the Investigators' Report and the Review Committee's Critique.

This document has not been reviewed by public or private party institutions, including those that support the Health Effects Institute; therefore, it may not reflect the views of these parties, and no endorsements by them should be inferred.

*A list of abbreviations and other terms appears at the end of this volume.

During the course of the work, there were severe delays in setting up the new study on air pollution and autism in Catalunya, Spain. Hence the current report is focused solely on the analysis of brain structural and functional measures in Generation R. A final report on the Spanish study will be published at a later date.

This Critique provides the HEI Review Committee's evaluation of the study. It is intended to aid the sponsors of HEI and the public by highlighting both the strengths and limitations of the study and by placing the Investigators' Report into a broader scientific perspective.

SCIENTIFIC BACKGROUND

Neuroimaging is a powerful tool that allows in vivo visualization of brain structure and function. These techniques are noninvasive and free of ionization radiation, making them suitable for research applications in children. Dr. Guxens used various neuroimaging techniques, such as structural MRI, diffusion tensor imaging (DTI), and functional MRI, which are described in Box 1.

Advances in neuroimaging have ushered in a new era of developmental neuroscience. The development of the brain occurs through the interaction of several complex synchronized processes, some of which are complete before birth, while others continue into adulthood. The brain of a newborn at 2–4 weeks of age is about 36% the size of an adult brain. The early postnatal period represents a time of dramatic change in brain structure and function. The brain grows to about 70% of its adult size by 1 year of age and to about 80% of adult size by age 2 years. Increases in brain volume during the first year of life is greatest in the cerebellum, followed by subcortical areas, and then the cerebral cortex. By age 5 years, brain size is about 90% of adult size. Substantial remodeling of gray and white matter continues, however, into the third decade of life. The brain is exceptionally complex and has a dynamic structure that is constantly evolving throughout life. The brain structure and function at any time is a product of interactions between genetic, epigenetic, internal physiological environment, and external environmental factors (Lenroot and Giedd 2006; Tau and Peterson 2010). Box 2 summarizes the major structures and functions of the brain.

APPROACH

The study by Dr. Guxens assessed the possible relationship of air pollution exposure during pregnancy and childhood with brain outcomes in children. Brain structural and functional measures were studied in Generation R — an existing birth cohort in Rotterdam, the Netherlands. Mother–child pairs were recruited during pregnancy or at birth from 2002–2006 and followed up until 2015.

Dr. Guxens and colleagues used air pollution data and high-resolution neuroimaging data collected in about 800 school-age children and in about 3,100 pre-adolescents. About 400 children underwent imaging at two time points. Early life exposure was estimated at the residential address level for various air pollutants using existing land-use regression (LUR) models, mainly from the European ESCAPE project. They applied single pollutant regression models to assess the association between early life air pollution exposure and brain structural and functional measures corrected for important confounders. Additionally, they used multipollutant models using a deletion/substitution/addition (DSA) approach.

METHODS

The aims of the study are detailed in Critique Table 1. These aims were to investigate the possible relationship of air pollution exposure during pregnancy and childhood with brain outcomes in children by assessing:

- (Aim 1) brain structural morphology (brain volumes, cortical thickness, and cortical surface area),
- (Aim 2) brain structural connectivity (white matter microstructure), and
- (Aim 3) brain functional connectivity (connectivity scores among brain areas).

Dr. Guxens and colleagues used high-resolution neuroimaging data collected in school-age children (age 6–10) and in pre-adolescents (age 9–12). MRI measurements of structural morphology were performed at both time points. Measurements of structural connectivity and of functional connectivity were performed at both time points as well, but for the Guxens study they used these data in pre-adolescents only. Thus, Aim 1 was pursued in both school-age children and pre-adolescents, whereas Aims 2 and 3 were investigated in pre-adolescents only. In both time points, they used a scanning platform specifically dedicated for the study, though a different scanner was used for each time point. The Investigators' Report provides the detailed protocol that was followed for the measurements.

In addition to the MRI measurements, cognitive function of the school-age children was assessed by using an array of tasks from the Dutch version of the Developmental Neuropsychological Assessment test (NEPSY-II). For this analysis, tests were chosen in the attention and executive functioning domain and the memory and learning domain.

Exposure was estimated at the residential address level for 14 air pollutants using existing LUR models, mainly from the European ESCAPE project (e.g., Beelen et al. 2013; Eeftens et al. 2012). Those models were based on air pollution measurements between February 2009 and February 2010 at 40 to 80 sites spread across the Netherlands and Belgium. For some analyses, prenatal and childhood exposure was estimated using back and forward extrapolation methods based on a few continuous-reference monitoring sites to match the exact period of interest for six pollutants (nitrogen oxides [NO_x], NO_2, PM_{10}, PM_{COARSE}, $PM_{2.5}$, and $PM_{2.5}$absorbance [absorbance

Box 1: Various Magnetic Resonance Imaging (MRI) Methods Used in the Guxens Study[a]

Structural or anatomical MRI generates static measurements of morphological brain features by discriminating among gray matter, white matter, and cerebrospinal fluid. Images are formed from 3-dimensional volume elements called *voxels*. Each voxel is assigned a single value based on the relaxation time of the tissue. The size of the voxel determines the spatial resolution or fineness of detail that can be distinguished in an image. Clinically, anatomical MRI is used for medical diagnosis and classifying disease stage (e.g., identifying tumors); researchers use anatomical MRI to assess morphological features of the brain, including whole brain volume, volumes of specific regions or subregions, and cortical thickness.

Diffusion Tensor Imaging (DTI) provides in vivo data on white matter integrity and fiber connectivity between brain structures by characterizing myelination patterns and neuroanatomical changes in white matter microstructure. Water molecules diffuse through brain tissue in isotropic (equal in all directions) fashion in cerebral spinal fluid and cell bodies but anisotropic (greater in one direction vs. other directions) in white matter tracts. Diffusional anisotropy is increased in regions where white matter is coherent, highly myelinated, and tightly packed, and decreased in areas where white matter is not as organized. By measuring the direction and flow of anisotropy within a voxel, DTI provides an estimate of the neural fiber connectivity within each voxel. DTI scans produce two kinds of data: (1) an integrity measure, usually quantified using fractional anisotropy, which is linked to axon packing and myelination, and (2) mean diffusivity reflecting water content and density.

Functional MRI (fMRI) provides an indirect measure of neuronal activity that is assessed by changes in oxygenation states of blood. Neuronal activation increases local deoxyhemoglobin concentration; the increase is rapidly followed by a surge of oxyhemoglobin through the neurovascular coupling system, which leads to an increase of the MRI signal above baseline. fMRI can be either conducted in a resting state or task related. Task-related fMRI assesses regional activation that occurs when a specific task is completed and seeks to identify those brain regions associated with the task-related activity. Resting state fMRI (rs-fMRI) was used in the current study. It measures activity in the brain when a participant is not performing an explicit task and detects spontaneous synchronous activity between distant brain regions. Sets of regions that share temporally correlated activity at rest are believed to constitute functional networks including visual, sensorimotor, auditory processing networks, and default mode network. The latter network of interacting brain regions is active when a person is not focused on the outside world, and the brain is at wakeful rest.

[a] Method description largely based on Horton et al. 2014.

Box 2: Major Structures and Functions of the Brain[a]

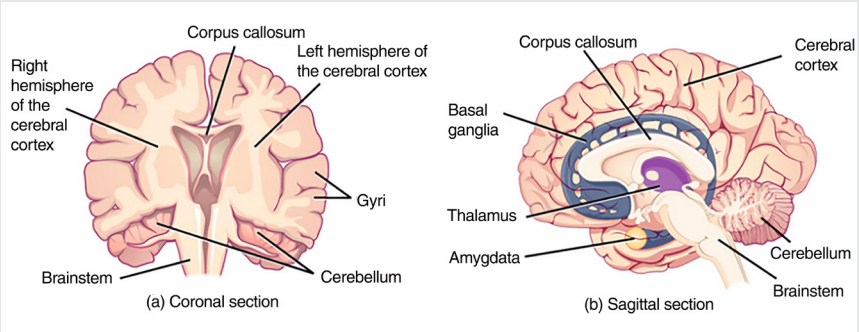

The brain can be divided into three basic structural units: the hindbrain, the midbrain, and the forebrain. The hindbrain includes the upper part of the spinal cord, most of the brainstem, and the cerebellum. This part of the brain controls the body's vital functions such as respiration and heart rate. The cerebellum (little brain) coordinates movement, posture, and balance. The midbrain is the uppermost part of the brainstem and controls some reflex actions and is part of the circuit involved in the control of eye movements and other voluntary movements. The forebrain is by far the largest part of the human brain and contains the entire cerebrum and several structures directly nestled within it, such as the thalamus.

Cerebrum. The cerebrum is the largest part of the forebrain and accounts for about two thirds of the total brain's mass. It contains the cerebral cortex and several subcortical structures, including the hippocampus, basal ganglia, and amygdala. Right beneath the cerebral cortex is the corpus callosum.

Corpus callosum. The most prominent white matter structure is the corpus callosum, which consists of about 200 million myelinated fibers, most of which connect homologous areas of the left and right cortex. The functions of the corpus callosum can generally be thought of as integrating the activities of the left and right cerebral hemispheres, including functions related to the unification of sensory fields, memory storage and retrieval, attention and arousal, enhancing language, and auditory functions.

Hippocampus. Located deep within the brain, the hippocampus has a major role in learning and memory.

[a] Largely based on Lenroot and Giedd 2006. From: *https://openstax.org/books/biology/pages/1-introduction*. OpenStax. Available under Creative Commons license *CC BY 4.0*.

(Box 2 continues next page)

Box 2 (Continued). *Major Structures and Functions of the Brain*[a]

Basal ganglia. The basal ganglia consist of the caudate nucleus, putamen, globus pallidus (palladium), subthalamic nucleus, nucleus accumbens, and substantia nigra. The basal ganglia have long been known to play a role in the control of movement and muscle tone but more recently have been shown to be involved in circuits that mediate higher cognitive functions, attention, and affective states.

Amygdala. The amygdala is a small, almond-shaped complex of nerve cells that receive input from both the olfactory system and the cerebral cortex. It performs a primary role in the processing of memory, decision-making, and emotional responses, including fear, anxiety, and aggression. The amygdala might be best known as the part of the brain that drives the *fight or flight* response. Although it is often associated with the body's fear and stress responses, it also plays a pivotal role in memory.

Thalamus. The thalamus is a mostly a gray matter structure, located at the top of the brain stem, with many essential relaying roles that range from perception, movement, and the body's vital functions. It acts as a two-way relay station, sorting, processing, and directing signals from the spinal cord and midbrain structures up to the cerebrum in the forebrain and, conversely, from the cerebrum down the spinal cord to the nervous system.

of the $PM_{2.5}$ fraction]). For the remaining pollutants (polycyclic aromatic hydrocarbons [PAHs], organic carbon [OC], copper [Cu], iron [Fe], silicon [Si], zinc [Zn], and two oxidative potential measures), assumptions were made that the contrast remained constant over time because there were no historical data available for those pollutants.

Guxens and colleagues applied single pollutant regression models to assess the association between early life air pollution and brain structural and functional measures corrected for important potential confounders, such as maternal smoking, prepregnancy body mass index and socioeconomic status. Missing confounder data — for example, up to 41% of data on paternal psychological distress — were imputed using standard techniques. To increase statistical power in the first round, a potential sampling bias was introduced by deliberately selecting more school-age children with child behavior problems and with mothers who reported certain exposures during pregnancy (e.g., exposure to drugs, nicotine, alcohol, and psychiatric medication). All analyses used inverse probability weighting to increase the chance the results would be representative for the study population initially recruited (about 9,600). In a sensitivity analysis for the global white matter microstructure outcomes, they applied a correction for exposure measurement error using the bootstrap method from Szpiro and colleagues (2011).

Critique Table 1 summarizes the data and analyses conducted by aim. Single-pollutant analyses were used for each brain outcome separately, with one pollutant from one exposure window added to the model at a time. The number of outcome measurements was very large — for example, for the cortical thickness and connectivity scores measures — about 140,000 to 320,000 suboutcomes were analyzed depending on the brain measure. Hence, analyses of those brain outcomes were corrected for multiple comparisons using a Monte Carlo approach. In contrast, analyses of other brain outcomes, including brain volumes and white matter microstructure outcomes, were not corrected for multiple testing; for those outcomes, multipollutant models were run instead. Those multipollutant models consider the correlation matrix of air pollutants and simultaneously correct for multiple testing. The investigators chose multipollutant analyses using the DSA approach (Sinisi and van der Laan 2004). DSA uses an iterative selection algorithm to fit a generalized linear model predicated on the power of cross-validation to select the best predictive model for each brain outcome. They picked the pollutants in the multipollutant model using the criterion that any exposure variable selected in at least 10% of the runs would go into a final model; each DSA model was run 200 times.

SUMMARY OF RESULTS

Several air pollutants were associated with brain structural morphology, structural connectivity, and functional connectivity in children. Critique Table 2 presents a summary of the results. In short, exposure to air pollution during early life showed the following associations:

- No associations with global brain volumes including total brain, gray matter, and white matter in school-age children or pre-adolescents. Air pollution exposure during pregnancy and childhood was associated with some differences in region-specific brain volumes in pre-adolescents only, such as a smaller volume in the hippocampus and corpus callosum, but only for a few pollutants (e.g., PAHs, Cu, OC, and oxidative potential). Some unexpected associations were reported in some brain regions as well.
- Associated with a thinner cortex in various regions of the brain in both school-age children and pre-adolescents, for various air pollutants including $PM_{2.5}$, $PM_{2.5}$absorbance and PM_{COARSE}.
- Associated with impaired cognitive function in one domain (attention and executive function), in school children, but only for $PM_{2.5}$. No associations were observed for the other cognitive function outcomes, such as in the memory and learning domain.
- Associated with fractional anisotropy and mean diffusivity, both globally and in several individual white matter tracts in pre-adolescents. In particular, the global measures of structural connectivity was associated for almost half of the air pollutants under investigation, including $PM_{2.5}$ and NO_2.

Critique Table 1. Summary of Data and Analyses Conducted to Study Air Pollution and Brain Outcomes in Children

Analysis / Age of the Children	Children (*n*)	Pollutants	Exposure Windows	Brain Outcomes	Details of the Analysis
AIM 1 — Structural Morphology					
School-age children	783	4 Pollutants: NO_2, PM_{COARSE}, $PM_{2.5}$, $PM_{2.5}$ absorbance	Pregnancy	4 Brain volumes (global and 9 region-specific volumes) Cortical thickness Cognitive function (e.g., attention and executive function, memory and learning)	Volume and thickness outcomes: Linear regression models corrected for important potential confounders[a]; no multipollutant analysis; thickness was corrected for multiple testing Cognitive function: Negative binomial models for attention task and linear regression for memory task; in addition, meditation analysis to investigate cortical thickness as a mediator in the $PM_{2.5}$–cognitive function relationship
Pre-adolescents	3,133	14 Pollutants: NO_x, NO_2, PM_{10}, PM_{COARSE}, $PM_{2.5}$, $PM_{2.5}$absorbance, PAHs, OC, Cu, Fe, Si, Zn, 2 oxidative potential measures	Pregnancy Childhood	Brain volumes Cortical thickness and surface area	Same as volume and thickness outcomes above, but also included a multipollutant analysis, using the DSA approach
AIM 2 — Structural Connectivity					
Pre-adolescents	2,954	14 Pollutants (see above)	Pregnancy Childhood	2 White matter microstructure outcomes (global and 12 individual tracts): - Fractional anisotropy (tendency for preferential water diffusion in white matter tracts) - Mean diffusivity (magnitude of average water diffusion in all directions within brain tissue)	Same as volume and thickness outcomes above, but also included a multipollutant analysis; no correction for multiple testing In a sensitivity analysis, they applied a correction for exposure measurement error using the bootstrap method from Szpiro et al. 2011 (global measures only)
AIM 3 — Functional Connectivity					
Pre-adolescents	2,197	6 Pollutants: NO_x, NO_2, PM_{10}, PM_{COARSE}, $PM_{2.5}$, $PM_{2.5}$absorbance	Pregnancy 0–2 years 2–5 years 5–9 years	Connectivity scores amongst the different brain areas	Same as volume and thickness outcomes above; no multipollutant analysis; the analysis was corrected for multiple testing

Cu = copper, DSA = deletion/substitution/addition, Fe = iron, NO_x = nitrogen oxides, NO_2 = nitrogen dioxide, OC = organic carbon, $PM_{2.5}$ = PM with aerodynamic diameter ≤2.5 µm, $PM_{2.5}$absorbance = absorbance of the $PM_{2.5}$ fraction, PM_{10} = PM with aerodynamic diameter ≤10 µm, PM_{COARSE} = PM with aerodynamic diameter between 10 µm and 2.5 µm, PAH = polycyclic aromatic hydrocarbon, Si = silicon, Zn = zinc.

[a] Parental confounders include parental education, ethnicity, and household income; maternal age, height, prepregnancy body mass index, psychological distress during pregnancy, smoking and alcohol use during pregnancy, maternal parity, maternal intelligence quotient, and family status; and the child's confounders include genetic ancestry, sex, and age at the scanning session. Additionally, corpus callosum volume, cerebellum volume, and subcortical brain volumes were adjusted for intracranial volume.

Critique Table 2. Summary of Results on the Associations of Air Pollution Exposure During Early Life Exposure with Brain Outcomes in Children[a]

Analysis / Age of the Children	Brain Outcome	Key Results Based on Single Pollutant Models
AIM 1 Structural Morphology		
School-age children	4 Global brain volumes	No associations
School-age children	9 Region-specific volumes	No associations
School-age children	Cortical thickness	No associations other than the following in the expected direction: (−) Cortical thickness in 6 brain regions (precuneus, pars opercularis, pars orbitalis, rostral middle frontal, superior frontal, cuneus) — $PM_{2.5}$ (−) Cortical thickness in 1 brain region (lateral orbitofrontal) — PM_{COARSE} (−) Cortical thickness in 1 brain region (fusiform) — $PM_{2.5}$absorbance
School-age children	Cognitive function	No associations other than the following in the expected direction: (+) number of inhibition errors in the attention and executive function domain — $PM_{2.5}$ About 15% of the $PM_{2.5}$ association with cognitive impairment was mediated through the reduced cortical thickness
Pre-adolescents	4 Global brain volumes	No associations
Pre-adolescents	9 Region-specific volumes	No associations other than the following in the expected direction: (−) Corpus callosum — OC and one measure of oxidative potential (ESR) (−) Hippocampus — PM_{COARSE}, PAHs, Cu and one measure of oxidative potential (DTT) (+) Amygdala — Si (+) Nucleus accumbens — Zn (+) Putamen — PM_{COARSE} Associations reported in the unexpected direction: (−) Amygdala — OC and PAHs (+) Cerebellum — PM_{10}, PM_{COARSE}, $PM_{2.5}$, $PM_{2.5}$absorbance (+) Palladium — PM_{COARSE}
Pre-adolescents	Cortical thickness	No associations other than the following in the expected direction: (−) Cortical thickness in 1 brain region (postcentral gyrus) — OC (−) Cortical thickness in 1 brain region (rostral middle frontal gyrus) — $PM_{2.5}$absorbance and Cu (−) Cortical thickness in 1 brain region (lingual gyrus) — one measure of oxidative potential (DTT)
Pre-adolescents	Cortical surface area	No associations other than the following in the expected direction: (−) Cortical surface area in the pars trangularis — PM_{COARSE} Associations reported in the unexpected direction: (+) Cortical surface area in 3 brain regions (precentral gyrus, precuneus, pericalcarine cortex) — Zn (+) Cortical surface area in 1 brain region (precentral gyrus) — one measure of oxidative potential (ESR)

(Table continues next page)

Cu = copper, ESR = electron spin resonance, DTT = dithiothreitol, Fe = iron, NO_x = nitrogen oxides, NO_2 = nitrogen dioxide, OC = organic carbon, $PM_{2.5}$ = PM with aerodynamic diameter ≤2.5 µm, $PM_{2.5}$absorbance = absorbance of the $PM_{2.5}$ fraction, PM_{10} = PM with aerodynamic diameter ≤10 µm, PM_{COARSE} = PM with aerodynamic diameter between 10 µm and 2.5 µm, PAH = polycyclic aromatic hydrocarbon, Si = silicon, Zn = zinc.

[a] Expected direction mean in agreement with the authors' hypothesis about the negative effect that air pollution would have on the outcome. A decrease in the association (−) indicates a worse outcome for the specified brain outcome, and an increase in the association (+) indicates a worse outcome for the specified brain outcome.

Critique Table 2 (*Continued*). Summary of Results on the Associations of Air Pollution Exposure During Early Life with Brain Outcomes in Children[a]

Analysis / Age of the Children	Brain Outcome	Key Results Based on Single Pollutant Models
AIM 2 Structural Connectivity		
Pre-adolescents	Global fractional anisotropy	Associations reported in the expected direction: (−) for NO_x, NO_2, PM_{10}, $PM_{2.5}$, $PM_{2.5}$absorbance, and OC (6 out of 14 pollutants)
Pre-adolescents	Fractional anisotropy in 12 individual white matter tracts	Associations reported in the expected direction: (−) for $PM_{2.5}$ in 4 individual tracts and for NO_x in 5 individual tracts
Pre-adolescents	Global mean diffusivity	Associations reported in the expected direction: (+) for all 14 pollutants except for PAHs
Pre-adolescents	Mean diffusivity in 12 individual white matter tracts	Associations reported in the expected direction: (+) for Si in 5 individual tracts, for Zn in 9 individual tracts, and for one measure of oxidative potential (DTT) in 1 individual tract
AIM 3 Functional Connectivity		
Pre-adolescents	Connectivity scores for the different brain areas	Associations reported higher air pollution exposure and higher connectivity (no a priori hypothesis on direction of associations): (+) NO_x — 15 brain regions (+) NO_2 — 20 brain regions (+) PM_{COARSE} — 2 brain regions (+) $PM_{2.5}$absorbance — 83 brain regions No associations reported for PM_{10} and $PM_{2.5}$

Cu = copper, ESR = electron spin resonance, DTT = dithiothreitol, Fe = iron, NO_x = nitrogen oxides, NO_2 = nitrogen dioxide, OC = organic carbon, $PM_{2.5}$ = PM with aerodynamic diameter ≤2.5 µm, $PM_{2.5}$absorbance = absorbance of the $PM_{2.5}$ fraction, PM_{10} = PM with aerodynamic diameter ≤10 µm, PM_{COARSE} = PM with aerodynamic diameter between 10 µm and 2.5 µm, PAH = polycyclic aromatic hydrocarbon, Si = silicon, Zn = zinc.

[a] Expected direction mean in agreement with the authors' hypothesis about the negative effect that air pollution would have on the outcome. A decrease in the association (−) indicates a worse outcome for the specified brain outcome, and an increase in the association (+) indicates a worse outcome for the specified brain outcome.

- Associated with higher brain functional connectivity among several brain regions in pre-adolescents (NO_x, NO_2, PM_{COARSE}, $PM_{2.5}$absorbance). No associations were reported for PM_{10} and $PM_{2.5}$. The identified areas with higher connectivity were located in regions that are part of the default mode network and the sensorimotor networks.
- The clinical relevance of the findings remain unclear.

HEI REVIEW COMMITTEE'S EVALUATION

In its independent review of the study, the HEI Review Committee complimented Dr. Guxens on her study and thought the research was well motivated and addressed important and novel questions about the potential relationships between air pollution and the developing brain. This type of research is emerging but remains distinctive — with only a handful of MRI studies in children so far.

The Committee noted several major strengths of the study. First, it recognized the benefits of using of an existing birth cohort that has neuroimaging data for a large subset of the cohort — the largest sample to date — and the wealth of individual-level covariate data, including physical exams, neuropsychological tests, and parent questionnaires that allow for a comprehensive assessment of confounding. The Committee thought the availability of high-resolution neuroimaging data was unprecedented, because MRI is a powerful tool that allows in vivo visualization of brain structure and function. Second, the large suite of air pollution exposure metrics estimated at the residential address level, while taking into account residential mobility, was considered another strength. The Committee also thought the analyses were comprehensive, straightforward, and clearly presented in the report. For example, the use of multiple imputation to account for missing covariate data, a correction approach to increase the chance that results would be representative for the study population initially recruited, and an assessment of measurement error show the rigor of the research undertaken. In addition, the mediation analysis to investigate whether schoolchildren who had reduced cortical thickness showed cognitive impairment was appreciated because it shed some light on whether the findings are clinically relevant. The Committee considered Dr. Guxens an exceptional recipient of HEI's Walter A. Rosenblith New Investigators Award and was impressed by her performance and successful completion of a pioneering project.

The study by Dr. Guxens documented associations between early life air pollution exposure and various measures of brain structural morphology, structural connectivity, and functional connectivity in children. For example, exposure to air pollution during early life was associated with a thinner cortex in various regions of the brain in both school-age children and pre-adolescents. Moreover, in pre-adolescents, exposure to air pollution during early life was associated with various differences in region-specific brain volumes, such as a smaller volume in the hippocampus and corpus callosum. In addition, associations were documented between exposure and white matter microstructure and higher brain functional connectivity among several brain regions.

The current study is the largest so far and adds to a limited evidence base. The few earlier studies in children that integrated air pollution epidemiology and neuroimaging suggest that various brain structures and functions could be affected by air pollution (de Prado Bert et al. 2018; Herting et al. 2019; Lopuszanska and Samardakiewicz 2020). Observations included smaller white matter surface area (e.g., Peterson et al. 2015) and microstructure (Pujol et al. 2016b); smaller volumes or less density or both within the caudate (e.g., Alemany et al. 2018; Mortamais et al. 2017; Pujol et al. 2016b); altered resting-state functional connectivity (Pujol et al. 2016a,b), and brain activity to sensory stimuli (Pujol et al. 2016a). Earlier MRI findings in children suggests air pollution exposure does not lead to differences in global brain volumes including total brain, gray matter, and white matter (Mortamais et al. 2017; Pujol et al. 2016a,b), which is consistent with the results of the current study. A new analysis of 186 children from the Brain Development and Air Pollution Ultrafine Particles in School Children (BREATHE) study in Barcelona, Spain, reported that prenatal exposure to $PM_{2.5}$ might be associated with a decreased corpus callosum volume, which was associated with a higher hyperactivity subscore. No associations were observed between $PM_{2.5}$ and volume measures in other brain structures (gray matter, white matter, and lateral ventricles), nor in measures of structural connectivity (Mortamais et al. 2019). The majority of MRI studies to date are based on subsets of children from two cohort studies: the BREATHE study in Barcelona and the Columbia Center for Children's Environmental Health (CCCEH) cohort in New York City. Those studies are limited by the cross-sectional nature of the analyses and the small sample size, which is partly due to the high costs of the MRI measurements.

Although the Review Committee broadly agreed with the investigators' conclusions, there are a few limitations identified by the Committee detailed below that should be considered when interpreting the results.

SUBSTANTIAL TEMPORAL AND SPATIAL MISALIGNMENT OF THE EXPOSURE DATA

The Committee had concerns about the exposure assessment because of the substantial temporal and spatial misalignment of the data. That issue is particularly important when studying the developing brain, which is exceptionally complex with potentially critical time windows of development. The study relies on an historical exposure assessment that is temporally misaligned with the health data by about 4–8 years later than the collection of the brain outcome data. Several issues of concern with the exposure assessment were noted by the Committee. First, the limited number of sites for

the PM and PM species (40) does not afford strong data support for the modeling; this might have led to over-smoothing in the pollution surfaces, particularly for some of the metals that likely have fine-scale variations, such as Cu, Fe, and Zn. Second, PM measurements were not measured simultaneously (with only 10 sites per round); this seems to have necessitated temporal adjustments that can introduce error because of differential accuracy in the temporal adjustment, depending on the spatial relationship between the research sites and the single continuous-reference monitor site. Third, the forward and back extrapolations used in some analyses to match the exact period of interest could introduce additional exposure error. Fourth, the Committee noted several general concerns regarding the use of standard linear regression for the exposure model development. For example, the algorithm may overfit the data when there are relatively few monitoring sites to train a model and a large number of potential predictor variables offered. Also, the algorithm could fail to capture potentially complex relationships within the data because it assumes the relationship between air pollution and a predictor is linear over the whole range of the predictor values and includes potential interactions among covariates to only a limited extent. Moreover, the algorithm could result in unstable and uninterpretable coefficient estimates when highly correlated predictors are included in one model. To try to alleviate those concerns, other modeling techniques have increasingly been applied to develop LUR models for air pollution exposure assessment, such as machine learning techniques. The few studies, however, that compared performance of different modeling techniques for exposure assessment report similar performance for the models, although those results may differ with the study setting, hampering a generic recommendation for one algorithm (e.g., Chen et al. 2019; Kerkhoffs et al. 2019; Weichenthal et al. 2016). Some, but not all, of these limitations in the exposure assessment were noted in the discussion section of the Investigators' Report and acknowledged by the study team. Although the Committee understands that Dr. Guxens and her team made best use of the exposure models available, the substantial temporal and spatial misalignment of the exposure data might have influenced the analysis of brain outcomes in unpredictable ways. An effort was made by the study team to adjust the analysis for exposure measurements error by using the bootstrap method from Szpiro et al. 2011, which was laudable, but was limited to a few brain outcomes only, and it is unclear whether the method has sufficient data support to derive reliable corrections.

STATISTICAL ANALYSES

The Committee thought the statistical analyses pursued was comprehensive, straightforward, and clearly presented. The analysis was hypothesis driven rather than an exploratory discovery-based analysis, and the main analyses were based on simple regression. The Committee appreciated the hypothesis provided after each aim, and the expected direction of the relationship for the many brain outcomes indicated under each table in the Investigators' Report. The Committee noted that the study was exploratory in many aspects, without much prior knowledge on which to build. For example, investigators had no expected direction for the relationship for some brain measure outcomes, such as for the connectivity scores for the different brain areas. In those cases, it was clearly stated by the investigators that there was no a priori hypothesis on the direction of the relationship.

The Committee noted two potential areas for future work to compliment the current analyses. They would recommend a broader exploration that uses some of the untargeted analyses. Those analyses could address some of the main challenges more fully, such as simultaneous testing of multiple hypotheses and consideration of (a) multiple correlated exposures, (b) exposure interactions and nonlinear exposure–response relations, and (c) temporal factors in exposures. The Committee thought that one could borrow from some of the approaches currently used in omics analyses in studies of the exposome (Agier et al. 2016; Chadeau-Hyam et al. 2013; Staffogia et al. 2017). Other valuable studies would be future longitudinal analyses with repeated MRI measurements to assess the effect of air pollution on the developmental trajectories of the brain outcomes included in the current cross-sectional analysis. The brain is exceptionally complex and has a dynamic structure that is constantly evolving throughout life and influenced by many factors (Lenroot and Giedd 2006; Tau and Peterson 2010). The investigators are well positioned to pursue such longitudinal analyses in the near future. The ongoing Generation R just finished a third round of MRI measurements on the same children who are now 13–17 years old. They used the same scanner as in the second time point, and it is expected that the investigators will now have sufficient statistical power for such an analysis. Unfortunately, there are fewer children (about 400) that underwent imaging at both the first and second time points, and the use of different scanners has prevented a longitudinal analysis using those data.

Although the Committee thought the analyses were generally well done, all brain outcomes should have been corrected for multiple comparisons because of the large number of analyses. Multiple comparison corrections are an imperative step in reducing Type I error in MRI brain research (Bennett et al. 2009; Lindquist and Mejia 2015). For example, for the brain volume outcomes, the investigators ran 364 regression models (14 pollutants × 13 brain volume outcomes × 2 exposure windows). The investigators justified their decision with their hypothesis-based approach to selecting only volumes in specific brain regions and argued that the use of the multipollutant modeling alleviates multiple testing issues.

MULTIPOLLUTANT MODELING

The Committee was not convinced that the multipollutant approach added much. The use of the DSA algorithm in

modeling the effects of multiple exposures on brain outcomes is said to provide a compromise between sensitivity and false discovery proportion compared with other methods. How stable the identified specific exposure associations are, however, remains open to question. Each DSA model was run 200 times, and the final model was identified as the one in which any exposure variable was selected in at least 10% of the runs — suggesting strongly that these findings are not particularly stable.

In addition, the Committee thought that the DSA approach for multipollutant modeling was not reliable because of the vastly different performance and data support for the various exposure models. Optimizing the prediction could favor those pollutants that are better supported and predicted than others. The Committee preferred some further analysis of multipollutant models, for example, using a manually supervised selection and combinations of variables to the DSA approach implemented, given the limitations of the data and exposure models.

Multipollutant modeling in general remains difficult in the presence of high correlations among pollutants, irrespective of the method (Dominici et al. 2010). In particular PM_{10}, $PM_{2.5}$, NO_x, NO_2, and $PM_{2.5}$absorbance were highly correlated (>0.7), as were Cu, Fe, and oxidative potential using electron spin resonance (>0.8), and Fe and Si (0.8). The correlation between PAHs and Cu was similarly high (0.7). Typically, somewhat lower correlations were reported for the other pollutant pairs. Likewise, the often-high correlation between prenatal and childhood exposure hampered the identification of a susceptible exposure window to tease out effects of pregnancy versus childhood exposure and an approach for how to allow for effects during both time periods. The correlation was typically around 0.60 between prenatal and childhood exposure. Thus, the Committee would like to emphasize that the individual pollutant results should be considered as indicators of the ambient air pollution mixture, and prenatal and childhood exposure should be viewed as indicators of early life exposure. Thus, when summarizing the results in this Critique, the Committee has focused on single pollutant results and did not distinguish between pregnancy and childhood exposures.

GENERALIZABILITY OF THE FINDINGS

The Committee had some concerns about the generalizability of the findings. On the one hand, some strengths are that in Generation R the overall response rate at recruitment was 61%, which is relatively high and laudable (Kooijman et al. 2016). In addition, all analyses used inverse probability weighting to increase the chance that the results would be representative for the study population initially recruited (about 9,600). The Committee appreciated this correction approach because indeed MRI data were available from only a subset of the cohort, which was due in part to the high cost of performing an MRI. Also, a potential sampling bias was introduced by deliberately selecting more school-age children with child behavior problems and with mothers who reported certain exposures during pregnancy (e.g., exposure to drugs, nicotine, alcohol, and psychiatric medication). Nevertheless, the Committee thought the generalizability of the results was still reduced because the current study population is a convenience sample. Particularly noteworthy is that 26% of mothers smoked and about 50% drank alcohol during pregnancy at recruitment — much higher rates than the average consumption during pregnancy in the Netherlands (Lanting et al. 2015). Moreover, participants were recruited from Rotterdam, which hosts one of the largest seaports in the world and has associated refineries located upwind of the population studied. Although those issues might not affect the internal validity, they could affect the generalizability of the findings.

SUMMARY AND CONCLUSION

Dr. Guxens and colleagues have conducted a novel study that uses data from an existing birth cohort (Generation R) in Rotterdam, the Netherlands, one of the few to address important and novel questions about the potential relationships between air pollution and the developing brain. The availability of high-resolution neuroimaging data for a large subset of the cohort — the largest sample to date — was unprecedented; the wealth of individual-level covariate data and the large suite of air pollution exposure metrics estimated were considered to be strengths of the study. The study documented associations between early life air pollution exposure and various measures of brain structural morphology, structural connectivity, and functional connectivity in children. Although the Review Committee broadly agrees with the investigators' conclusions, it noted a few limitations that should be considered when interpreting the results.

The Committee had concerns about the exposure assessment because of the substantial temporal and spatial misalignment of the data. That issue is particularly important when studying the developing brain, which is exceptionally complex with potentially critical time windows of development. Furthermore, all brain outcomes, including brain volume outcomes, should have been corrected for multiple comparisons because of the large number of analyses. The Committee was not convinced that the multipollutant approach added much, because, for example, it remains unclear how stable the identified specific exposure associations in the multipollutant analyses really are. High correlations were noted among many pollutants in the analyses and between prenatal and childhood exposure. Thus, it was not possible

to tease out independent pollutant associations and identify a susceptible exposure window during pregnancy and early childhood. Additionally, some study design features affected the generalizability of the findings.

Overall, the insights drawn from the current study, along with a few other brain imaging studies in children, are noteworthy and should provide impetus for further research. Because the brain has a dynamic structure that is constantly evolving throughout life, longitudinal studies beginning as early as possible are the best means to assess the effect of air pollution on the developmental trajectories of the brain outcomes included in the current cross-sectional analysis. Also, further analyses should be encouraged, for example, to investigate whether children with worse brain outcomes showed poorer cognitive function or other adverse neurodevelopmental outcomes. Those analyses would shed light on whether the brain outcome findings are clinically relevant, but this so far remains unclear.

ACKNOWLEDGMENTS

The Review Committee thanks the ad hoc reviewers for their help in evaluating the scientific merit of the Investigators' Report. The Committee is also grateful to Hanna Boogaard and Annemoon van Erp for their oversight of the study, to Hanna Boogaard for her assistance in preparing its Critique, to Carol Moyer for editing of this Report and its Critique, and to Kristin Eckles and Hope Green for their roles in preparing this Research Report for publication.

REFERENCES

Agier L, Portengen L, Chadeau-Hyam M, Basagaña X, Giorgis-Allemand L, Siroux V, et al. 2016. A systematic comparison of linear regression-based statistical methods to assess exposome-health associations. Environ Health Perspect 124:1848–1856.

Alemany S, Vilor-Tejedor N, García-Esteban R, Bustamante M, Dadvand P, Esnaola M, et al. 2018. Traffic-related air pollution, *APOE* ε4 status, and neurodevelopmental outcomes among school children enrolled in the BREATHE project (Catalonia, Spain). Environ Health Perspect 126:087001; doi:10.1289/EHP2246.

Beelen R, Hoek G, Vienneau D, Eeftens M, Dimakopoulou K, Pedeli X, et al. 2013. Development of NO_2 and NO_x land use regression models for estimating air pollution exposure in 36 study areas in Europe — The ESCAPE project. Atmos Environ 72:10–23.

Bennett CM, Wolford GL, Miller MB. 2009. The principled control of false positives in neuroimaging. Soc Cogn Affect Neurosci 4:417–422.

Bongaerts E, Nawrot TS, Van Pee T, Ameloot M, Bové H. 2020. Translocation of (ultra)fine particles and nanoparticles across the placenta: A systematic review on the evidence of in vitro, ex vivo, and in vivo studies. Part Fibre Toxicol 17:56.

Calderón-Garcidueñas L, Engle R, Mora-Tiscareño A, Styner M, Gómez-Garza G, Zhu H, et al. 2011. Exposure to severe urban air pollution influences cognitive outcomes, brain volume and systemic inflammation in clinically healthy children. Brain Cogn 77: 345–355.

Calderón-Garcidueñas L, Mora-Tiscareño A, Styner M, Gómez-Garza G, Zhu H, Torres-Jardón R, et al. 2012. White matter hyperintensities, systemic inflammation, brain growth, and cognitive functions in children exposed to air pollution. J Alzheimers Dis 31:183–191; doi:10.3233/JAD-2012-120610.

Chadeau-Hyam M, Campanella G, Jombart T, Bollolo L, Portengen L, Vineis P, et al. 2013. Deciphering the complex: Methodological overview of statistical models to derive OMICS-based biomarkers. Environ Mol Mutagen 54:542–557.

Chen J, de Hoogh K, Gulliver J, Hoffmann B, Hertel O, Ketzel M, et al. 2019. A comparison of linear regression, regularization, and machine learning algorithms to develop Europe-wide spatial models of fine particles and nitrogen dioxide. Environ Int 130:104934.

de Prado Bert P, Mercader EMH, Pujol J, Sunyer J, Mortamais M. 2018. The effects of air pollution on the brain: a review of studies interfacing environmental epidemiology and neuroimaging. Curr Environ Health Rep 5:351–364.

Dominici F, Peng RD, Barr CD, Bell ML. 2010. Protecting human health from air pollution: shifting from a single-pollutant to a multipollutant approach. Epidemiology 21:187–194.

Eeftens M, Beelen R, De Hoogh K, Bellander T, Cesaroni G, Cirach M, et al. 2012. Development of land use regression models for $PM_{2.5}$, $PM_{2.5}$ absorbance, PM_{10} and PM_{coarse} in 20 European study areas: Results of the ESCAPE project. Environ Sci Technol 46:11195–11205.

Herting MM, Younan D, Campbell CE, Chen JC. 2019. Outdoor air pollution and brain structure and function from across childhood to young adulthood: A methodological review of brain MRI studies. Front Public Health 7:332.

Horton MK, Margolis AE, Tang C, Wright R. 2014. Neuroimaging is a novel tool to understand the impact of environmental chemicals on neurodevelopment. Curr Opin Pediatr 26:230–236.

Kerckhoffs J, Hoek G, Portengen L, Brunekreef B, Vermeulen RCH. 2019. Performance of prediction algorithms for modeling outdoor air pollution spatial surfaces. Environ Sci Technol 53:1413–1421.

Kooijman MN, Kruithof CJ, van Duijn CM, Duijts L, Franco OH, van IJzendoorn MH, et al. 2016. The Generation R Study: Design and cohort update 2017. Eur J Epidemiol 31:1243–1264.

Landrigan PJ. 2002. The worldwide problem of lead in petrol. Bull World Health Organ 80:768.

Lanting C, van Dommelen P, van der Pal-de Bruin KK, Bennebroek Gravenhorst J, van Wouwe JP. 2015. Prevalence and pattern of alcohol consumption during pregnancy in the Netherlands. BMC Public Health 15:723.

Lenroot RK, Giedd JN. 2006. Brain development in children and adolescents: Insights from anatomical magnetic resonance imaging. Neurosci Biobehav Rev 30:718–729.

Levy BS, Nassetta WJ. 2003. Neurologic effects of manganese in humans: A review. Int J Occup Environ Health 9:153–163.

Lindquist MA, Mejia A. 2015. Zen and the art of multiple comparisons. Psychosom Med 77:114–125.

Lopuszanska U, Samardakiewicz M. 2020. The relationship between air pollution and cognitive functions in children and adolescents: a systematic review. Cogn Behav Neurol 33:157–178.

Mortamais M, Pujol J, van Drooge BL, Macià D, Martínez-Vilavella G, Reynes C, et al. 2017. Effect of exposure to polycyclic aromatic hydrocarbons on basal ganglia and attention-deficit hyperactivity disorder symptoms in primary school children. Environ Int 105:12–19.

Mortamais M, Pujol J, Martínez-Vilavella G, Fenoll R, Reynes C, Sabatier R, et al. 2019. Effects of prenatal exposure to particulate matter air pollution on corpus callosum and behavioral problems in children. Environ Res 178:108734.

Peterson BS, Rauh VA, Bansal R, Xuejun H, Toth Z, Nati G, et al. 2015. Effects of prenatal exposure to air pollutants (polycyclic aromatic hydrocarbons) on the development of brain white matter, cognition, and behavior in later childhood. JAMA Psychiatry 72:531–540; doi:10.1001/jamapsychiatry.2015.57.

Pujol J, Martínez-Vilavella G, Macià D, Fenoll R, Alvarez-Pedrerol M, Rivas I, et al. 2016a. Traffic pollution exposure is associated with altered brain connectivity in school children. NeuroImage 129:175–184.

Pujol J, Fenoll R, Macià D, Martínez-Vilavella G, Alvarez-Pedrerol M, Rivas I, et al. 2016b. Airborne copper exposure in school environments associated with poorer motor performance and altered basal ganglia. Brain Behav 6:e00467.

Saenen ND, Martens DS, Neven KY, Alfano R, Bové H, Janssen BG, et al. 2019. Air pollution-induced placental alterations: An interplay of oxidative stress, epigenetics, and the aging phenotype? Clin Epigenet 11:124.

Sinisi SE, van der Laan MJ. 2004. UC Berkeley Division of Biostatistics Working Paper Series (Working 1889 Paper 143) — Loss-Based Cross-Validated Deletion/Substitution/Addition Algorithms in Estimation. Available: *https://biostats.bepress.com/ucbbiostat/paper143* [accessed 6 July 2021].

Stafoggia M, Breitner S, Hampel R, Basagaña X. 2017. Statistical approaches to address multi-pollutant mixtures and multiple exposures: The state of the science. Curr Environ Health Rep 4:481–490.

Szpiro AA, Sheppard L, Lumley T. 2011. Efficient measurement error correction with spatially misaligned data. Biostatistics 12:610–623; doi:10.1093/biostatistics/kxq083.

Tau GZ, Peterson BS. 2010. Normal development of brain circuits. Neuropsychopharmacology 35:147–168.

U.S. Environmental Protection Agency. 2016. Integrated Science Assessment (ISA) for Oxides of Nitrogen — Health Criteria (Final Report, Jan 2016). EPA/600/R-15/068. Washington, DC:U.S. EPA.

U.S. Environmental Protection Agency. 2019. Integrated Science Assessment (ISA) for Particulate Matter (Final Report, Dec 2019). EPA/600/R-19/188. Washington, DC:U.S. EPA.

van den Hooven EH, Pierik FH, de Kluizenaar Y, Hofman A, van Ratingen SW, Zandveld PYJ, et al. 2012. Air pollution exposure and markers of placental growth and function: The generation R study. Environ Health Perspect 120:1753–1759.

Weichenthal S, van Ryswyk K, Goldstein A, Bagg S, Shekkarizfard M, Hatzopoulou M. 2016. A land use regression model for ambient ultrafine particles in Montreal, Canada: A comparison of linear regression and a machine learning approach. Environ Res 146:65–72.

RELATED HEI PUBLICATIONS

Number	Title	Principal Investigator	Date
Research Reports			
208	Mortality and Morbidity Effects of Long-Term Exposure to Low-Level $PM_{2.5}$, BC, NO_2, and O_3: An Analysis of European Cohorts in the ELAPSE Project	B. Brunekreef	2021
193	Particulate Air Pollutants, Brain Structure, and Neurocognitive Disorders in Older Women	J.C. Chen	2017
190	The Effects of Policy-Driven Air Quality Improvements on Children's Respiratory Health	F. Gilliland	2017
189	Ambient Air Pollution and Adverse Pregnancy Outcomes in Wuhan, China	Z. Qian	2016
188	Adverse Reproductive Health Outcomes and Exposure to Gaseous and Particulate-Matter Air Pollution in Pregnant Women	J. Wu	2016
183	Development of Statistical Methods for Multipollutant Research		
	Part 1. Statistical Learning Methods for the Effects of Multiple Air Pollution Constituents	B.A. Coull	2015
	Part 2. Development of Enhanced Statistical Methods for Assessing Health Effects Associated with an Unknown Number of Major Sources of Multiple Air Pollutants	B.A. Coull	2015
	Part 3. Modeling of Multipollutant Profiles and Spatially Varying Health Effects with Applications to Indicators of Adverse Birth Outcomes	J. Molitor	2016
177	National Particle Component Toxicity (NPACT) Initiative: Integrated Epidemiologic and Toxicologic Studies of the Health Effects of Particulate Matter Components	M. Lippman	2013
119	Manganese Toxicokinetics at the Blood–Brain Barrier	R.A. Yokel	2004
89	Reproductive and Offspring Developmental Effects Following Maternal Inhalation Exposure to Methanol in Nonhuman Primates	T. Burbacher	1999
12	Neurotoxicity of Prenatal Carbon Monoxide Exposure	L.D. Fechter	1987
Special Report			
17	Traffic-Related Air Pollution: A Critical Review of the Literature on Emissions, Exposure, and Health Effects	HEI	2010
Perspective			
3	Understanding the Health Effects of Ambient Ultrafine Particles	HEI	2013

Copies of these reports can be obtained from HEI; PDFs are available for free downloading at www.healtheffects.org/publications.

ABBREVIATIONS AND OTHER ITEMS

CI	confidence interval
Cti	estimated air pollution concentration at the time period *ti*
Cu	copper
Cyearly	estimated yearly air pollution concentration
DSA	deletion/substitution/addition
DTI	diffusion tensor imaging
ESCAPE	European Study of Cohorts for Air Pollution Effects
FA	fractional anisotropy
Fe	iron
fMRI	functional magnetic resonance imaging
ISA	Integrated Science Assessment
ISGlobal	Barcelona Institute for Global Health
IRR	incidence rate ratio
LUR	land-use regression
MD	mean diffusivity
MRI	magnetic resonance imaging
NDE	natural direct effect
NEPSY-II	Developmental Neuropsychological Assessment test
NIE	natural indirect effect
NO_2	nitrogen dioxide
NO_x	nitrogen oxides
OC	organic carbon
OP^{DTT}	oxidative potential using dithiothreitol
OP^{ESR}	oxidative potential using electron spin resonance
PAH	polycyclic aromatic hydrocarbon
PM	particulate matter
$PM_{2.5}$	PM with aerodynamic diameter ≤2.5 μm
$PM_{2.5}$absorbance	absorbance of the $PM_{2.5}$ fraction
PM_{10}	PM with aerodynamic diameter ≤10 μm
PM_{COARSE}	PM with aerodynamic diameter between 10 μm and 2.5 μm
QDEC	Query, Design, Estimate, Contrast
rs-fMRI	resting-state functional magnetic resonance imaging
Si	silicon
TRANSPHORM	Transport related air pollution health effects integrated methodologies for assessing particulate matter
U.S. EPA	U.S. Environmental Protection Agency
Zn	zinc

HEI BOARD, COMMITTEES, and STAFF

Board of Directors

Richard A. Meserve, Chair *Senior of Counsel, Covington & Burling LLP; President Emeritus, Carnegie Institution for Science; former Chair, U.S. Nuclear Regulatory Commission*

Enriqueta Bond *President Emerita, Burroughs Wellcome Fund*

Jo Ivey Boufford *President, International Society for Urban Health*

Homer Boushey *Emeritus Professor of Medicine, University of California–San Francisco*

Michael T. Clegg *Professor of Biological Sciences, University of California–Irvine*

Jared L. Cohon *President Emeritus and Professor, Civil and Environmental Engineering and Engineering and Public Policy, Carnegie Mellon University*

Stephen Corman *President, Corman Enterprises*

Martha J. Crawford *Dean, Jack Welch College of Business and Technology, Sacred Heart University*

Michael J. Klag *Dean Emeritus and Second Century Distinguished Professor, Johns Hopkins Bloomberg School of Public Health*

Alan I. Leshner *CEO Emeritus, American Association for the Advancement of Science*

Karen C. Seto *Frederick Hixon Professor of Geography and Urbanization Science, Yale School of the Environment*

Research Committee

David A. Savitz, Chair *Professor of Epidemiology, School of Public Health, and Professor of Obstetrics and Gynecology, Alpert Medical School, Brown University*

Jeffrey R. Brook *Senior Research Scientist, Air Quality Research Division, Environment Canada, and Assistant Professor, University of Toronto, Canada*

Amy H. Herring *Sara & Charles Ayres Professor of Statistical Science and Global Health, Duke University*

Barbara Hoffmann *Professor of Environmental Epidemiology, Institute of Occupational, Social, and Environmental Medicine, University of Düsseldorf, Germany*

Heather A. Holmes *Associate Professor, Department of Chemical Engineering, University of Utah*

Neil Pearce *Professor of Epidemiology and Biostatistics, London School of Hygiene and Tropical Medicine*

Ivan Rusyn *Professor, Department of Veterinary Integrative Biosciences, Texas A&M University*

Evangelia (Evi) Samoli *Associate Professor of Epidemiology and Medical Statistics, Department of Hygiene, Epidemiology and Medical Statistics, School of Medicine, National and Kapodistrian University of Athens, Greece*

Gregory Wellenius *Professor, Department of Environmental Health, Boston University School of Public Health*

Review Committee

Melissa Perry, Chair *Professor and Chair, Department of Environmental and Occupational Health, George Washington University Milken Institute School of Public Health*

Sara D. Adar *Associate Professor and Associate Chair, Department of Epidemiology, University of Michigan School of Public Health*

Kiros Berhane *Professor and Chair, Department of Biostatistics, Mailman School of Public Health, Columbia University*

Michael Jerrett *Professor and Chair, Department of Environmental Health Sciences, Fielding School of Public Health, University of California- Los Angeles*

Frank Kelly *Henry Battcock Chair of Environment and Health and Director of the Environmental Research Group, Imperial College London School of Public Health*

Jana B. Milford *Professor, Department of Mechanical Engineering and Environmental Engineering Program, University of Colorado-Boulder*

HEI BOARD, COMMITTEES, and STAFF

Jennifer L. Peel *Professor of Epidemiology, Colorado School of Public Health and Department of Environmental and Radiological Health Sciences, Colorado State University*

Eric J. Tchetgen Tchetgen *Luddy Family President's Distinguished Professor, Professor of Statistics and Data Science, The Wharton School, University of Pennsylvania*

Officers and Staff

Daniel S. Greenbaum *President*

Robert M. O'Keefe *Vice President*

Ellen K. Mantus *Director of Science*

Donna J. Vorhees *Director of Energy Research*

Annemoon M. van Erp *Deputy Director of Science*

Thomas J. Champoux *Director of Science Communications*

Jacqueline C. Rutledge *Director of Finance and Administration*

Emily Alden *Corporate Secretary*

Lee Ann Adelsheim *Research Assistant*

Palak Balyan *Consulting Staff Scientist*

Hanna Boogaard *Consulting Principal Scientist*

Sofia Chang-DePuy *Digital Communications Manager*

Aaron J. Cohen *Consulting Principal Scientist*

Dan Crouse *Senior Scientist*

Robert M. Davidson *Staff Accountant*

Philip J. DeMarco *Compliance Manager*

Kristin C. Eckles *Senior Editorial Manager*

Elise G. Elliott *Staff Scientist*

Hope Green *Editorial Project Manager*

Joanna Keel *Research Assistant*

Yi Lu *Staff Scientist*

Lissa McBurney *Senior Science Administrator*

Janet I. McGovern *Executive Assistant*

Martha Ondras *Research Fellow*

Pallavi Pant *Senior Scientist*

Allison P. Patton *Senior Scientist*

Quoc Pham *Science Administrative Assistant*

Anna S. Rosofsky *Staff Scientist*

Robert A. Shavers *Operations Manager*

Eva Tanner *Staff Scientist*

Eleanne van Vliet *Staff Scientist*

HEALTH
EFFECTS
INSTITUTE

75 Federal Street, Suite 1400
Boston, MA 02110, USA
+1-617-488-2300
www.healtheffects.org

RESEARCH
REPORT

Number 209
February 2022